

AD-A207 482

POTENTIAL FOR A NEAR TERM VERY LOW ENERGY ANTIPROTON  
SOURCE AT BROOKHAVEN NATIONAL LABORATORY(U) AIR FORCE  
ASTRONAUTICS LAB EDWARDS AFB CA G D NORDLEY APR 89

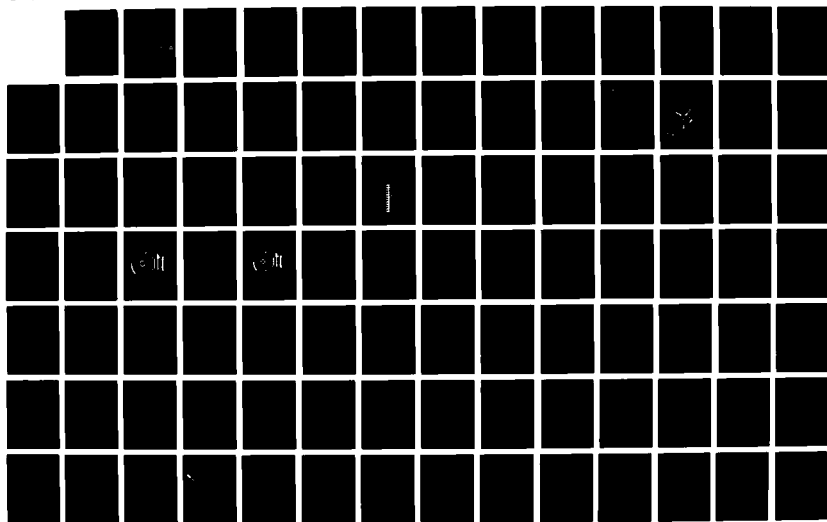
1/3

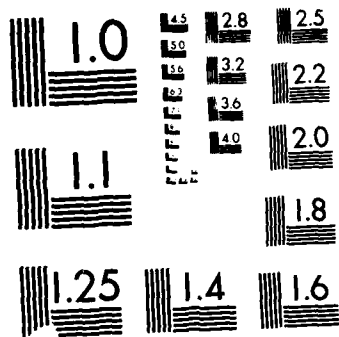
UNCLASSIFIED

AFAL-SR-89-001

F/G 20/7

NL





UTION TEST CHART  
 1010-A

(4)

AD-A207 482

## Potential for a Near Term Very Low Energy Antiproton Source at Brookhaven National Laboratory

A compilation of reports provided under task 1 of the AL/DoE Memorandum of Agreement for Applied Research In Energy Storage support from Brookhaven National Laboratory

April 1989

Editor: Gerald D. Nordley

DTIC  
ELECTE  
MAY 08 1989  
S H D  
cb

### Approved for Public Release

Distribution is unlimited. The AL Technical Services Office has reviewed this report, and it is releasable to the National Technical Information Service, where it will be available to the general public, including foreign nationals.

### Astronautics Laboratory (AFSC)

Air Force Space Technology Center  
Space Division, Air Force Systems Command  
Edwards Air Force Base,  
California 93523-5000

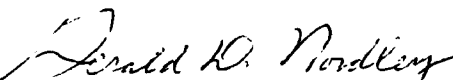
89 5 5 076

## NOTICE


When U.S. Government drawings, specifications, or other data are used for any purpose other than a definitely related government procurement operation, the government thereby incurs no responsibility nor any obligation whatsoever, and the fact that the government may have formulated, furnished, or in any way supplied the said drawings, specifications, or other data is not to be regarded by implication or otherwise, as conveying any rights or permission to manufacture, use, or sell any patented invention that may in any way be related thereto.

## FOREWORD

This special report comprises the papers provided by Brookhaven National Laboratory (BNL) as the final report of the effort performed under task 1 of the Air Force Astronautics Laboratory/Department of Energy-BNL Memorandum of Agreement for support of Applied Research In Energy Storage (ARIES). This special report has been reviewed and approved in accordance with the distribution statement on the cover an on the DD form 1473.

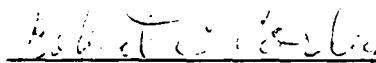


GERALD D. NORDLEY, Major, USAF  
Research Staff Manager, ARIES  
Air Force Astronautics Laboratory



SEYMOUR BARON  
Associate Director  
Brookhaven National Laboratory

FOR THE DIRECTOR



ROBERT C. CORLEY  
Chief, Astronautical Sciences Division

## REPORT DOCUMENTATION PAGE

Form Approved  
OMB No. 0704-0188

1a. REPORT SECURITY CLASSIFICATION Unclassified			1b. RESTRICTIVE MARKINGS		
2a. SECURITY CLASSIFICATION AUTHORITY			3. DISTRIBUTION / AVAILABILITY OF REPORT Approved for public release. Distribution is unlimited.		
2b. DECLASSIFICATION / DOWNGRADING SCHEDULE					
4. PERFORMING ORGANIZATION REPORT NUMBER(S) AFAL-SR-86-001			5. MONITORING ORGANIZATION REPORT NUMBER(S)		
6a. NAME OF PERFORMING ORGANIZATION Air Force Astronautics Laboratory		6b. OFFICE SYMBOL (If applicable) LSX	7a. NAME OF MONITORING ORGANIZATION		
6c. ADDRESS (City, State, and ZIP Code) Edwards Air Force Base, CA 93523-5000			7b. ADDRESS (City, State, and ZIP Code)		
8a. NAME OF FUNDING / SPONSORING ORGANIZATION		8b. OFFICE SYMBOL (If applicable)	9. PROCUREMENT INSTRUMENT IDENTIFICATION NUMBER		
8c. ADDRESS (City, State, and ZIP Code)			10. SOURCE OF FUNDING NUMBERS		
PROGRAM ELEMENT NO. 62302F		PROJECT NO. 5730	TASK NO. 00	WORK UNIT ACCESSION NO. 5E	
11. TITLE (Include Security Classification) POTENTIAL FOR A NEAR-TERM LOW ENERGY ANTIPROTON SOURCE AT BROOKHAVEN NATIONAL LABORATORY (U)					
12. PERSONAL AUTHOR(S) Nordley, Gerald D., Editor					
13a. TYPE OF REPORT Special Report		13b. TIME COVERED FROM _____ TO _____		14. DATE OF REPORT (Year, Month, Day) 89/04	
15. PAGE COUNT					
16. SUPPLEMENTARY NOTATION					
17. COSATI CODES			18. SUBJECT TERMS (Continue on reverse if necessary and identify by block number)		
FIELD	GROUP	SUB-GROUP	>Low Energy Antiproton Source; Beam Deceleration; Antiproton Production Rates. (f-1)		
20	07				
20	08				
19. ABSTRACT (Continue on reverse if necessary and identify by block number)					
<p>The resolution of key issues in the use of antimatter for applications ranging from aerospace materials analysis in the near term and propulsion energy storage in the far term requires experiments with low energy, relatively slow moving, or thermal, antiprotons. There is no United States source of antiprotons at that energy; therefore, a task was initiated with Brookhaven National Laboratory to determine what would be required in time, equipment, and money to create a source producing antiprotons at a rate (approx <math>10^{14}</math>/yr) sufficient to support applications experiments. The estimate eventually derived from this first order analysis was approximately \$8.6M for an initial source of 20 KeV antiprotons plus another roughly estimated \$5M for cooling to increase the production rate to <math>10^{14}</math> - <math>10^{15}</math> antiprotons per year. - Key 100 152</p> <p>10 - 154 pages</p>					
20. DISTRIBUTION / AVAILABILITY OF ABSTRACT <input checked="" type="checkbox"/> UNCLASSIFIED/UNLIMITED <input type="checkbox"/> SAME AS RPT. <input type="checkbox"/> DTIC USERS			21. ABSTRACT SECURITY CLASSIFICATION Unclassified		
22a. NAME OF RESPONSIBLE INDIVIDUAL Gerald D. Nordley, Maj, USAF			22b. TELEPHONE (Include Area Code) (805) 275-5653		22c. OFFICE SYMBOL LSX

POTENTIAL FOR A NEAR TERM VERY LOW ENERGY ANTIPROTON SOURCE  
AT BROOKHAVEN NATIONAL LABORATORY

EXECUTIVE SUMMARY

1. Background

In 1983, the Air Force Rocket Propulsion Laboratory, now the Air Force Astronautics Laboratory (AFAL) commissioned an aggressively openminded study of potential new sources for propulsion energy [1]. This study was needed because propulsion systems based on conventional chemical reactants were approaching their physical limits of performance well short of the fuel efficiency needed for significantly lower cost access to space. Antiproton propulsion technology was one of the items in the study which was not ruled out for scientific reasons, however difficult it might be from an engineering standpoint. A follow-on study [2] indicated that there might be reasonable engineering solutions to the challenges of economically producing, storing and using antimatter as a propulsive energy source; but that large amount of work had to be done to demonstrate that any set of specific solutions would be feasible. The scale-up of antiproton production from the current femtogram level to a level of a gram or more per year was identified as a major issue.

Antiproton propulsion technology was selected for emphasis by Project Forecast II, the 1985 United States Air Force study to identify future missions for the Air Force and the technology base needed to support them [3]. In response to the Project Forecast II initiative, the AFAL began a series of projects aimed at investigating technology bases which must be established for the concept of antimatter propulsion to be feasible [4]. Among these was the availability of a source of very "low" energy antiprotons which could be used for near term experiments to establish the viability of potential antiproton based technologies.

Brookhaven National Laboratory investigators [5] were already exploring production of high luminosity antiproton beams by the Alternating Gradient Synchrotron (AGS) in mid range energies (below 10 GeV/c) as a means of increasing the signal for cross section measurements of certain rare nuclear reactions involving combinations of "charmed" quarks called "charmonium". In this context, "high



luminosity" meant  $10^6$  to  $10^7$  antiprotons per second. The new beams would be unique in the 2 to 10 GeV/c momentum band and supplement the badly oversubscribed Low Energy Antiproton Ring (LEAR) at the Centre Européen des Recherches Nucléaires (CERN) at lower energies. The luminosity of these beams amounts to an antiproton production rate of picograms per year, sufficient for many applications oriented experiments. Table 1 estimates of antiproton technology growth with antiproton availability.

Other experimenters had been advocating use of very low energy antiprotons (less than 200 MeV) for use in radiotherapy and imaging [6]. A potential for use of antiprotons in the testing and analysis of aerospace materials follows directly from the proposed medical work [4].

In March 1986, the AFAL established the Applied Research In Energy Storage (ARIES) office to pursue the Project Forecast II propulsion initiatives in high energy density matter and antimatter. In July 1986 a Memorandum of Agreement (MOA) between the Department of Energy for BNL and the AFAL was established for the support of the ARIES activity.

As part of this memorandum of agreement, BNL was tasked to provide a first order analysis of the engineering and associated cost required for a near term low energy antiproton facility capable of producing approximately  $10^{14}$  antiprotons per year. This analysis was presented to the AFAL/Rand Corporation panels evaluating the potential of low energy antiproton technology held in 1987. This study resulted in a strong endorsement for the creation of a low energy antiproton facility in the United States [7].

## 2. Task Results

The results of AFAL sponsored BNL task comprise the following papers:

a. In the paper, "A thought on Very Low Energy Antiprotons," Y. Y. Lee of BNL estimates that  $1.9 \times 10^5$  antiprotons per pulse could be produced by the AGS and decelerated through the BNL Linac to thermal energies. If the antiprotons are "cooled" (made to travel at essentially the same velocity) in the booster ring prior to deceleration, then the yield can be increased to  $1.33 \times 10^8$  per pulse.

b. The report of the ADD-AGS Superconducting Stretcher Committee, Compiled and Edited by L. G. Ratner, follows. This facility, if built, could possibly be used as a high energy (antiproton accumulator ring to increase the flux of antiprotons.

c. In "A Conceptual Design for A Very Low Energy Antiproton Source," Lee and Lowenstein address directly the engineering and cost implications of an initial 20 keV antiproton source. A realistic estimate of \$8.6M is derived for a  $10^5$  per pulse class antiproton source.

d. Donald Lazarus' Proceedings of the August 1986 antiproton meeting at BNL summarizes a number of physics experiments which have been proposed or could benefit from an intense antiproton source at BNL.

e. In "Trapping Decelerated Antiprotons," A Hershcovitch and Y. Y. Lee propose a gated electrostatic trap for accumulation of antiprotons from the above low energy source. It is pointed out that such a trap would be relatively inexpensive (compared to a new low energy storage ring, for instance) and could in theory store several billion antiprotons for a period of hours.

f. "Low Energy Antiproton Possibilities at BNL" by Y.Y. Lee and D. I. Lowenstein provides a background exposition of BNL's accelerator facilities and summarizes the previous studies for the benefit of the proceedings of the RAND workshop. The authors point out BNL's emphasis on heavy ion acceleration and collision physics and the compatibility of this commitment with the very high luminosity proton beams needed for and intense antiproton source.

g. "A High Intensity Hadron Facility, AGS II," also by Lee and Lowenstein, was furnished following the completion of the task but is included here because it bears on increasing proton beam luminosity and thus eventual antiproton yield. This technical note discusses the possibility of increasing AGS protons per pulse to  $2.5 \times 10^{14}$  and decreasing AGS cycle time to 0.4 seconds per pulse by the early 1990's.

### 3. Conclusion

An increase in proton production rate by a factor of 16 over that used by Lee to project a low energy antiproton production rate of  $10^8$  per pulse implies an annual production capacity in excess of  $10^{15}$  antiprotons per year, or several nanograms, with a mature facility, including the various improvements in cooling and proton production. One nanogram would be sufficient to run a two kilowatt annihilation energy conversion experiment for 10 seconds. Thus it seems that a relatively small increase of about \$20M in the ongoing BNL accelerator program would be enough provide the capacity to conduct



meaningful antiproton energy conversion experiments, including possibly small rocket thrusters, in the mid 1990's. An investment of half this size would provide an initial very low energy antiproton source for a large number of physics experiments and initial exploration of medical and materials applications.

#### REFERENCES

1. Forward, Robert L., 'Alternate Propulsion Energy Sources,' AFRPL TR 83-067, AF Astronautics Laboratory, Edwards, CA, 1983.
2. Forward, Robert L., 'Antiproton Annihilation Propulsion', AFRPL TR 85-003, AF Astronautics Laboratory, Edwards, CA, 1985.
3. Project Forecast II Directors Report (Classified), AFSC TR 86-004, Air Force Systems Command, Andrews AFB, 1986.
4. Nordley, G. D., "Air Force Antimatter Technology Program," IH-87-020, AFAL, 1987.
5. Bachman, M. et. al. "Development of a Time Purified/Separated Beam and High Precision Cross Section Measurements," An AGS Proposal, BNL, 1 May 1984.
6. Gray, L., and T. E. Kalogeropoulos, "Possible Biomedical Applications of Antiproton Beams I.; In Vivo Direct Density Measurements: Radiography," IEEE Transactions on Nuclear Science, Vol. NS-29, No. 2, April 1982.
7. Augenstein, B. W., F. E. Mills, B. E. Bonner, M. M. Nieto, Proceedings of the Antiproton Science and Technology Workshop, 6-9 October, 1987, AFAL-CP-88-002, AFAL, Edwards AFB CA, 1988.

Table 1. Potential Uses of Antimatter with Time And Availability

TIME-FRAME & Cost	SCALE (Numbers of Antiprotons Needed)	ANNIHILATION ENERGY AVAIL.
Some Research Now in Progress	<b>FEMTOGRAM ( <math>6 \times 10^8</math> )</b> Low Kinetic Energy Nuclear Physics Experimental Non-destructive Analysis of Solids Vacuum Measurement Antiproton Atomic Physics Imaging Experiments	15 Joules
2 - 5 Years Circa \$10M	<b>PICOGRAM ( <math>6 \times 10^{11}</math> )</b> Small Volume 3D Density Imaging in Solids Gravitational Mass Measurements High Density Quark-Gluon Plasmas 3D Etching in Crystals Radiotherapy, Microcauterization Experiments Annealing Experiments in Crystals, Metals	$1.5 \times 10^2$
5 - 10 Years Circa \$50M	<b>NANOGRAM ( <math>6 \times 10^{14}</math> )</b> Longer Range or Higher Res. Imaging, Analysis Small Energy Deposition Experiments, kW Commercial Aerospace NDA, NDE Ultrahigh Pressure State Experiments	$1.5 \times 10^5$
15 Years ? Circa \$100M	<b>MICROGRAM ( <math>6 \times 10^{17}</math> )</b> Small Scale Industrial Interior Welding Energy Conversion , 100 lbf Thruster Experiments General Medical Use General Analytic Use (Criminology, Drugs, Toxics) Condensed Antihydrogen Experiments	$1.5 \times 10^8$
20 - 50 Years Circa \$700M	<b>MILLIGRAM ( <math>6 \times 10^{20}</math> )</b> Deep Space Probes, 10lbf, hours, 1200s lsp Large Engine Experiments 100,000 lbf, 900s lsp	$1.5 \times 10^{11}$
50-100 Years ? Circa \$10 <sup>11</sup>	<b>GRAM ( <math>6 \times 10^{23}</math> )</b> Space Transportation (35mg/20 tons to LEO ) Space-Based Production?	$1.5 \times 10^{14}$

Note: "Annihilation Energy Available" excludes neutrinos

## TABLE OF CONTENTS

<u>PAPER</u>	<u>PAGE</u>
A Thought on Very Low Energy Antiprotons - Y.Y. Lee	1
AGS Superconducting Stretcher Ring - L. G. Ratner, ed.	5
A Conceptual Design for a Very Low Energy Antiproton Source - Y.Y. Lee and D. I. Lowenstein	75
Proceedings of the August 1988 Meeting on Antiprotons -D. Lazarus, ed.	81
Trapping Decelerated Antiprotons - A Herscovitch and Y.Y. Lee	163
Low Energy Antiproton Possibilities at BNL - Y.Y. Lee and D. I. Lowenstein	169
A High Intensity Hadron Facility - Y.Y. Lee and D. I. Lowenstein	183

## A THOUGHT ON VERY LOW ENERGY ANTIPROTON\*

Y. Y. LEE  
AGS Department  
Brookhaven National Laboratory  
Associated Universities, Inc.  
Upton, NY 11973

### INTRODUCTION

It has been proposed to use the AGS Booster<sup>1</sup> as a time stretcher purifier for the antiprotons of momentum 0.65 to 5.2 GeV/c.<sup>2</sup> In this note, we would like to extend the idea to very low energy of tens of keV antiprotons.

A brief description of the system is as follows. In each AGS cycle the booster field is set to accept antiprotons of momentum 3.5 GeV/c, where one expects maximum production of antiprotons, after injecting protons into the AGS. The AGS extracts three rf buckets of protons from either H10 or I10 to strike an antiproton production target. The antiprotons will be collected by an appropriate lens system (e.g. lithium lens) and transported to the booster area and injected into the booster through the channel identical to its extraction channel. Since antiproton is the antiparticle of the proton, injection of the antiproton is identical to the extraction of the protons. Once the antiprotons are injected and captured in the booster, one can either accelerate or decelerate them in the booster. After deceleration to 200 MeV kinetic energy, they can be further decelerated through the linac and an RFQ preinjector down to ion source energy.

### ANTI-PROTONS WITHOUT COOLING

Assuming standard production rate at AGS energies of

$$10^{-6} \text{ antiprotons/m-str/\%/interacting protons}$$

antiprotons at 3.5 GeV/c, one can estimate the number of antiprotons which can be accumulated in the booster acceptance of 50 mm-mr and 2% momentum bite. Realistically the AGS proton beam at 30 GeV/c can be focused down to 1 mm spot size, and therefore the angular acceptance one can expect in each dimension would be

$$50 \text{ mm-mr}/0.5 \text{ mm} = 100 \text{ mr.}$$

And the solid angle subtended would be 0.04 steradians.

\*Work performed under the auspices of the U.S. Department of Energy.

Because of the finite length of the target, the collection efficiency would be reduced further. For a 10 cm long target, particle production studies show that only one-third of the particles fall into the useable phase space, and thus the effective solid angle becomes

$$0.04/3 \text{ str} = 13.3 \text{ mstr.}$$

The antiproton production rate is therefore

$$\begin{aligned} N_p &= 10^{-6} \times 13.3 \times 2(\%) \times N_p/3 \\ &= 8.89 \times 10^{-6} N_p \end{aligned}$$

where  $N_p$  is number of incident protons and the factor 3 is to correct for interacting versus incident protons.

The post booster AGS will accelerate  $0.5 \times 10^{13}$  protons/bucket and if one uses three of those buckets for the production per cycle

$$N_p = 8.89 \times 10^{-6} \times 1.5 \times 10^{13} = 1.33 \times 10^8 \text{ antiprotons/pulse at } 3.5 \text{ GeV/c.}$$

If one decelerates the collected antiprotons, assuming rf system has enough debunching to take care of the antiproton beam energy spread (i.e. while making the bunch longer, reduce the energy spread), then the betatron phase space decreases by the factor  $1/P^2$ . The normalized emittance of the collected beam at 3.5 GeV/c is 186.5 mm-mr and this emittance will be trimmed through the deceleration process. The normalized acceptance of the booster at 200 MeV linac energy is 34.3 mm-mr. Figure 1 shows the resultant antiproton intensity as a function of final decelerated energy in the booster.

#### DECELERATION THROUGH THE LINAC

The decelerated antiprotons can be extracted near the booster injection channel, and transported through either injection transport system with its dipoles reversed or separate transport system to the 200 MeV linac. The beam can be decelerated through the linac to a kinetic energy of 750 keV at the "entrance" of linac tank 1. The acceptance of the system is dominated by the normalized admittance<sup>3</sup> at the 750 keV point of 10 mm-mr. Thus one will lose beam intensity through the 200 MeV linac by a factor of

$$(10/34.3)^2 = 0.085$$

and in addition by an additional factor of two due to beam bunching efficiencies. As a result

$$1.9 \times 10^5 \text{ antiprotons}$$

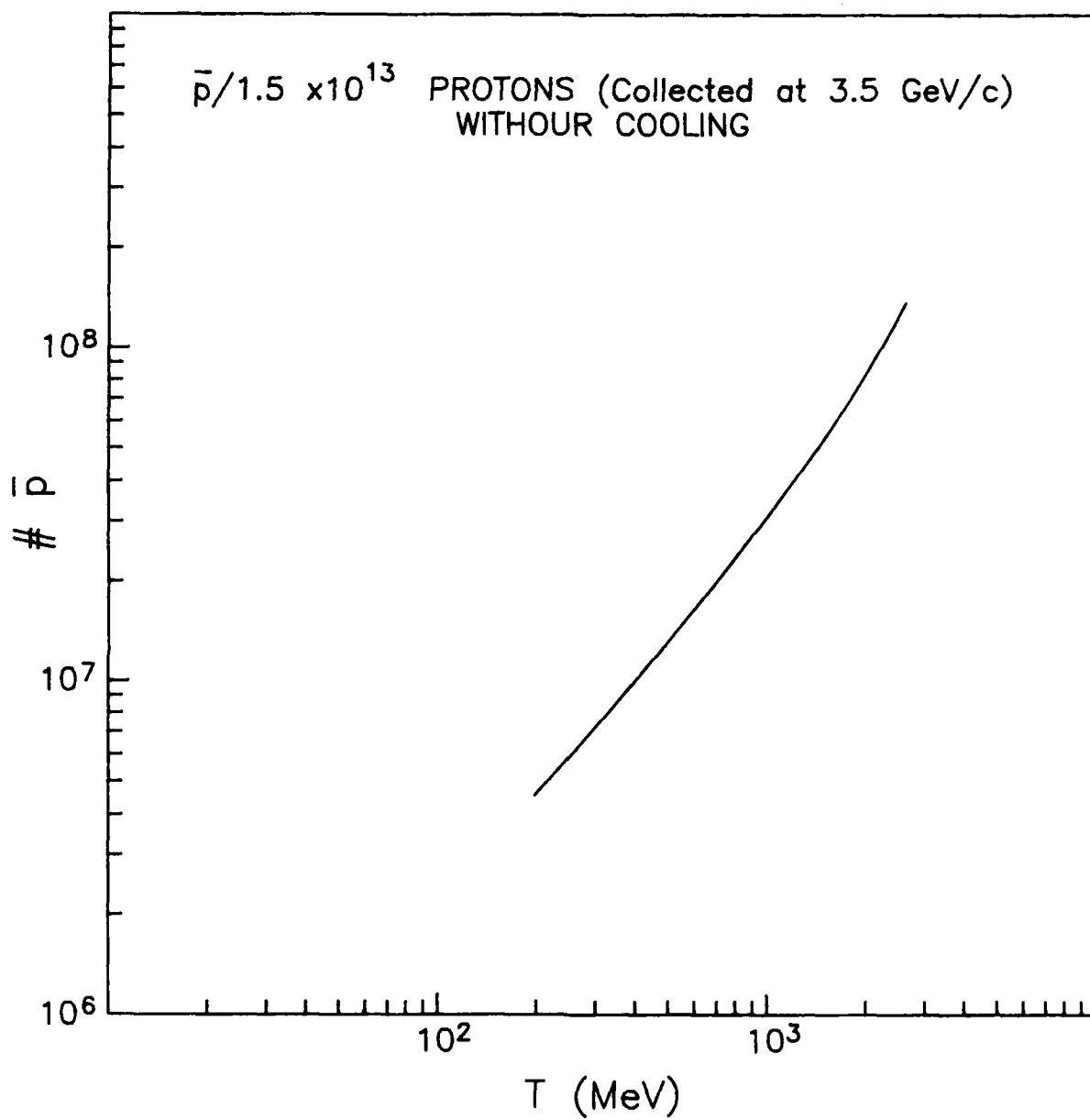
will survive to 750 keV. The antiprotons can be further decelerated through the RFQ preinjector to energies of 20 keV.

#### EFFECT OF COOLING

If one cools the antiprotons in the booster to less than 10 mm-mr normalized or 14.6 mm-mr at 200 MeV energy, theoretically half of the  $1.33 \times 10^8$  antiprotons collected at 3.5 GeV/c could be decelerated to 750 keV and then to 20 keV.

#### REFERNCES

1. AGS booster conceptual design report, BNL 34989 R (1985)
2. A.S. Carroll, Y.Y. Lee, D.C. Peaslee, and L.S. Pinsky, to be published
3. G.W. Wheeler et. al. Particle Accelerators Vol. 9 No. 1/2 (1979)



**AGS SUPERCONDUCTING STRETCHER RING**

(Evaluation of Technical and Cost/Schedule Aspects of a 30 GeV Proton  
Duty Cycle Extending Superconducting Storage Ring for the AGS)

ADD-AGS Superconducting Stretcher Committee

G.M. Bunce, G.F. Dell, J.W. Glenn, C.L. Goodzeit,  
L.G. Ratner, P.A. Thompson

Consultants

D.P. Brown, J.G. Cottingham, E.D. Courant, W. Frey,  
H.C. Hseuh, E. Jablonski, S.Y. Lee, P.V. Mohn, L. Repeta,  
J. Sandberg, R.T. Sanders, A. Soukas, J. Tuozzolo

Compiled and Edited by L.G. Ratner

November 1986

**AGS DEPARTMENT**  
**BROOKHAVEN NATIONAL LABORATORY**  
**UPTON, NEW YORK 11973**



## AGS SUPERCONDUCTING STRETCHER RING

(Evaluation of Technical and Cost/Schedule Aspects of a 30 GeV Proton  
Duty Cycle Extending Superconducting Storage Ring for the AGS)

### ADD-AGS Superconducting Stretcher Committee

G.M. Bunce, G.F. Dell, J.W. Glenn, C.L. Goodzeit,  
L.G. Ratner, P.A. Thompson

### Consultants

D.P. Brown, J.G. Cottingham, E.D. Courant, W. Frey, H.C. Hseuh,  
E. Jablonski, S.Y. Lee, P.V. Mohn, L. Repeta, J. Sandberg, R.T. Sanders,  
A. Soukas, J. Tuozzolo

Compiled and Edited by L.G. Ratner

November 1986

### Acknowledgements

We gratefully thank Ms. Kathy Brown and Ms. Joan Depken for a superb effort in producing this manuscript.

#### DISCLAIMER

This report was prepared as an account of work sponsored by an agency of the United States Government. Neither the United States Government nor any agency thereof, nor any of their employees, nor any of their contractors, subcontractors, or their employees makes any warranty, express or implied, or assumes any legal liability or responsibility for the accuracy, completeness, or usefulness of any information, apparatus, product or process disclosed, or represents that its use would not infringe privately owned rights. Reference herein to any specific commercial product, process, or service by trade name, trademark, manufacturer, or otherwise, does not necessarily constitute or imply its endorsement, recommendation, or favoring by the United States Government or any agency thereof. The views and opinions of authors expressed herein do not necessarily state or reflect those of the United States Government or any agency, contractor, or subcontractor thereof.

## TABLE OF CONTENTS

I.	Introduction. . . . .	1
II.	Siting and Size . . . . .	3
	Fig. II-1 - Layout of ring . . . . .	4
	Fig. II-2 - Layout of ring with contour lines . . . . .	5
	Fig. II-3 - Tunnel enclosure . . . . .	7
	Table II-1 - Radiation shielding thickness . . . . .	8
III.	Conventional Facilities . . . . .	9
	Table III-1: Cost Summary . . . . .	10
IV.	Lattice and Stretcher Properties. . . . .	11
	Fig. IV-1   Cell lattice functions. . . . .	12
	Fig. IV-2   Insertion region lattice. . . . .	12
	Fig. IV-3   Superperiod lattice functions . . . . .	12
	Fig. IV-4   Particle survival at various energies . . . . .	18
	Fig. IV-5   Particle survival for $\Delta p/p < 2\%$ . . . . .	19
	Table IV-1a Stretcher parameters. . . . .	13
	Table IV-1b Parameters after lattice matching . . . . .	13
	Table IV-1c Components specification. . . . .	13
	Table IV-2   Random multipoles . . . . .	15
	Table IV-3   Parameters for tracking study . . . . .	17
V.	Stretcher Magnet System . . . . .	20
	Fig. V-1   Dipole cross section. . . . .	22
	Fig. V-2   Cell layout . . . . .	23
	Fig. V-3   Quadrupole cross section. . . . .	24
	Table V-1   Stretcher magnet parameters . . . . .	25
	Table V-2   Magnet cost estimate. . . . .	27
	Table V-3   Power supplies cost estimate. . . . .	28
VI.	Stretcher Cryogenic System. . . . .	29
	Table VI-1   Heat loads. . . . .	30
	Table VI-2   Cost estimate . . . . .	31

## Table of Contents (continued)

VII.	Stretcher Vacuum System . . . . .	32
	Fig. VII-1 Layout. . . . .	34
	Table VII-1 Specification . . . . .	33
	Table VII-2 Cost estimate . . . . .	35
VIII.	Stretcher Control and Instrumentation . . . . .	36
IX.	AGS Ejection - Stretcher Injection/Extraction . . . . .	38
	Fig. IX-1 Time sequence of injected bunches into stretcher. . . . .	40
	Fig. IX-2 Transfer line-AGS to stretcher. . . . .	42
	Fig. IX-3 Vertical bend-AGS to stretcher. . . . .	43
	Fig. IX-4 Injection into stretcher. . . . .	45
	Fig. IX-5 Extraction from stretcher . . . . .	47
	Fig. IX-6 Transfer line stretcher to SEB. . . . .	49
	Table IX-1 Examples of repetition periods for synchronous transfer. . . . .	38
	Table IX-2 AGS/Stretcher transfer line components. .	41
	Table IX-3 Stretcher to SEB transfer line components . . . . .	48
	Table IX-4 Magnets and power supplies- cost estimates. . . . .	50
	Table IX-5 RF system physics parameters. . . . .	51
	Table IX-6 RF system cost estimate . . . . .	53
X.	$\bar{p}$ Option. . . . .	54
XI.	Schedule. . . . .	56
	Table XI-1 Schedule S.C. magnet systems. . . . .	57
	Table XI-2 Schedule cryogenics systems . . . . .	58
	Table XI-3 Schedule conventional facilities. . . . .	59
	Table XI-4 Critical item schedule (overall schedule). . . . .	60
XII.	Cost Summary. . . . .	61
	Table XII-1 Cost estimate . . . . .	62

## SUMMARY

A limited study between July and November 1986 was done by the ADD-AGS Committee to determine a location, design, and cost of a superconducting stretcher ring external to the AGS tunnel. A location which allows reasonable transfer lines from the AGS to the stretcher and from the stretcher to the existing slow beam switchyard was found for a 30 GeV proton stretcher ring. Such a ring can be built without interfering with the ongoing AGS program and could be commissioned by extracting one AGS bunch per cycle. Construction time would be three years preceded by about 1-1/2 years of engineering and fabrication of tooling for superconducting magnet construction. The cost (including contingencies) is estimated at \$40.8M in 1986 dollars. The transfer lines were designed to permit the transfer of polarized protons. As outlined in the next section, this is impossible in the present "in-the-ring" stretcher design. In addition, it appears feasible to use this ring as an accumulator of antiprotons and then reinject them into a reversed magnetic field AGS for acceleration/deceleration (25 MeV - 30 GeV) and extraction to the SEB experimental area.

## I. INTRODUCTION

The need and potential for a fixed energy stretcher ring specifically for high extraction efficiency for slow beam and its desirable features were outlined in the Report of the AGS Task Force on the 10-Year Plan in February 1984 and in the AGS Stretcher Study (BNL 37752) in January 1986. The present report is not a detailed design study, but it does show the technical feasibility and gives an "educated guess" cost estimate for a 30 GeV superconducting ring to stretch the 35% AGS duty cycle to  $\sim 100\%$  and which is located outside the AGS ring tunnel.

This report is in response to the memo from E.B. Forsyth and D. Lowenstein dated June 30, 1986, setting up an interdepartmental committee to examine the design, location and cost of a superconductor stretcher ring placed outside the AGS which would provide beams for the SEB program. In the process of considering this charge, we also took into consideration the use of polarized protons in the stretcher and the use of the stretcher as a  $\bar{p}$  accumulator.

When we considered the transfer of polarized protons, we found that special care must be taken in order to preserve polarization. This is accomplished by separating the required vertical bends, which are needed because the stretcher is about 4 meters below the AGS, from the horizontal bends. Although the necessary vertical bends are large, there is no net effect on the spin direction. The horizontal bends do not affect a vertical polarization. Knowing that the "in-the-ring" stretcher design is also at a different height from the AGS (1 meter above), we looked at the effects on polarized protons. In this case, it is necessary to bend horizontally while the beam is being pitched up (transfer to stretcher) and down (transfer from stretcher). The transfers are accomplished over approximately one AGS superperiod, so the intervening horizontal bends are about  $30^\circ$ , with the vertical bend of  $\pm 45$  mrad. At 30 GeV, the precession angle is  $57\times$  the bend angle. Each vertical bend causes a  $142^\circ$  spin precession in the vertical plane, with a  $1700^\circ$  horizontal spin precession in-between. The present "in-the-ring" stretcher design would exclude polarized proton running. The only likely fix would be a redesign to put the stretcher at the AGS level.

Another consideration was the use of the ring as an accumulator for antiprotons. The location of the ring about 4 meters below the AGS makes for a rather simple arrangement for a production target and transfer

lines without any complex shielding. The ring could indeed accumulate antiprotons at 3.5 GeV/c and reinject into the AGS (reversed field) for acceleration/deceleration and extraction. The  $\bar{P}$  flux in this ring would be about 1/3 of what could be obtained using the AGS booster because the aperture is smaller. The stretcher ring magnet coil I.D. is 120 mm and making this larger is not trivial from both the technical and economic sides.

The other considerations leading to the chosen parameters are outlined in the following sections.

## II. SITING AND SIZE

The basic premise for this study was to provide a stretcher with minimal interruption of the SEB program. This implies penetrations only for injection and ejection and the ability to commission the ring in a parasitic mode. It also implies that the area interior to the AGS ring should be avoided since it contains many pipes, cables, conduits, cooling facilities, and the ring magnet power supply. Construction in this area would deleteriously impact the AGS program. A third point to consider is whether to build a new experimental area or locate the ring in such a position that the present SEB is usable. Since the prime directive requires SEB operation not to be interrupted, the construction of a new area would have to duplicate shielding, magnets, power supplies, facilities, etc., as well as a new building. The committee felt that this option was far too expensive and decided to concentrate its efforts on a location where the beam could be fed into the present switchyard. A location which meets the requirements for reasonable injection and transfer lines to the appropriate AGS points, exists between Building 911 and the HITL tunnel and stretches from the AGS ring to slightly past Rutherford Drive.

Initially we started out with a  $1/4$  AGS, but even without straight-sections and with 6T fields, it was very tightly packed and was not feasible. Even an AGS size machine would have inadequate straight section length to achieve an extraction efficiency high enough to prevent superconducting magnets from going normal. These considerations and the real estate led us to a "race-track" machine. The arcs will have  $\sim 1/3$  AGS radius and the two straight sections will have sufficient length to make the effective circumference equal about  $13/24$  AGS. (See Fig. II-1 and Fig. II-2.) The arcs and the extraction transfer line will have superconducting magnets, but the injection transfer line and the straight-sections will have conventional iron magnets, septa, and kickers at room temperature.

Excavation will be necessary for the stretcher outside the AGS tunnel and with the need for shielding a machine with a flux of  $5 \times 10^{13}$  proton per sec, it was decided to place the machine at a lowered elevation consistent with not having water table difficulties. The stretcher floor is put at 60', while the AGS floor is at 70'. Stretcher midplane will be 63' and the AGS midplane is 75'. The top of the berm will be at 91', a distance of 28' from the stretcher midplane and the tunnel will



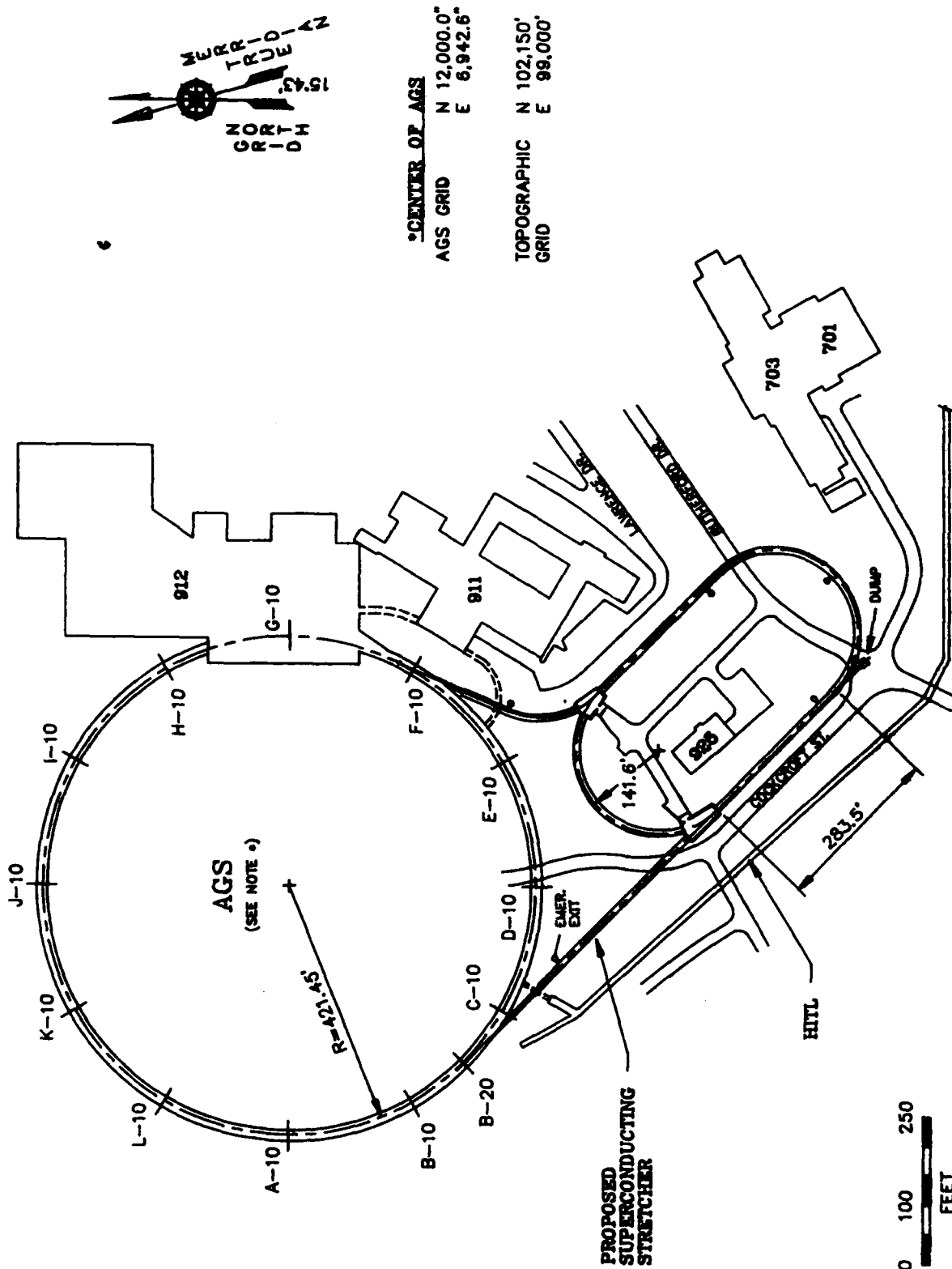


Fig. II-1. Layout of Ring

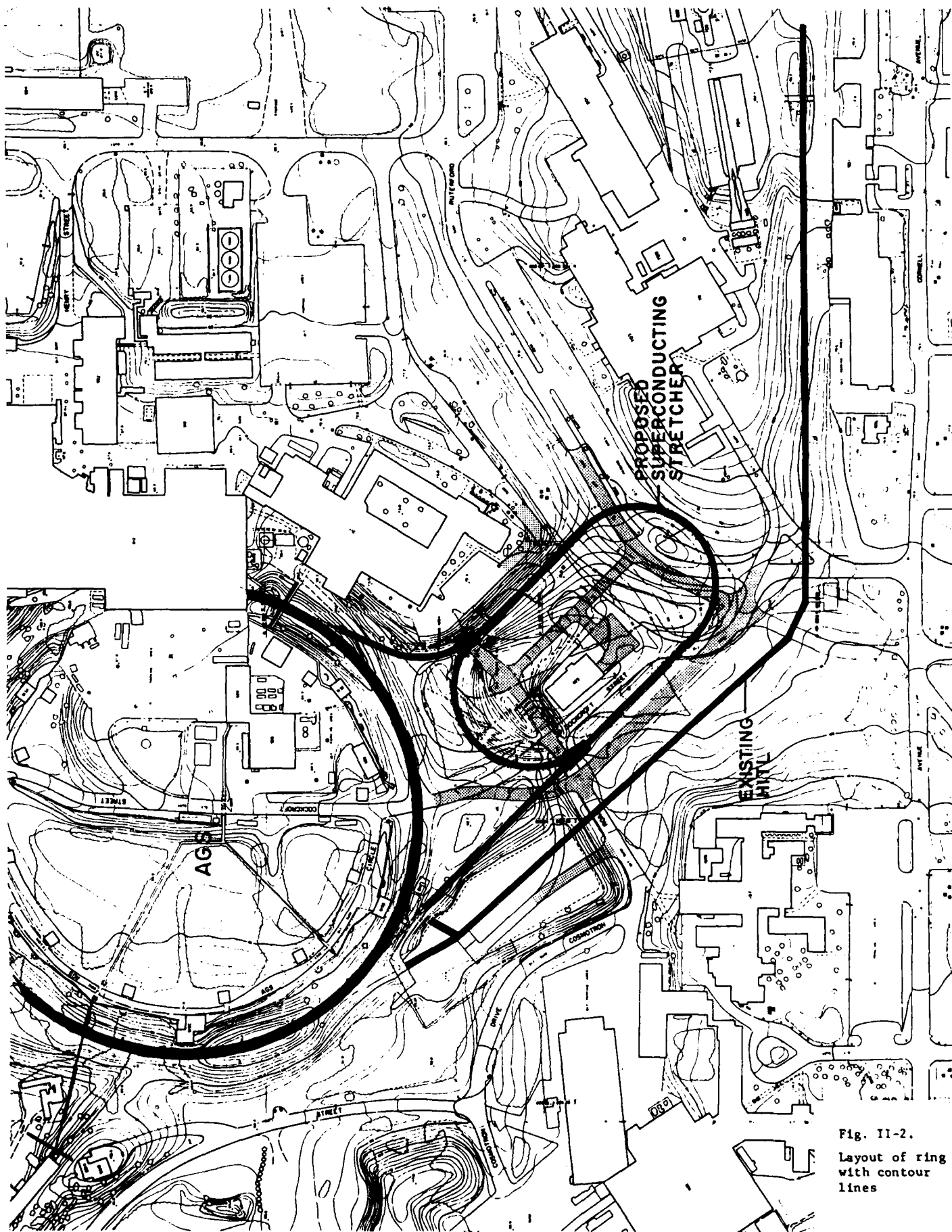


Fig. II-2.  
Layout of ring  
with contour  
lines

be covered with 23' of earth. (See Fig. II-3.) In general, this shielding should lead to radiation levels of the order of 0.5 mrem/Hr at ground level provided losses are kept to reasonable levels (< 1%).

It should be noted that one could not operate at the loss levels of > 1% and that one of the major design goals of this machine is to limit these losses to < 1%. However, the following loss rates were used to calculate doses.

1. Proton Intensity  $6 \times 10^{13}$  protons/sec
2. Losses-a) Injection < 1%
3. Losses-b) Extraction < 5%
4. Losses-c) Arcs < 1% distributed = < 0.1%/magnet

Dose calculation:

$$H(r,d) = 1.5 \times 10^{-14} S E^{0.8} e^{-d/107}/r^2$$

H is in Sv      S = proton flux

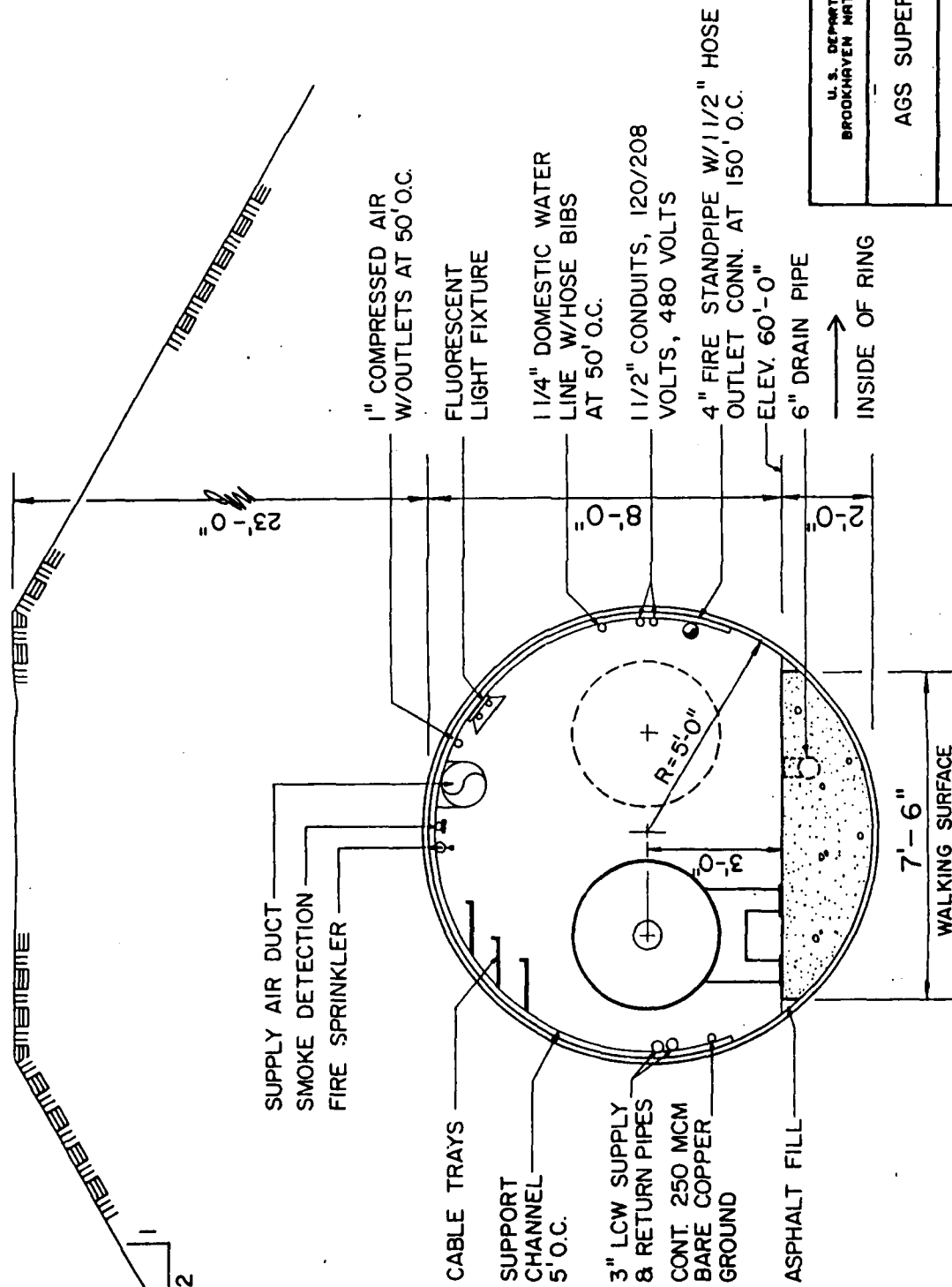
r in meter    d in g/cm<sup>2</sup>

$$D(\text{rem}) = 1.5 \times 10^{-12} \times 6 \times 10^{11} \times 30^{0.8} \times \exp(-\rho r/107)/(r+2)^2$$

$$= 13.6 \exp(-\rho r/107)/(r+3)^2 \text{ for 1\% loss}$$

$$D(\text{rem/hr}) = 4.9 \times 10^7 \exp(-1.68 r)/(r+2)^2$$

$$\text{for 1\% loss, } \rho = 1.8 \text{ gm/cm}^2$$



TUNNEL CROSS SECTION

U. S. DEPARTMENT OF ENERGY BROOKHAVEN NATIONAL LABORATORY
AGS SUPER-STRETCHER
TUNNEL/ENCLOSURE TYPICAL SECTION
MS
Doc. No.

Fig. II-3

Thus the shielding thickness (in meters of sand) for the various parts of the AGS is given by the following table:

TABLE II-1: Radiation Shielding Thickness

	<u>Loss</u>	<u>D(0.5 mrem/hr)</u> <u>meters</u>	<u>D(50 mrem/hr)</u> <u>meters</u>
Transfer lines	0.1%	7	4.5
Injection	1%	8.5	5.5
Extraction	5%	9	6.5
Arcs	0.1%	7	4.5

Twenty-three feet of sand (7 meters) will be in place at all points. Machine design to reduce losses and, if necessary, some concrete could be used to replace sand.

The density of concrete is approximately 2.4 so 0.75 meters of concrete can be substituted for 1 meter of sand.

### III. CONVENTIONAL FACILITIES

The following preliminary cost estimate is based on the present design criteria and using unit costs derived from recent construction contracts on the BNL site, namely using costs from the Heavy Ion Transfer Line, Radiation Effects Facility, and Neutral Particle Beam Test Facility. These cost factors were escalated to 1986 dollars. The plot plans, sections, and beam geometry were used to test the feasibility of such a facility at the proposed location.

The attached budget estimate could vary from 10 to 15 percent, up or down, depending on future refinements to the design parameters. We have estimated the cost of the facility using the same materials and methods as the recent HITL project.

There are two areas within the estimate which impact the cost in an extraordinary way. First the need for a new primary power source requires running a new 13.8 KV 1000 MCM feeder from the main sub-station (B.603) to the facility, a distance of approximately 1/2 mile. In addition, a new 12000 KVA sub-station is needed for the required load.

Secondly, we require the extensive use of steel sheet piling during construction, due to the depth of the tunnel floor (El. 60.0'). This technique is needed due to the present topographical conditions adjacent to the AGS and Service building. The protection of existing utilities in the area also requires heavy sheeting and shoring techniques during construction.

Finally, we have applied the usual engineering (A/E) and contingency factors to the totals. The escalation factor is not applied for any future years. This would be required as our estimates are based on current year costs. A detailed breakdown of the following cost estimate has been made and is available.

**TABLE III-1: Super Stretcher - Cost Summary**  
**Conventional Facilities**

---

---

I.	Improvements to Land	\$ 880K
II.	Earthwork	1,520K
III.	Magnet Tunnel	1,741K
IV.	Mechanical Work	444K
V.	Electrical Work	261K
VI.	Modifications to B-925	105K
VII.	Power Supply Buildings	<u>94K</u>
	Sub-Total	5,045K
VIII.	Engineering @ 15%	757K
IX.	Contingency @ 21%	<u>1,218K</u>
	Total Cost	\$7,020K

---

#### IV. LATTICE AND STRETCHER PROPERTIES

##### A. Parameters

The conceptual design of the superconducting stretcher has a circumference = .553 of the AGS circumference = 446.3 m and an arc length of  $0.339 \times \text{AGS} = 273.48$  m. The two straight sections are each 86.4m long made up of four FODO cells with different cell lengths. The circumference is determined mainly by the RF beam transfer requirements and the arc length by the magnet capability and the site requirement. Since the ring is a race track design, the stretcher will have a superperiodicity of 2. The arc contains twenty-four FODO cells with a cell length of 11.395 meters. Each 1/2 cell has two dipoles with 1.5 m effective length with a field of 4.36 T at  $B_p = 100$  Tm. The maximum  $\beta$ -functions in the arc are 27.5 m and 16.3 m in the Y and X planes respectively. The maximum dispersion function is 1.94 m. Figures IV-1 and IV-3 show the lattice functions for a cell and a superperiod.

The insertion regions have an integral number of cells and the symmetric mid-point has a magnet. These magnets will be room temperature as will be the septa, kickers, etc., needed for injection and extraction. The maximum  $\beta$ -functions in the insertions will be 44.2 m and 45.1 m in the x and y planes respectively. The maximum dispersion is 1.95 m. Each of the four cells has a phase advance of approximately  $90^\circ$ , which makes the insertion look like a unit transformation for the beam. Figure IV-2 shows the lattice functions in the insertion region. The large values of the  $\beta$ -functions result in a more efficient extraction process.

The stretcher parameters are listed in Table IV-1a.



# AGS SUPERCONDUCTING STRETCHER

CELL: MUX=.2396 MUY=.115

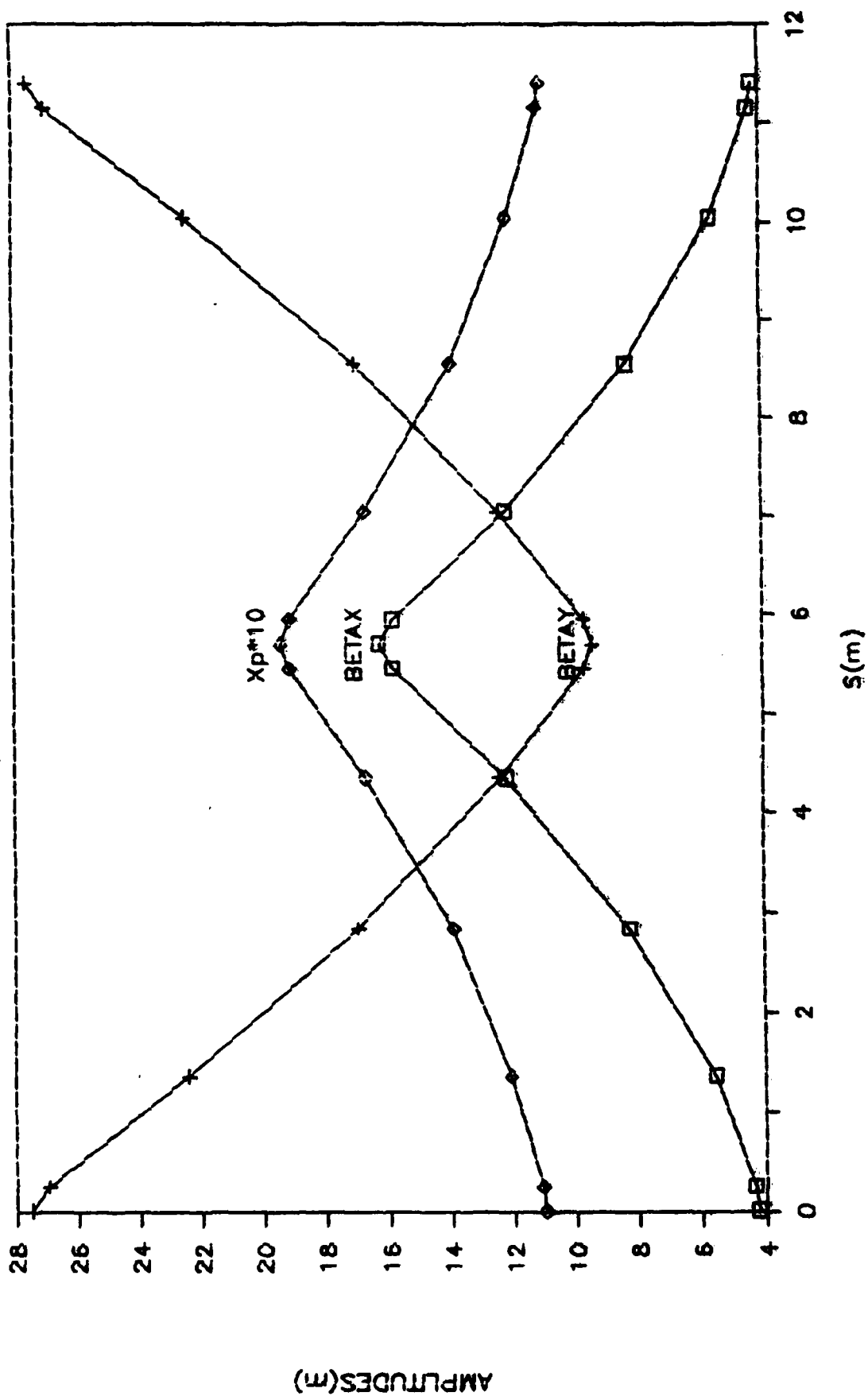


Fig. IV-1. Cell Lattice Functions

## AGS SUPERCONDUCTING STRETCHER

PHASE ADVANCES = 2\*pi/INSERTION

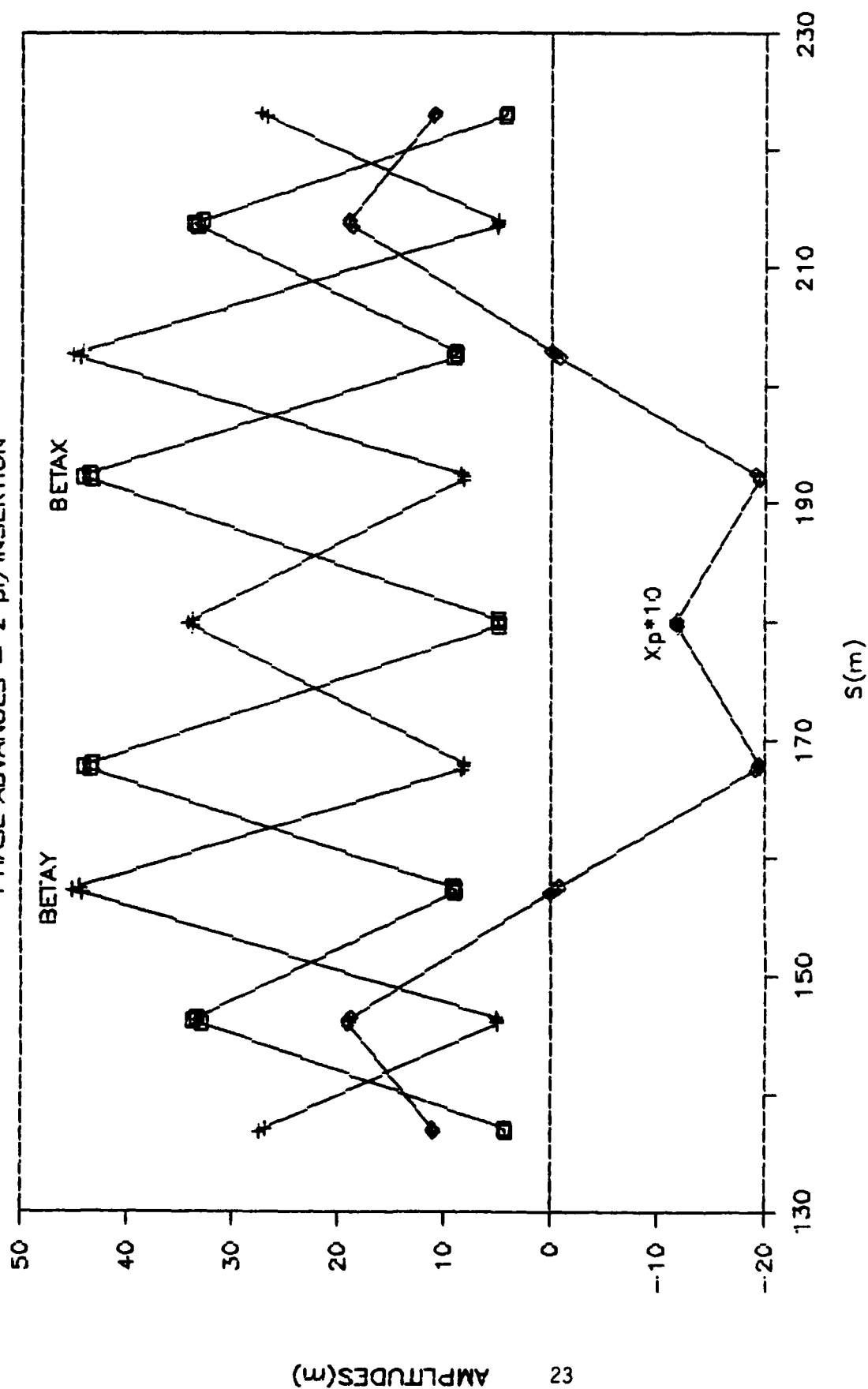


Fig. IV-2. Insertion Region Lattice

# AGS SUPERCONDUCTING STRETCHER

$Q_x=7.75$   $Q_y=4.76$  TWO SUPERPERIODS

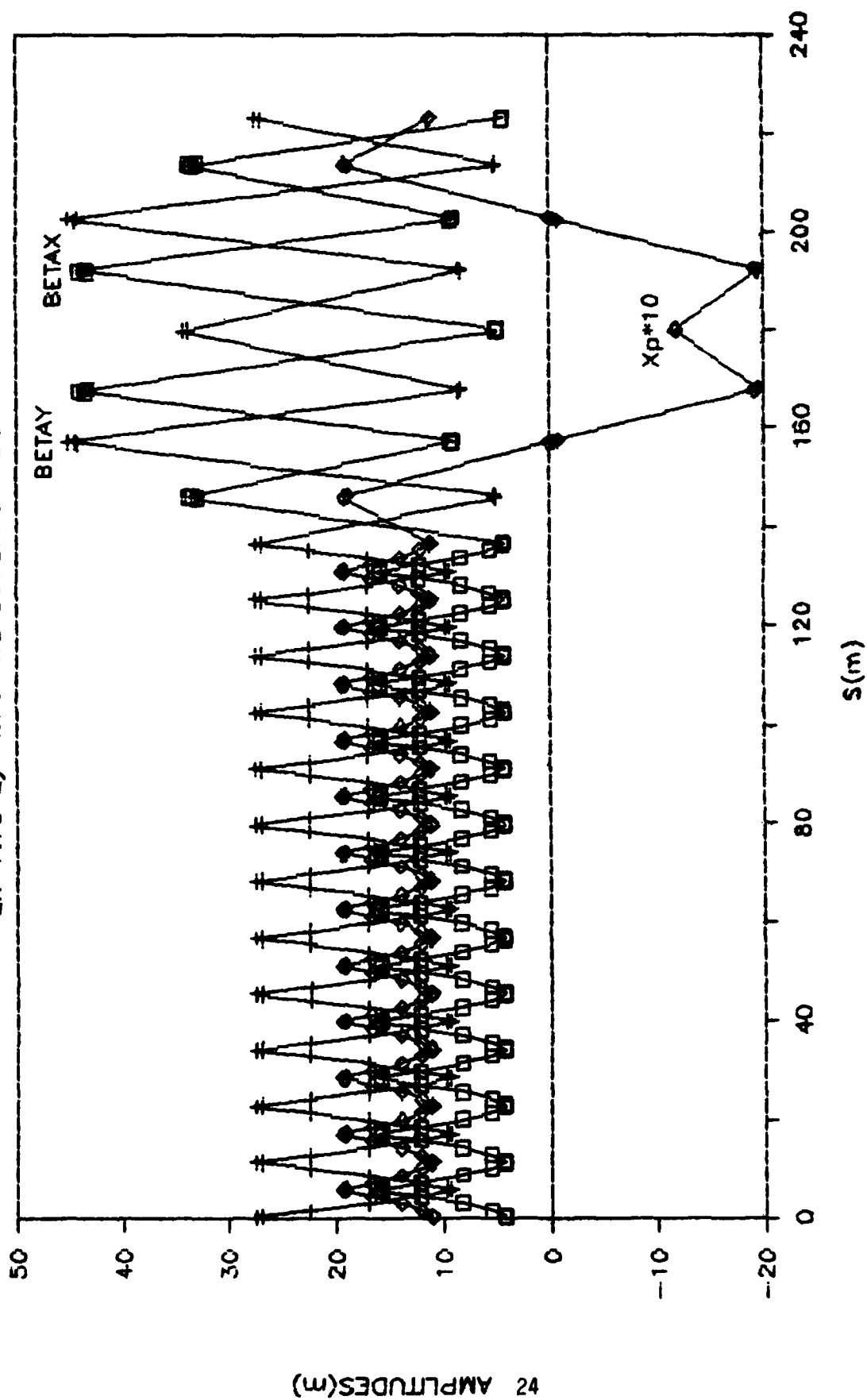


Fig. IV-3. Superperiod Lattice Functions

Table IV-1a: Stretcher Parameters.

Circumference	446.34 m
Arc length	273.48 m
Number of cells	24
Cell length	11.395 m
Number of dipoles	96
Length of dipoles	1.5 m
Bending angle (degrees)/dipole	3.75
Sagitta	12.27 mm
Bend radius	22.922 m
Dipole B @ 100 Tm	4.363 T
Number of quadrupoles	48
BY (max)	27.5 m
BX (max)	16.3 m
Xp (max)	1.94
Insertion length	86.429 m
Number of cells	4
BY (max)	44.17 m
BY (max)	45.12 m
Xp (max)	1.95 m

TABLE IV-1b: Parameters after lattice function matching.

Tune	
QX	7.75
Qy	4.76
$\mu_X$ (phase advance/cell)	$0.2396 \cdot 2\pi$
$\mu_Y$ (phase advance/cell)	$0.115 \cdot 2\pi$
X phase advance/insertion	$1 \cdot 2\pi$
Y phase advance/insertion	$1 \cdot 2\pi$
$\gamma_T$	7.11
Chromaticity	
Cx	-8
Cy	-7.2
Tune vs Amplitude	
Axx	-2.2
Axy	166
Ayy	-72.9

TABLE IV-1c: Integrated Strength of Components

QF	0.2278 1/m
QD	-0.1614 1/m
Q4	0.1402 1/m
Q3	-0.1336 1/m
Q2	0.1278 1/m
Q1	-0.1104 1/m
SF	0.1769 1/m <sup>2</sup>
SD	-0.2368 1/m <sup>2</sup>

The emittance of the AGS booster at high intensity operation is expected to be  $50 \pi \text{ mm-mrad}$  at 200 MeV injection energy. The normalized emittance would be  $34 \pi \text{ mm-mrad}$ . Therefore, the emittance at 30 GeV would be  $1.1 \pi \text{ mm-mrad}$ . Allowing an increase of 3 in the emittance, we would expect a maximum emittance of  $3.3 \pi \text{ mm-mrad}$ . The emittance is likely to decrease when the transition jump across the transition energy in the AGS is added. In the following estimate of the beam size, we shall assume the emittance of  $3.3 \pi \text{ mm-mrad}$ . The momentum aperture is expected to be less than 0.2%.

$$\begin{aligned}\text{Emittance} &= 3.3 \pi \text{ mm-mrad} \\ 6\sigma_Y &= 24.7 \text{ mm} \\ 6\sigma_X &= 18.2 + 10 = 28.2 \text{ mm}\end{aligned}$$

Since the sagitta of the dipole is 12.3 mm, the beam size ( $6\sigma$ ) is expected to be 68.7 mm. The tracking results of RHIC, SSC, and Fermilab, indicate that 60% of the coil i.d. can be considered as linear aperture for a large size magnet. We therefore require a dipole magnet with a minimum coil i.d. of 115 mm.

If we choose to have an integral number of cells for the insertion region, the symmetric midpoint of the insertion must have a magnet. It would be nice to have the insertion work like a unit transformation for the beam particles from arc to arc. We therefore look for a phase advance of integer  $\times 2\pi$ . The task can be accomplished by the four cells; each has a phase advance of approximately  $90^\circ$ . Table IV-1b lists parameters after the lattice function matching.

The machine operates around  $Q_x = 7.75$  and  $Q_y = 4.76$  in a tune space without half-integer and third-integral resonances. The natural chromaticity is  $C_x = -8.0$  and  $C_y = -7.2$ . Since the momentum amplitude at this energy may not be very large, a chromatic correction may not be needed at all. The important chromatic effect may come from the systematic sextupole field from the superconducting magnets. This effect could be corrected, however, by two families of sextupoles in the arc. The unit transfer matrix in the insertion then has the merit that the arc behaves like a machine with 24 superperiods and Table IV-1c lists the quadrupole components and the sextupole requirements.

To facilitate resonance slow spill, extraction sextupoles will be placed in the insertion region. The strength will be discussed in the extraction scheme.

## B. Preliminary Tracking Study

Tracking studies have been made on this preliminary lattice. The purpose of the tracking study is to determine whether such a stretcher, using superconducting dipoles, can be expected to work at its nominal energy of 30 GeV and whether any compromises of operation are necessary at other energies.

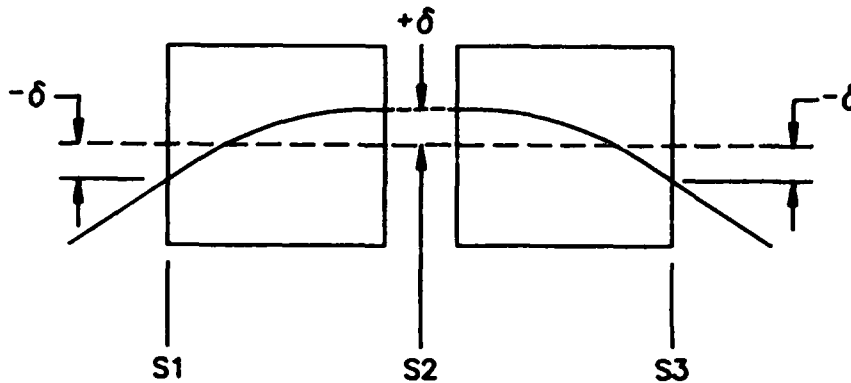
The following assumptions are made for the tracking study:

1. Insertion quadrupoles have conventional iron construction and have negligible random multipole coefficients.
2. Arc quadrupoles are superconducting, have an ID 10.4 cm and random multipole coefficients that scale from RHIC quadrupoles
3. Arc dipoles are superconducting, have a coil ID of 12 cm, and have random multipole coefficients that scale from RHIC dipoles as  $B_n(S) = (r(R)/r(S))^{n+1/2} b_n(R)$ , where R and S denote RHIC and the Stretcher.
4. Dipoles can be designed to have nearly zero systematic multipoles at one chosen excitation; this is assumed to be true at 30 GeV.
5. Random multipoles are assumed to arise from construction tolerances and are thus independent of momentum. A table of the random multipoles follows.

TABLE IV-2.

DIPOLE		DIPOLE	QUADRUPOLE
n	$\sigma b_n(m^{-n})$	$\sigma a_n(m^{-n})$	$\sigma b_n(m^{-n}) - \sigma a_n(m^{-n})$
1	4.63E-3	0.0	1.40E-2
2	2.70E-1	7.60E-2	4.00E-1
3	1.90E+0	3.40E+0	.78E+1
4	9.00E+1	2.40E+1	1.76E+2
5	5.80E+2	1.00E+3	.39E+4
6	2.43E+4	6.81E+3	.27E+5
7	1.43E+5	2.68E+5	1.78E+6
8	5.83E+6	1.76E+6	.377E+8
9	3.40E+7	6.39E+7	.76E+9
10	1.38E+9	4.25E+8	.16E+11
11	7.80E+9	1.54E+10	

6. Half cells are 5.7 m long and contain two 1.5 m long dipoles having bending radii of 22.918 m.
7. The effects of individual multipoles are manifested as a kick  $r'$ :  $r' = \Delta B_n l / B_0 \rho = \sum c_n r^n l / \rho$  with  $c_n = b_n + i a_n$  and  $r = x + i y$ .
8. The effect of the 1.2 cm sagitta in the dipoles is an extra displacement  $\delta$  of the particle from the magnet axis. Each dipole is split into two sections and has a kick at the center as well as at each end. The geometry is shown below:



Kick at s1 and s3:  $r' = \sum c_n (r_1 - \delta)^n l / 4\rho$  with  $i=1$  or  $3$  and  
 Kick at s2:  $r' = \sum c_n (r_2 + \delta)^n l / 2\rho$  with  $\delta = \pm 6.1$  mm.

9. a) The normalized emittance from the AGS is estimated as  $68\pi$  mm mrad using a two-fold growth factor during the AGS acceleration cycle.
- b) The emittance at 30 GeV is  $\approx 2\pi$  mm mrad.

Tracking has been done for 1000 turns at various emittances, and the results are plotted on Fig. IV-4. The plot can be interpreted as a measure of the survival of a test particle at any energy as its emittance is increased, or it can be interpreted as a measure of the survival at various energies for a normalized emittance of  $68\pi$  mm mrad.

There seems to be no difficulty with particles having  $\epsilon_n = 68\pi$  mm mrad for energies  $2 < E < 30$  GeV.

Runs have also been made up to  $\Delta P/P = \pm 2.0\%$  and have given almost identical results. (See Fig. IV-5.) As the momentum spread at 30 GeV is expected to be  $\sim \pm 0.2\%$ , the tracking study indicates no difficulty with 30 GeV operation.

For  $\bar{p}$  operation, the momentum spread acceptance is  $\pm 1\%$  with an emittance of  $40\pi$ . This is about 1/3 of the acceptance of the proposed AGS Booster for use in this mode.

The following values of the parameters (Table IV-3) for the lattice were used in this study. They are slightly different than those listed in Table IV-1.

TABLE IV-3.

---

---

Arc Quads: QF  $\beta_x = 16.136$  m,  $\beta_y = 9.313$  m

QD  $\beta_x = 4.195$  m,  $\beta_y = 27.264$  m

$X_p = 1.95$  m,

$\nu_x = 7.82175$ ,

$\nu_y = 4.82615$ ,

$CH_x$  (natural) = -8.413,

$CH_y$  (natural) = -7.402

SF = -0.1877 m<sup>-2</sup>

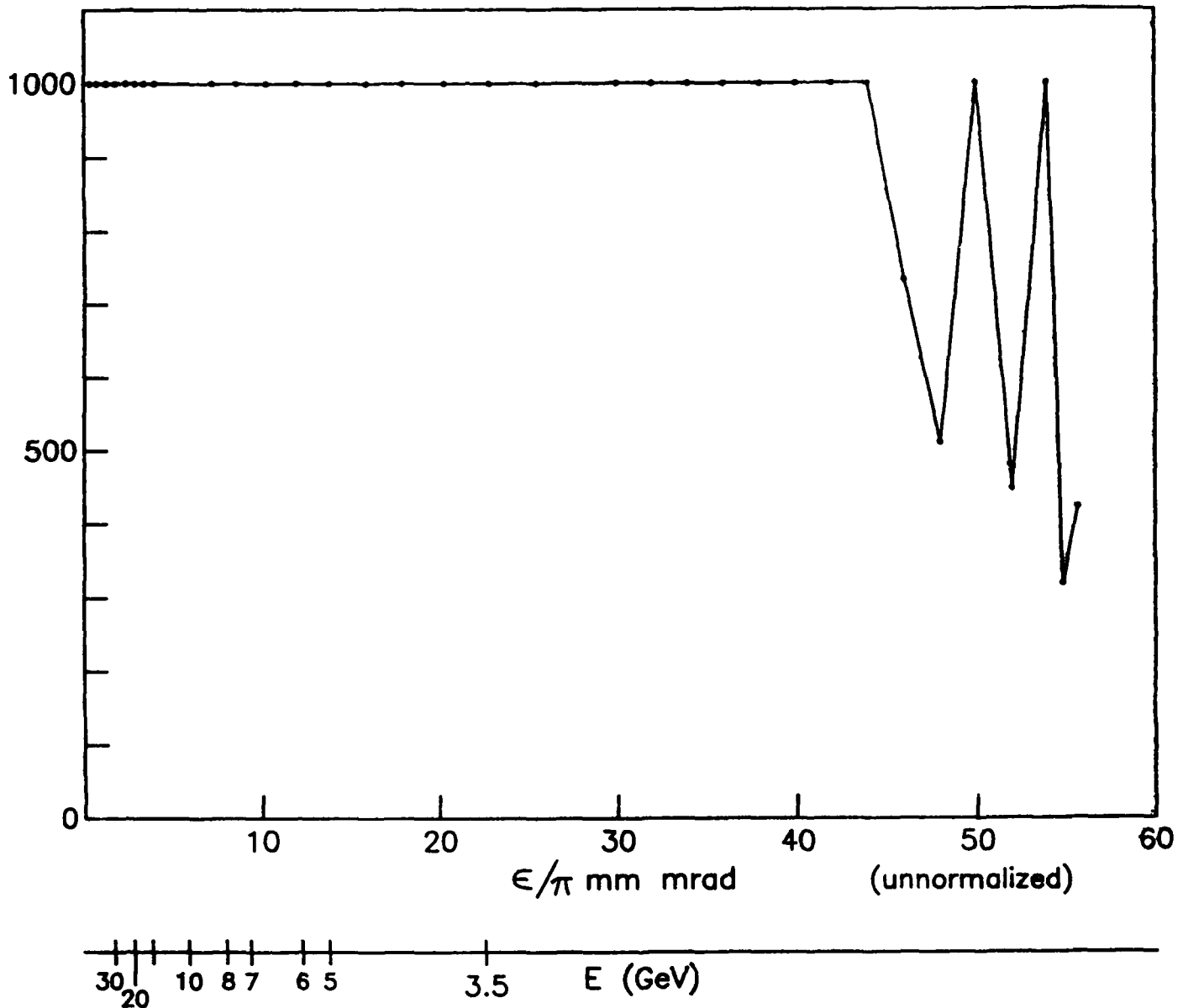
SD = 0.2478 m<sup>-2</sup>

Integrated sextupole strength  
for zero chromaticity

---



$$\Delta p/p = 0$$



Dependence of the survival of a test particle on its initial emittance. Launching conditions:  $\epsilon_x = \epsilon_y$  and  $x' = y' = 0$ . The plot can also be used with the energy scale on the abscissa to determine the survival of a test particle with  $\epsilon_n = 68\pi$  mm mrad at various energies. The low energy tracking does not include magnet field quality deterioration below about 2 GeV.

Fig. IV-4 Particle Survival at Various Energies.

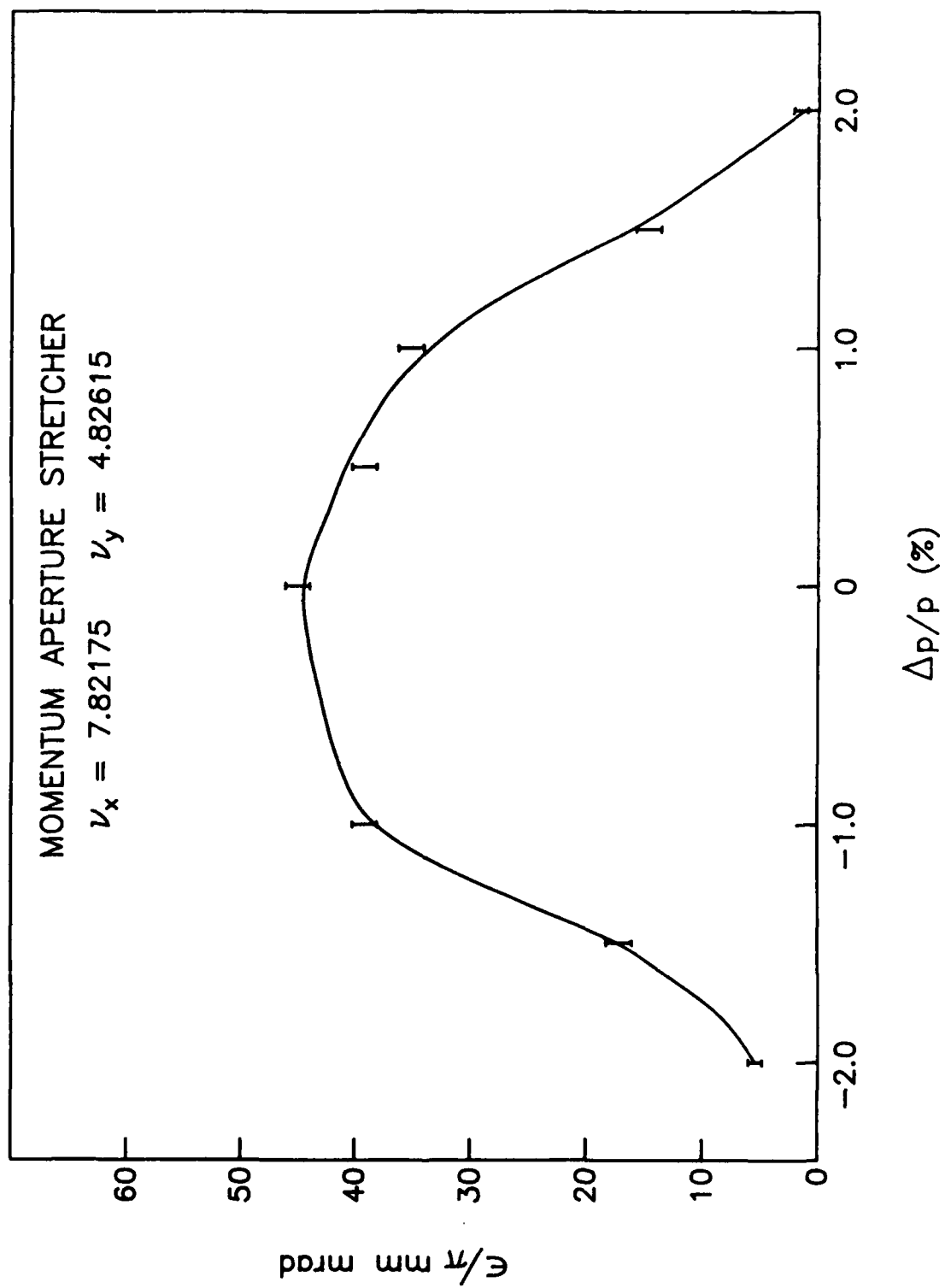


Fig. IV-5. Particle survival for  $\Delta p/p = \pm 2\%$ .

## V. STRETCHER MAGNET SYSTEMS

There are 24 cells with 2 dipoles/half cell for a total of 96 dipoles and 48 quadrupoles in the two superconducting arcs. There are 7 room temperature quadrupoles in each insertion to give the total circumference 32 cells. In addition, there will be 48 0.1 m sextupoles and 48 correctors.

The basic power supply will be a 50V, 6500 Amp supply with regulation of the order of 3 parts per  $10^5$  for the arcs and of 3 parts per  $10^4$  for the 70° bend and the superconducting vertical bending magnets in the extraction line.

The basic parameters of the magnets for the Stretcher are listed in Table V-1. The dipoles field strength of 4.36 Tesla was chosen to have arcs approximately 1/3 of the AGS. The magnets should be economical to construct and rely as much as possible on existing superconducting magnet technology in order to minimize R&D requirements. The dipole field strength level can be obtained with single layer coil cosine  $\theta$  magnets. Such a design has been proposed for the magnets for RHIC; in the case of the AGS Stretcher, the aperture of the magnets would be scaled up from 8 cm to 12.6 cm. The length of the magnets have been selected on the basis of a cost trade-off between aperture and length of individual magnets. Since the radius of the arcs is only about 23 meters, it appeared that the optimum dipole length would be about 1.5 meters for a relatively small sagitta. It has also been assumed that the operating field of 4.36 Tesla can be reliably obtained with a single layer coil based on presently obtainable high current density, fine filament, niobium-titanium superconductor.

The dipole cross section is shown in Fig. V-1. The superconductor cable is the same as that used for the RHIC magnets with 52 turns per coil. The coils are insulated with injection molded phenolic-glass composite and held in compression by the welded yoke halves. The coil mass which consists of the coil-yoke assembly in its helium containment shell is supported on folded post supports which have been developed and tested at FNAL for the SSC magnets. Since the individual components are rather short, it would be uneconomical for each to have its own cryostat. Thus, the elements that make up one complete cell are mounted in a single cryostat about 11.4 meters long. The arrangement of the elements in the cell cryostat is shown in Fig. V-2. Each element is joined to its neighbor by a transition section in the helium containment shell so that only one of the complex and expensive expansion assemblies to take care of thermal contraction of the bus work and magnets is required per cell.

The quadrupole, which is shown in cross section in Fig. V-3, is also a scaled-up version of the corresponding RHIC magnets. It uses the same superconducting cable and cold mass construction as the RHIC quadrupoles. However, the magnets are much shorter being only .46 and .33 meter effective length for the horizontal and vertical quadrupoles. Sextupole and dipole correction elements are also provided in each cell. These correctors are based on the proposed RHIC correctors which are wound with monolithic superconductor of about 1 mm diameter. These correctors are incorporated into the ends of the quadrupole.

Table V-2 and V-3 give the cost estimates for the magnet system and for the power supplies.

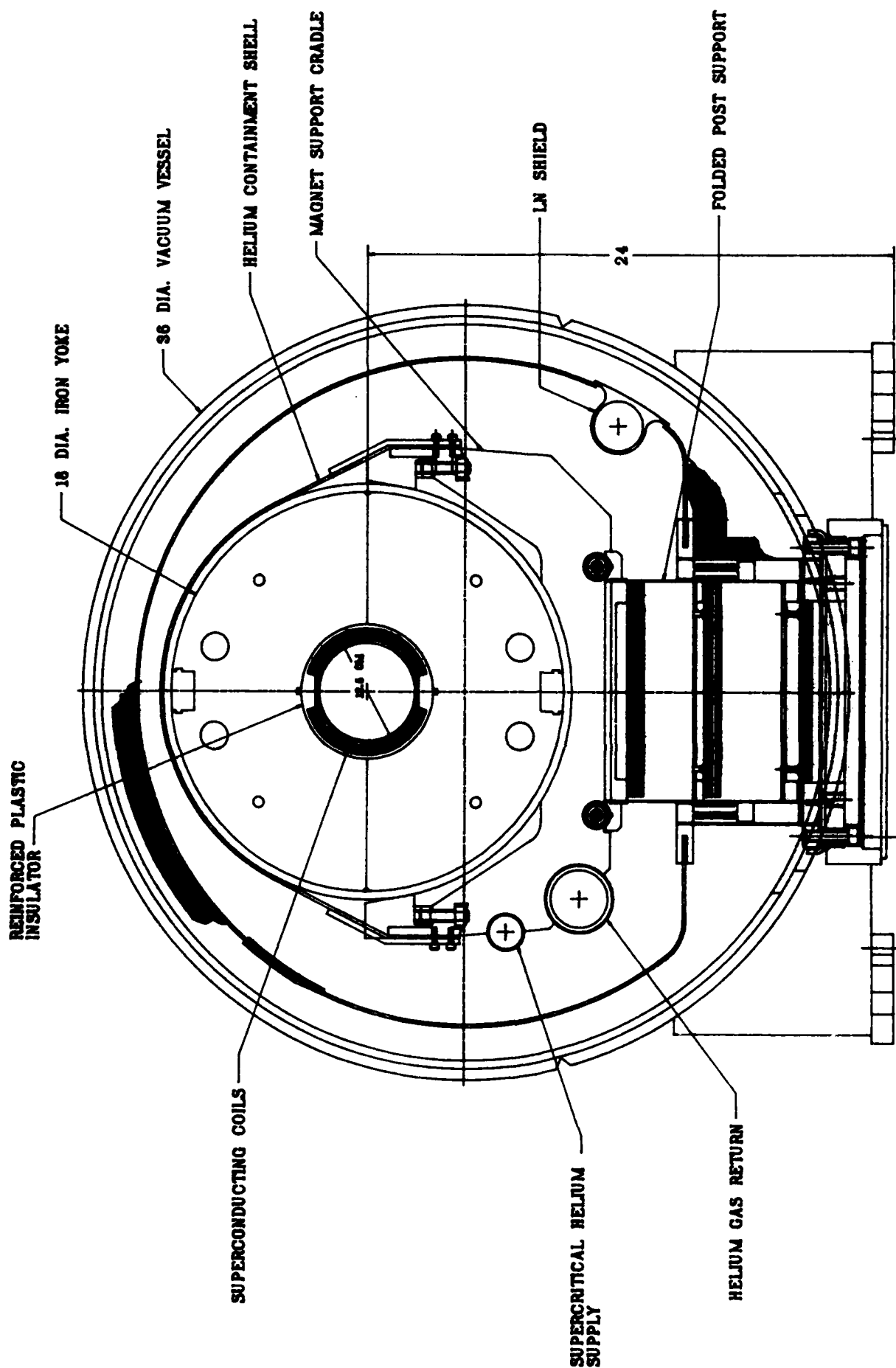
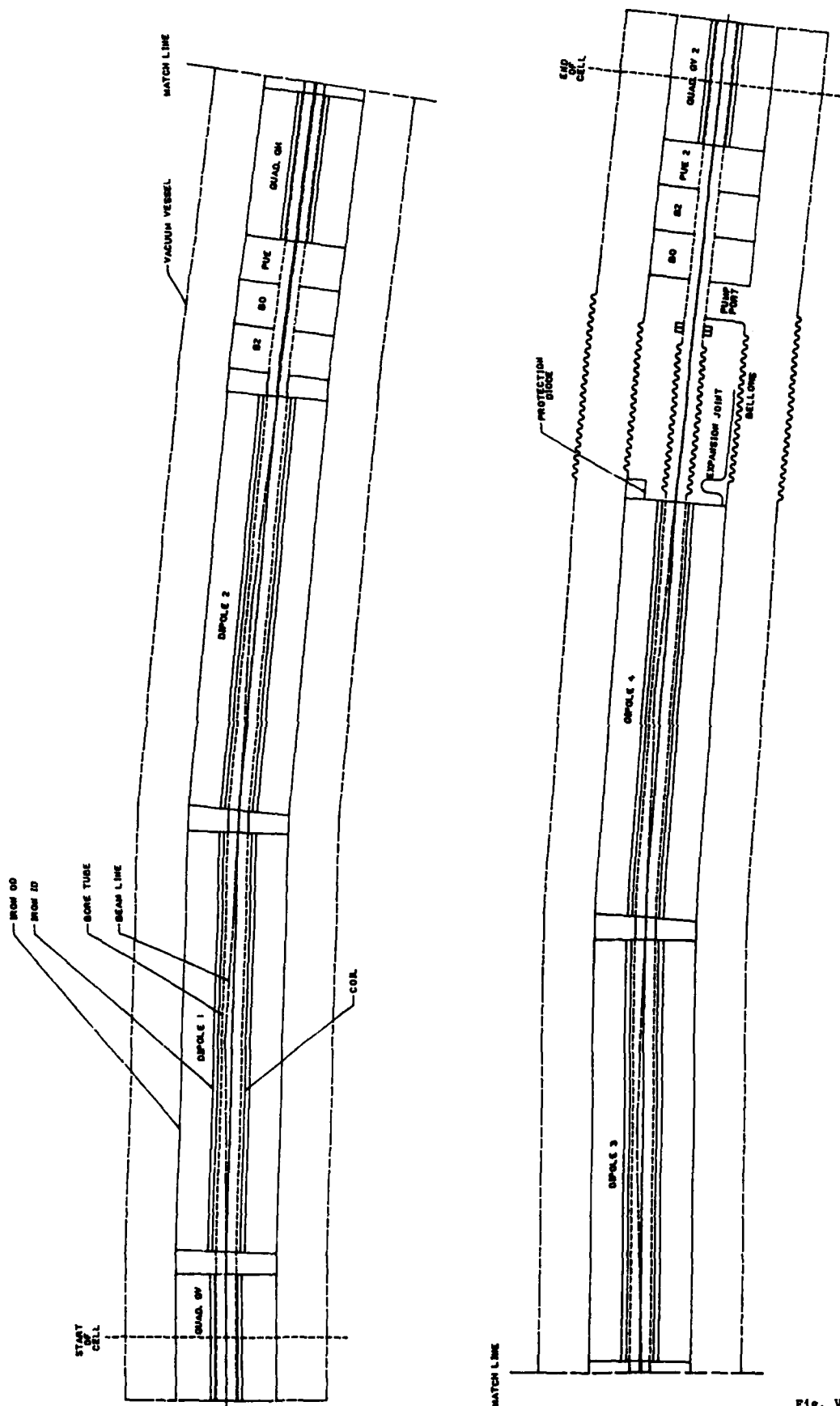


Fig. V-1

CROSS SECTION  
SUPERCONDUCTING AGS STRETCHER DIPOLE



AGS STRETCHER  
CELL LAYOUT

Fig. V-2

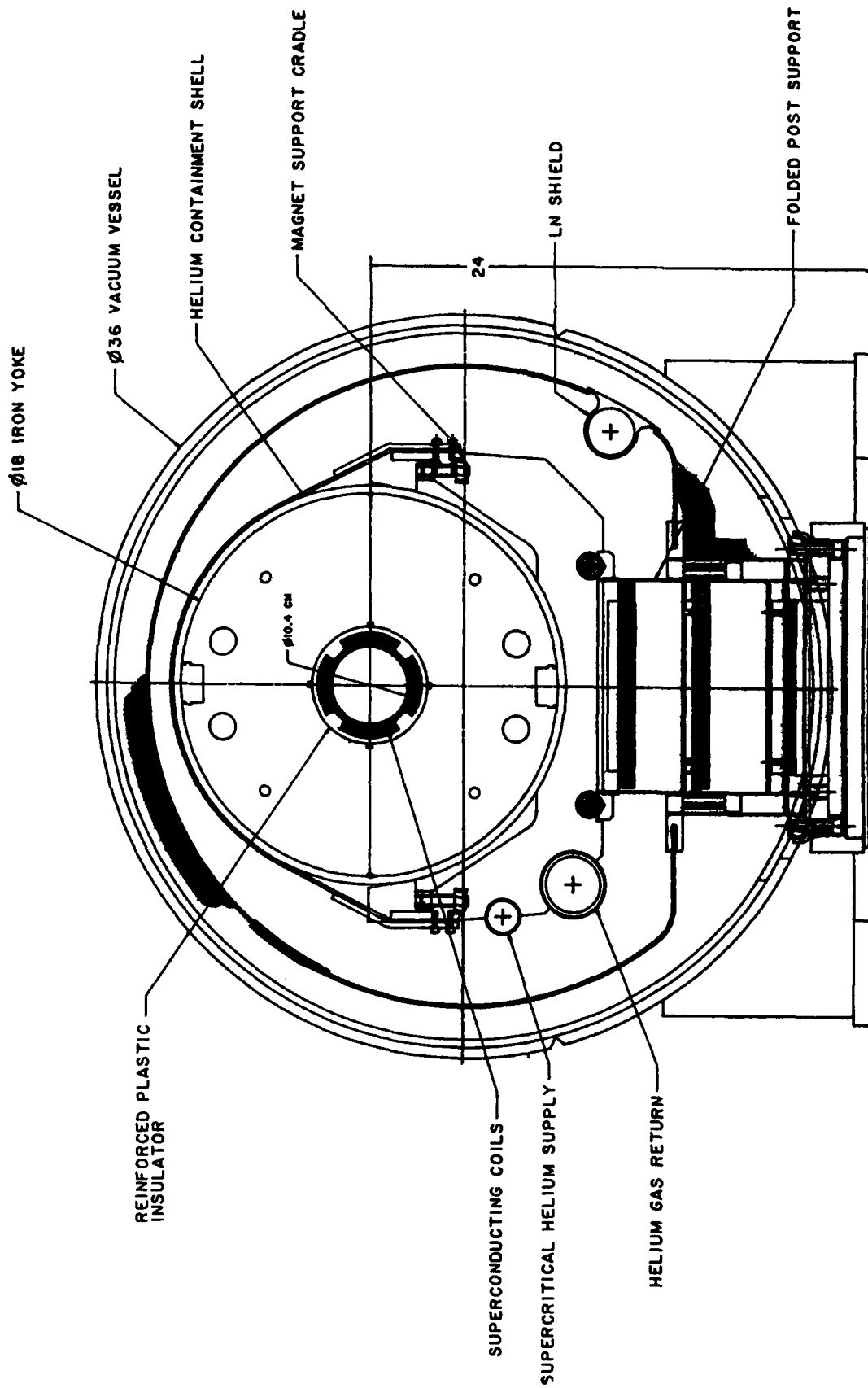


Fig. V-3

# CROSS SECTION SUPERCONDUCTING AGS STRETCHER QUADRUPOLE

**TABLE V-1: Superconducting AGS Stretcher Magnet Parameter Table**

**DIPOLLES:**

Number	96
Central field	4.36 Tesla
Operating current	5800 A
Quench current	6400 A
Magnetic length	1.5 meter
Inner diameter, coil	12.5 cm
Inner diameter, iron	16.5 cm
Outer diameter, iron	45.0 cm
Iron volume	.21 M <sup>3</sup>
Iron mass	1.6 Ton
Superconductor	RHIC cable
Turns/coil	52
Strands/cable	30
Strand diameter	.648 mm
Copper/superconductor	1.8
JC, strand @ 4.2K and 5T	2700 A/sq. mm
Cable width (bare)	9.73 mm
Cable mid-thickness (bare)	1.166 mm
Keystone angle	1°
Cable length	380 M

**QUADRUPOLES:**

Number, horizontal	24
Number, vertical	24
Gradient	50 Tesla/meter
Magnetic length (H)	.46 meter
Magnetic length (V)	.33 meter
Inner diameter, coil	10.4 cm
Inner diameter, iron	14.0 cm
Outer diameter, iron	45.0 cm
Iron volume	0.1 M <sup>3</sup>
Iron mass	0.6 Ton
Superconductor	Same as for dipole
Number of turns/coil	22
Cable length (H/V)	150/140 M

**SEXTUPOLES AND CORRECTORS:**

Number of each	48
Magnetic length	.1 M
Inner diameter, coil	10.4 cm
Inner diameter, iron	12.0 cm
Outer diameter, iron	20.0 cm
Superconductor	1 mm dia. wire
Turns/coil (sextupole)	100
Turns/coil (dipole)	600
Iron mass	37 kg



The bore tube parameters are as follows:

TABLE V-1. (Continued)  
Stretcher Magnet Parameters

---

BORE TUBE	
I.D.	90 mm
Wall	4 mm
Bend Radius	22.94 meter
HELIUM VESSEL	
I.D.	450 mm
VACUUM VESSEL	
O.D.	36 inches

---

TABLE V-2. Cost Estimate for Stretcher Magnet System

<b>Main Magnet System:</b>				
Number of cells	24			
Dipoles/cell	4			
Quadrupoles/cell	2			
Sextupoles/cell	2			
Correctors/cell	2			
Slot length/cell (m)	11.395			
Total cell length (m)	273.48			
Total dipoles	96			
Total quadrupoles	48			
Total sextupoles	48			
Total correctors	48			
Spool pieces	4			
<hr/>				
<b>Unit Costs:</b>	<b>Materials</b>	<b>Labor</b>	<b>Total</b>	<b>Hours</b>
Dipole ea.	\$ 12,169	\$ 2,988	\$ 15,157	103
Long quadrupole ea.	5,402	3,161	8,562	125
Short quadrupole ea.	4,696	3,106	7,802	122
Sextupoles, ea.	1,024	1,812	2,836	60
Correctors, ea.	1,024	1,812	2,836	60
Cell cryostat, ea.	18,976	11,016	29,992	403
Cell cryogenic test ea.	600	3,224	3,824	118
Cell interconnections ea.	3,780	1,171	4,951	39
<hr/>				
Sub-total/cell	\$ 86,226	\$ 28,926	\$115,152	1,457
Shop support @ 25%		7,231	7,231	364
<hr/>				
Cell, ea.	\$ 86,226	\$ 36,157	\$122,383	1,821
Spool pieces, ea.	25,000		25,000	
70° bend transfer line	430,224	180,405	610,628	9,085
2 vertical bend magnets	47,694	21,386	69,081	765
14 insertion quads N4Q36	658,000	142,000	800,000	3,520
<hr/>				
<b>Total Cost Summary</b>				
Main magnet system	\$2,169,431	\$ 867,771	\$3,037,203	25 man-years
Transfer line magnets	477,918	201,791	679,709	5 man-years
Magnet tooling	875,000		875,000	5 man-years
Installation and survey	13,000	102,000	115,000	2 man-years
(14) N4Q36	658,000	142,000	800,000	2 man-years
<hr/>				
Sub-total	\$4,293,349	\$1,313,562	\$5,506,912	40 man-years
Magnet EDIA@30%(excl.N4Q36)		352,469	352,469	11 man-years
<hr/>				
Sub-total	\$4,293,349	\$1,666,031	\$5,959,381	51 man-years
Contingency @ 20%			\$1,191,876	10 man-years
<hr/>				
Total			\$7,151,257	61 man-years

TABLE V-3. Stretcher Magnet Systems Power Supplies

COST ESTIMATE					
<u>Item</u>	<u>Voltage</u>	<u>Current</u>	<u>Quantity</u>	<u>Cost/Unit</u>	<u>Total Cost</u>
Dipole P.S.	50	6,500	1	\$ 110,000	\$110,000
Quadrupole P.S.	50	6,500	1	110,000	110,000
Quadrupole Bypass P.S.	50	1,000	1	18,000	18,000
Sextupole, 2 families	25	300	2	30,000	60,000
Corrector, a0, b0	10	150	80	2,250	180,000
Special, a0, b0	10	150	16	3,750	60,000
Corrector, a1, b1	10	300	4	7,500	30,000
Quench Protection					72,000
Dump Resistor					10,000
Cable Trays					250,000
Insertion Quadrupoles	30	2,400	14	18,000	252,000
Vertical Bending Magnets	50	6,500	1	85,000	85,000
70° Bending P.S.	50	6,500	1	85,000	85,000
-----					
Engineering and Installation:					\$1,322,000
		<u>Man-Years</u>	<u>Total Cost</u>		
Engineering		3	\$ 153,000		
Technician		6	282,000		
Electrician		2	94,000		
-----					
Total Labor			\$ 529,000		
Total Materials			1,322,000		
Material + Labor			1,851,000		
Contengency @ 20%			370,200		
Total System			2,221,200		

## VI. STRETCHER CRYOGENIC SYSTEM

The refrigerator and compressors for the Superconducting Stretcher will be housed in the area interior to the stretcher ring in (existing) Building 925. Electric power for the compressors and other cryogenic equipment will be supplied from a substation located near this building.

The present estimate of the refrigeration load is about 1.5 kW and a refrigerator of 3 kW capacity is chosen for the basis of the cost estimate. It is expected that the load will grow somewhat as the design progresses and that the final design refrigeration margin will decrease from the present factor of 2.0 to a final value of about 1.5. In order to make the cost more realistic now, a higher refrigerator capacity is chosen to approximate more nearly the final capacity expected.

The refrigerator will be installed over a pit so that the vacuum tank can be lowered to expose the internals of the cold box for servicing. A cold helium circulating compressor and a cold vacuum pump will be used to obtain the correct flow and temperature conditions for the magnets in the ring. They may be physically located in the refrigerator, but are estimated separately because they were not included in the refrigerator cost estimate. Oil-injected screw compressors will circulate the gas through the system. They will require about 1 MW of power. Helium buffer tanks will provide local storage for the helium gas working inventory. Much of the helium inventory will be stored as liquid in the 10,000 liter liquid storage dewar when the machine is warm. If it is desired, or necessary, the entire inventory could be transferred to the gas storage area at Building 919. Allowance for installation of the refrigerator pit and the pads for the compressors and the liquid dewar has been made in the cost estimate.

A process control computer system is provided to perform data logging and control functions for the entire cryogenic system. A dual cryogenic (80 K) helium purifier is provided to remove impurities from the make-up gas before it is introduced to the system. Special heat exchangers and heaters will be required to facilitate cool down and warm-up of the magnets. Vacuum-jacketed piping will be used to transport the cryogens from the refrigerator to the magnets and back.

TABLE VI-1

AGS SUPERCONDUCTING STRETCHER HEAT LOAD ALLOWANCE  
(S.C. ARCS + CONV. STRAIGHTS)

	<u>4K</u> <u>Liquid</u> <u>g/s</u>	<u>4K</u> <u>Refrigerator</u> <u>W</u>	<u>80K</u> <u>Refrigerator</u> <u>W</u>
<u>Ring Magnet Syste:</u>			
Dipole, 1.5 m (96 @ 4W + 25W)	.0	384	2400
Quad, .5 m (48 @ 3W + 20W)	.0	144	960
Feedcan(2 @ 5W + 50W)	.0	10	100
End Box (2 @ 5W + 50W)	.0	10	100
Power Leads, 6.5kA(8 @.4g/s + 8W)	3.2	54	0
Power Lead Bundle 12x100A (10)	1.0	20	0
Piping and Valves	.0	20	100
<u>Total For Ring Magnets</u>	4.2	652	3660
<u>Extraction Magnet System:</u>			
Dipole, 1.5 m (26 @ 4W + 25W)	.0	104	650
Quad., .5 m (12 <sup>2</sup> 3W + 20W)	.0	36	240
Feedcan (1 @ 5W + 50W)	.0	5	50
End Box (1)	.0	5	50
Power Leads, 6.5A(2 @.4g/s + 8W)	.8	16	0
Power Lead Bundle, 12x100A (1)	.1	2	0
Piping and Valves	.0	10	50
<u>Total for Extraction Magnets</u>	.9	178	1040
<u>Auxilliary Systems:</u>			
Piping and Valves	.0	50	0
Liquid Helium Storage Dewar	.1	0	0
Cryogenic Purifier (25 g/s He)	.0	0	200
4K Transfer Lines	.0	30	0
80K Transfer Lines	.0	0	25
<u>Total for Auxilliary Systems</u>	.1	80	225
GRAND TOTAL — ALL SYTEMS	5.2	910	4925
Approx. liters/hour equivalent	<u>156.0</u>	<u>      </u>	<u>109</u>

TABLE VI-2: Estimated Cost for Stretcher Cryogenic System

System parameters for estimating purposes

Load = 918W @ 4.5K + 5.2 g/s lead flow = 1500 W equivalent refig.

Refrigerator capacity: 3000W @ 4.5K

Power input to cryogenic compressors: 1 MW

Forced flow cooling to magnets @ 4.5 ATM

Warmest magnet @ 4.5 K

System cold volume: 182 magnets @ 50 liters = 9100 liters

Estimated Cost:

Item No.	Description	Cost in K\$			Labor	
		Materials	Labor	Total	S & P	Other
1	3 kW helium refrigerator with compressors	2000	0	2000	.0	.0
2	Installation of refig. & compressors	500	0	500	.0	.0
3	Cryogenic control system	385	98	483	1.0	1.0
4	Circulating compressor (100 g/s)	75	24	99	.0	.5
5	Liquid helium storage dewar (10,000 l)	150	0	150	.0	.0
6	Helium gas buffer	50	24	74	.0	.5
7	Dual cryo. helium make-up purifier (25 g/s)	100	35	135	.0	.8
8	Cold vacuum pump	90	24	114	.0	.5
9	Helium distribution system	200	188	388	.0	4.0
10	Nitrogen Distribution system	75	71	146	.0	1.5
11	Magnet cooldown/warm-up system	75	47	122	.0	1.0
12	EDIA	40	392	432	4.0	4.0
TOTAL		\$3740	\$901	\$4641	5.0	13.8

Labor Cost Per Man-Year (K\$)

S & P  
Others

51  
47

## VII. STRETCHER VACUUM SYSTEM

The stretcher ring and the transport lines will have three distinct type vacuum systems: the warm bore sections, the cold bore sections and the insulating vacuum of the superconducting magnets.

The warm sections include most of the transfer lines to and from the stretcher ring and the straight sections between the arcs with the exception of a 70° bend in the transfer line from the stretcher to the AGS. The vacuum chambers will be made of 304L, 316L or 316LN stainless, 1.5 mm thick with I.D. ~ 100 mm. They will be pumped by the combination of the linearly distributed NEG strips and a few small ion pumps. Pressure of low  $10^{-9}$  Torr monitored by the ion pump current and the cold cathode gauges will be maintained.

The cold bore of the superconducting magnets in the two arcs and the 70° bend will cryogenically pump these sections to below  $10^{-9}$  Torr. Access ports at the center and both ends of each arc will be used for monitoring and roughing.

The insulating vacuum will also be part of the superconducting magnets. Turbomolecular pumps will be used to rough the vessels before cooldown. Activated charcoal panels will be mounted to cryopump any minor helium leak in the vessel.

The vacuum system layout and design specifications are given in Fig. VII-1 and Table VII-1, respectively.

TABLE VII-1: Stretcher Vacuum System Specification

---

---

Warm Sections (divided into 5 sectors)

1. Vacuum chambers
    - 316LN stainless, 100 mm O.D., 1.5 mm thick, 10 m long,  
w/Conflat flanges and linear NEG strips
  2. Pumps
    - 10 Turbopump Stations (2 per sector) through 4" valves
    - 10 diode ion pumps (20 l/s each, 2 per sector)
    - 450 m NEG strips
    - 6 NEG cartridges for injection/extraction areas
  3. Monitoring
    - 20 cold cathode/pirani gauge sets (2 per sector, one per TMP)
    - 10 ion pump current readouts
  4. Cold Sections (3 sectors, 2 arcs, one 68° bend)
    - a. Pumps
      - 6 Turbopump stations (2 per sector)
    - b. Monitoring
      - 15 cold cathode/pirani gauge sets (3 per sector, one per TMP)
  5. Insulating Vacuum
    - a. Pumps
      - 9 Turbopump stations
    - b. Monitoring
      - 18 cathode/pirani gauge sets
  6. Average Pressure ( $5 \times 10^{-9}$  Torr)
-



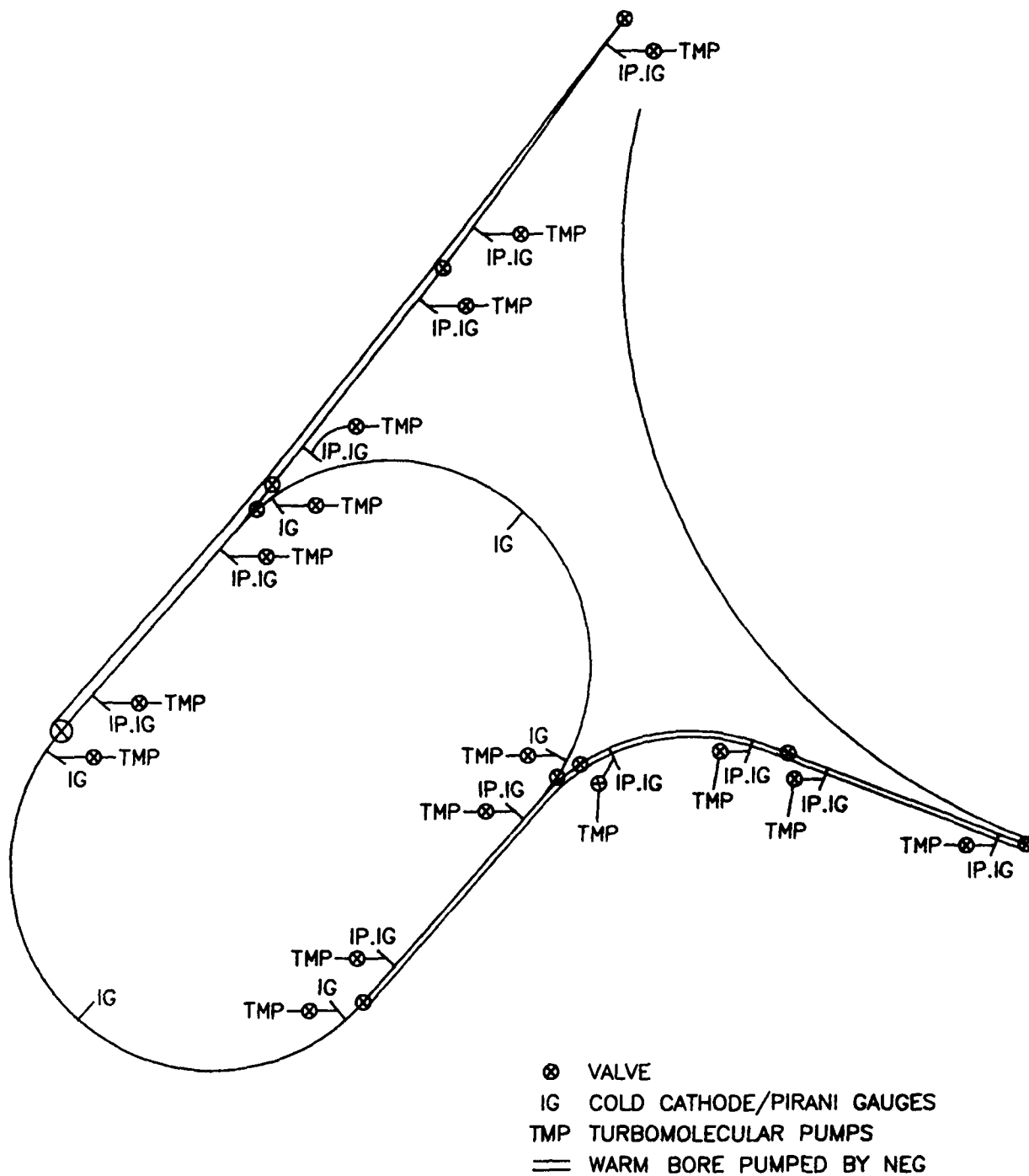


Fig. VII-1 Vacuum System Layout

TABLE VII-2: COST ESTIMATE - VACUUM SYSTEM

<u>Item</u>	<u>Description</u>	<u>FY1</u>	<u>FY2</u>	<u>FY3</u>	<u>K\$ Subtotal</u>
1	Valve	35	84		119
2	Roughing pump	38	275		313
3	Vacuum gauge	69	103		172
4	Ion pump		24	34	58
5	NEG pump			156	156
6	Vacuum chamber	150	111		261
7	Cabling		60	50	110
8	Charcoal		5	5	10
9	Vacuum control	<u>30</u>	<u>50</u>	<u>15</u>	<u>95</u>
	Subtotal	322	712	260	1294
	10% contingency	<u>32</u>	<u>71</u>	<u>26</u>	<u>129</u>
	<u>Total MSTC</u>	354	783	286	\$1423
10	Manpower - \$K (man-year)				
	<u>Construction</u>				
	S&P	102(2)	153(3)	102(2)	355(7)
	Tech.	94(2)	188(4)	282(6)	564(12)
	<u>Engineering</u>				
	S&P	102(2)	51(1)		153(3)
	Designer	141(3)	141(3)		282(6)
	<u>Total Manpower</u>	<u>439(9)</u>	<u>533(11)</u>	<u>384(8)</u>	<u>1354(28)</u>
	<u>VACUUM TOTAL</u>	<u>793</u>	<u>1316</u>	<u>670</u>	<u>\$2777</u>

### VIII STRETCHER CONTROL AND INSTRUMENTATION

We see no essential difference in the above systems in going from the "in-the-ring" design to the superconducting design. Of course, cables will go different routes and there may be some design changes for the cold environment. This should not significantly change the effort or cost and we use those given in the "in-the-ring" stretcher report. The following information is from that report with one modification, the use of 48 PUE units instead of 96.

#### A. Stretcher Beam Diagnostics System

The required elements are summarized below.

##### Summary of Stretcher Beam Diagnostic Elements

- Beam position monitoring system (one set of PUE's, H/V, at each lattice quadrupole location, 48 units).
- Beam current monitor (magnetic feedback transformer).
- Betatron tune measurement system (stripline drivers and monitors, analog/digital electronics).
- Movable scrape-off target (upstream of beam dump absorber).
- Distributed loss monitors (LRMs).
- Specific high precision loss monitors (4) for measurement of SEB extraction efficiency.
- Schottky scan noise spectrum measurement.
- Sweeping wire beam profile measurement.
- Beam transfer line (AGS-stretcher, stretcher-SEB switchyard) position and current monitor.

## B. Stretcher Control System

The control system for the stretcher is planned to be a straightforward extension of the system which will control the upgraded AGS. A prototype version of this system is now being installed for operation of the Heavy Ion Transfer Line project.

Briefly, this system has the architecture of a three-level hierarchy. At the lowest hierarchal level, microprocessor based Device Controllers acquire accelerator information and control accelerator devices and instruments. Real time synchronization is accomplished at this level. At the second level, microprocessor based entities called Stations serve to connect and monitor the Device Controller belonging to a given geographical area. The Stations connect to host/console computers (the highest hierarchal level) via a broadband Local Area Network. This link is currently a BNL developed LAN called RELWAY. This LAN includes Stations and host interface units called COMBOXes. The host/console computers are currently envisaged to be modern 32-bit workstations. These workstations provide computational resources and drive general purpose consoles which are already designed.

## **IX. AGS EJECTION - STRETCHER INJECTION/EXTRACTION**

### **I. AGS Ejection - Stretcher Injection**

The scenario described below individually kicks each of the 12 bunches out of the AGS and kicks them into the stretcher at the appropriate time as determined by the ratio of the machine circumferences. The design described below requires a pulse every 10  $\mu\text{sec}$  and therefore places severe demands on kicker power supplies. The repetition period may be increased to as much as 80  $\mu\text{s}$  without serious deterioration in the bunch structure or in the synchronization between the AGS and stretcher. Table IX-1 gives several choices of repetition period with the necessary stretcher circumferences. Furthermore, demands on the kicker power supplies can be alleviated by using an RF system in the stretcher so that one can maintain synchronism and allow a significantly long time between kicker pulses. We will include the cost of an RF system that will allow us to fill the stretcher at any desirable energy, with the thought in mind that the cost trade-offs between very fast kicker rep rate and RF system will have to be studied for any final design.

One can envision more exotic schemes for stretcher injection, but again trade offs of costs and efficiency will have to be investigated during a detailed design study. The 10  $\mu\text{sec}$  repetition period kickers plus an RF system give a maximum upper limit cost.

**TABLE IX-1: Examples of repetition periods of synchronous transfer between the AGS and Stretcher.**

<u>Kicker Repetition Period</u>	<u>AGS Turns + 11/12</u>	<u>Circumference ratio Stretcher/AGS</u>
5.16 $\mu\text{sec}$	1	.575
10.55 $\mu\text{sec}$	3	.553
29.41 $\mu\text{sec}$	10	.544
91.36 $\mu\text{sec}$	33	.538

#### A. AGS Ejection

A kicker magnet, kicking 1.1 mrad horizontally, will be used, in conjunction with a septum located at B10, to eject individual bunches from the AGS. The kicker and extraction system would be similar to the FEB extraction system with two additional requirements: 12 pulses are required, one each 10.34  $\mu$ seconds; the fall time must be less than 200 noseconds for the first pulse, 420 noseconds for the second pulse, and so on. (There are 220 noseconds between AGS bunches.) The Stretcher/AGS circumference ratio will be 0.553 so that after one bunch is extracted to the stretcher, after 3-11/12 AGS turns, the stretcher will have gone through a 7-1/13 (7.077) turns. At this point a second AGS bunch is extracted which arrives in the stretcher 112 noseconds behind the first bunch that was transferred. The time sequence for the first two pulses is indicated on Fig. IX-1. This is continued, emptying the AGS after 114  $\mu$ seconds.

As in the FEB line, the rise time of the kicker must be less than 200 noseconds for each pulse. The kicker would be located at an appropriate number of AGS wave lengths ( $1/4\lambda$ ,  $3/4\lambda$ , etc.) upstream of a horizontally-bending septum magnet leading to the AGS/Stretcher transfer line. The septum bend is 25 mrad and just compensates for the effect of the fields of AGS dipoles seen by the ejected beam, leaving the transfer line heading tangent to the AGS ring at the center of the B10 straight section.

We also assume that a beam clean-up system will be available in the AGS to reduce halo in preparation for extraction.

#### B. AGS/Stretcher Transfer Line

The heading of the extracted bunches is 15 degrees from the heading of the western straight section of the stretcher. The stretcher will be 12 feet below the AGS. It is important for the polarized proton program to separate the vertical-bending section from horizontal bends, as discussed in the Introduction. Therefore, we show the arrangement in Table IX-2 where we have two quads upstream to contain the beam, a horizontal bend of 15°, the vertical bending section, and a quad doublet, followed by horizontal and vertical bending magnets which steer the beam into the stretcher injection channel. Two 34 mrad vertical bends, each accomplished by a 6 foot warm dipole at 20 kgauss, are separated by 350' to bring the beam to the stretcher elevation. We show 3" diameter quads, as are used in AGS external lines. This is shown in Figs. IX-2 and IX-3.

# AGS/STRETCHER EXTRACTION

→ BUNCH DIRECTION

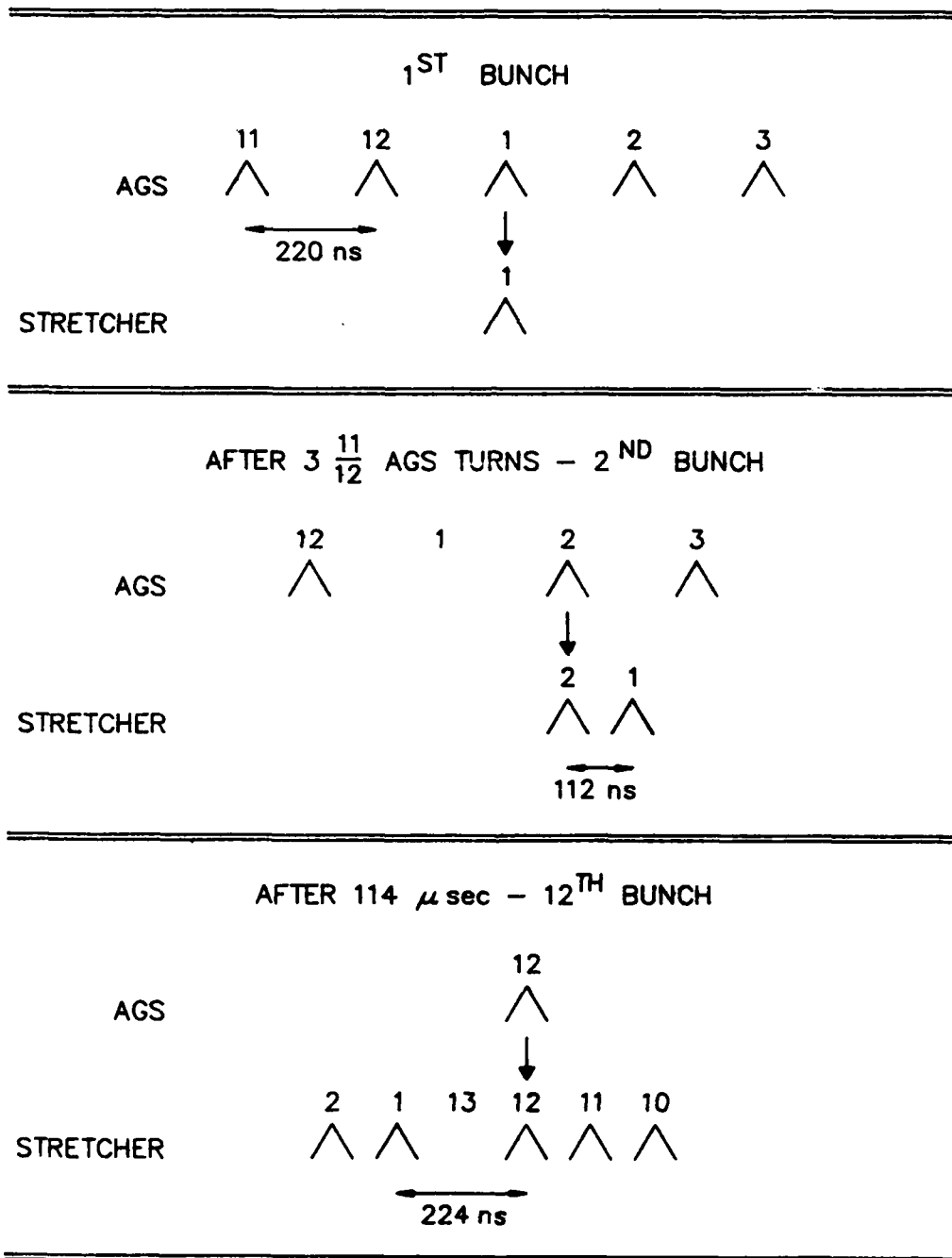


Fig. IX-1

TABLE IX-2: AGS/Stretcher Transfer Line Components, Coordinates

<u>Component</u>	<u>Flavor</u>	<u>Distance From B10</u>	<u>Bend</u>	<u>Heading of Beam After Component (From B10)</u>
AGS (B10)	—	—	—	0°H, 0°V
ASK1	Kicker (7D72*2)	-1/4λ	1.1 mrad, H	—
ASD1	Septum (2.3D9*1)	0	25 mrad, H	0° H, 0°V
ASQ1,2	2 x (N3Q18)	46'	—	15° H, 0°V
ASD2-9	8 x (7D79*3)	85'	15°, H	15° H, 0°V
ASP1	7D79*3	305'	-34 mrad, V	15° H, -34 mrad V
ASP2	7D79*3	655'	+34 mrad, V	15° H, 0° V
ASQ3,4	2x(N3Q18)	671'	—	15° H, 0° V
ASD10	7D79*3	685'	+1.7°, H	16.7° H, 0° V
ASP3	7D18*3	725'	+3 mrad, V	16.7° H, + 3 mrad V
ASD11-13	3 x (4D80*2) (Thin Lambertsons)	822' (-33') <sup>†</sup>	-30 mrad, H	15° H, -0.5 mrad V
ASK2,3	Kickers 2 x (2.6D120*1.7)	855' (0') <sup>†</sup>	+1.52 mrad, V	15° H, 0° V
Stretcher (West straight section)	—	—	—	15° H, 0° V
SA1-3	3 x (4D80*2) (Thin Lambertsons)	+33'	-30 mrad, H	13.3° H, +0.5 mrad V (Fast abort line)

\* Distances are to center of element or groups of elements, along beam line.

† Distances in parentheses are to center of stretcher west straight section.

Dipole notation: wDl\*g where w, l = pole width, length; g = gap all in inches.

Quadrupole notation: NdQl where d = inside diameter, l = length.

Thin Lambertson: 20° septum angle, 5 kgauss in gap.

ASK1: rise time < 200 nsec; fall time < 200 nsec 1st pulse;  
12 pulses, one each 10 μsec.

ASK2,3: rise time < 100 nsec; 12th fall time < 200 nsec; 12 pulses,  
one each 10 μsec.



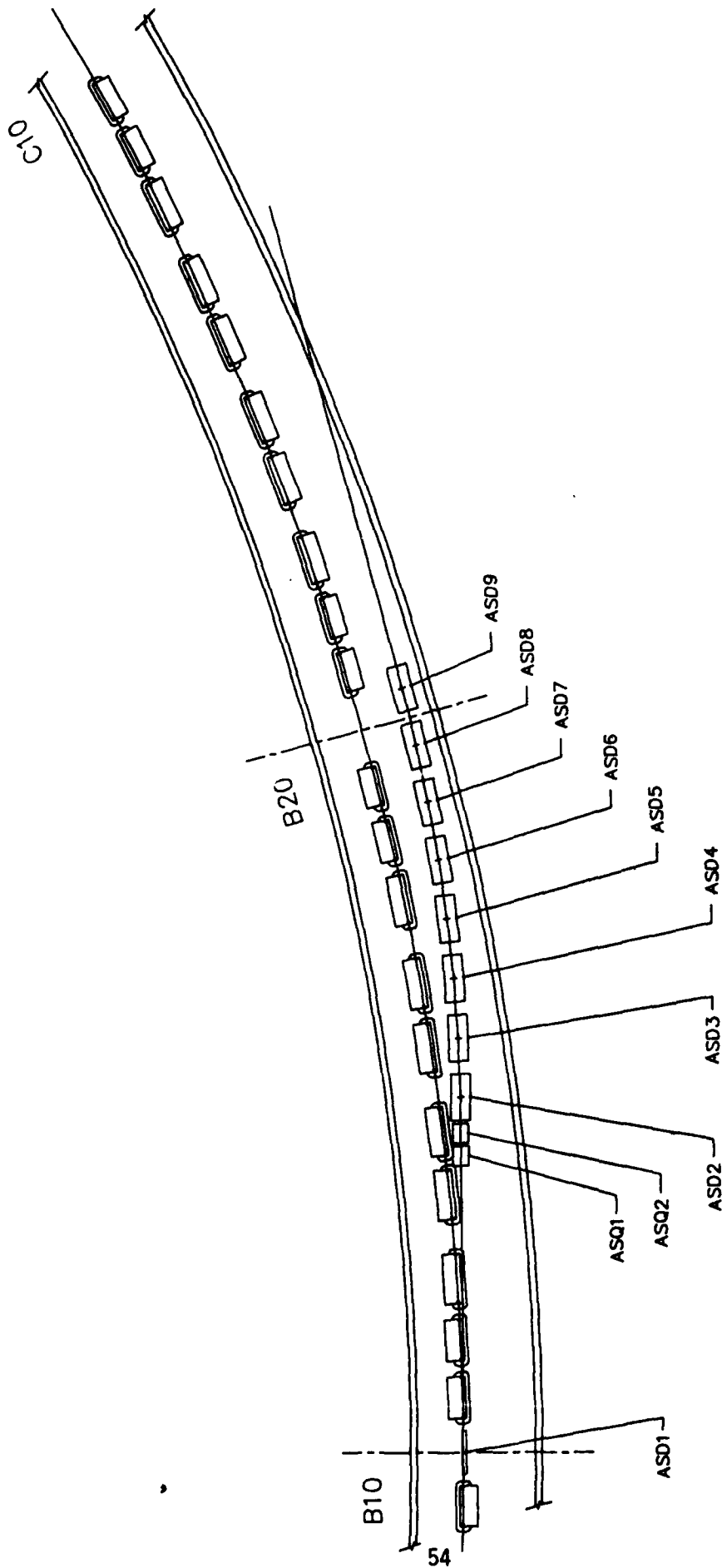


Fig. IX-2

TRANSFER LINE - AGS TO STRETCHER

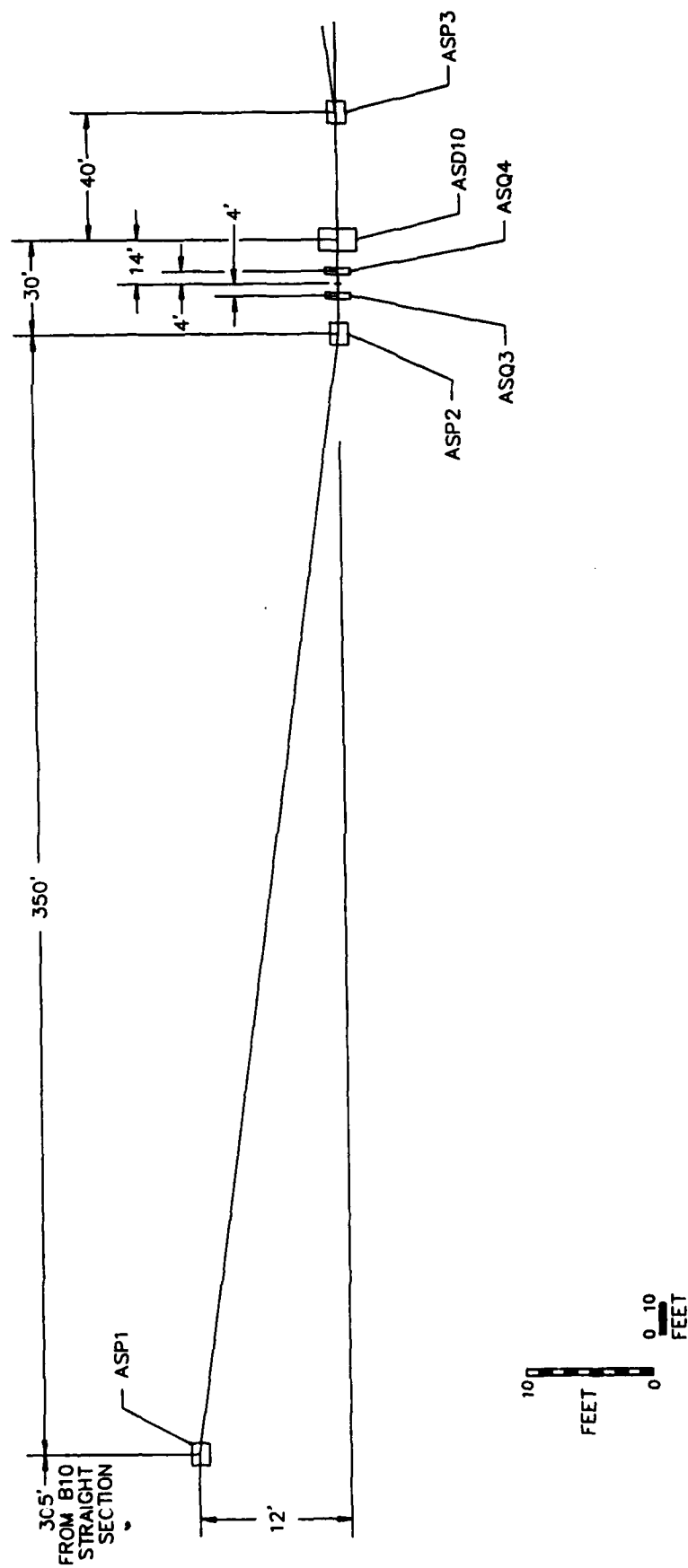


Fig. IX-3

VERTICAL BEND - ACS TO STRETCHER

### C. Stretcher Injection

Injection of each bunch into the stretcher will be done by thin Lambertsons bending horizontally followed by a vertical kicker magnet. This is shown on Fig. IX-4. The thin Lambertsons will nestle close to a vertical beta maximum and will correct the horizontal heading of the incident bunches to that of the west straight section. A 30 mrad bend is required to avoid the nearest quad in the stretcher lattice, which is 10 meters upstream. The beam will be left on a 0.5 mrad trajectory down, created by a small upstream pitching magnet, which crosses the stretcher at the center of the straight section. A vertical kicker here will then place the bunch in the stretcher, 112 nseconds behind the previously-stacked bunch.

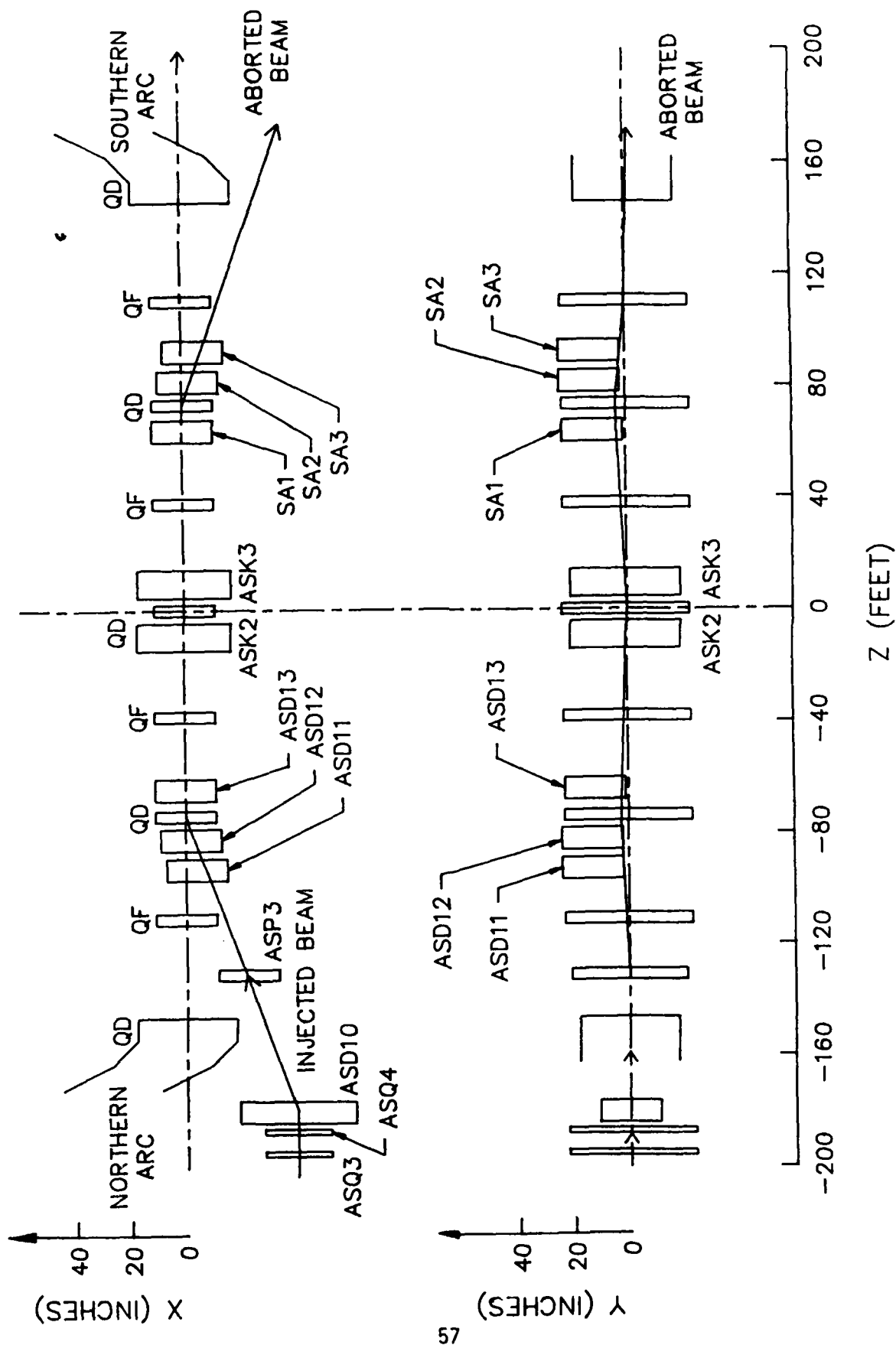
The thin Lambertsons each kick 15 kilogauss meters with a septum angle of 20 degrees. The required kicker aperture is 6.6 cm(V) x 4.3 cm gap. The kicker pulse rise time must be less than 100 nseconds, it must be capable of 12 pulses, one each 10 useconds, and the 12th fall time must be less than 200 nseconds (11th less than 310 nsec, etc.). Note that we fill 12/13 of the stretcher, leaving two interbunch distances (224 nsec.) as the maximum required fall time for this kicker.

### D. Debunching

Within 9 milliseconds the beam will debunch due to the different trajectories of the particles. Migration relative to the bunch center will have a width  $\sigma = 45$  nseconds, or  $2.5\sigma$  for one bunch spacing. At this time the beam can be extracted.

### E. Stretcher Extraction

We propose vertical resonant extraction. Four skew sextupoles will be placed to initiate the resonance condition and quadrupoles will be used to shift the vertical tune of the stretcher by the vertical chromaticity to sweep the resonance through the beam. Extraction would occur over the AGS cycle, typically 1.0 seconds. The tune-shift quads must be reset in a time short compared to this cycle-time, to avoid undue dead-time. Nonresonant beam, expected to be  $\sim 1\%$ , will be kicked out a separate extraction channel after the slow extraction process. The skew sextupole strength should be  $\int B'' dl = 33.5$  T/m for a beam rigidity of 100 T-m. For this strength the  $\Delta v$  from the quads will be 0.01. The straight section conventional magnet quadrupoles can be pulsed for  $\Delta v$ 's of this order of magnitude without significantly affecting the machine lattice.



STRETCHER INJECTION/FAST ABORT WESTERN STRAIGHT SECTION

Fig. IX-4

Two electrostatic septa, 5 cm aperture, 150 kV, and each 3 meters long, will be placed at the vertical  $\beta$  maximum just upstream of the center of the southern straight section. This is indicated on Fig. IX-5. A 0.6 mrad bend here will steer the extracted beam into three thin Lambertsons, bending horizontally. The thin Lambertsons bend 30 mrad, to the extraction transport channel. A small pitching magnet levels the beam after the Lambertsons.

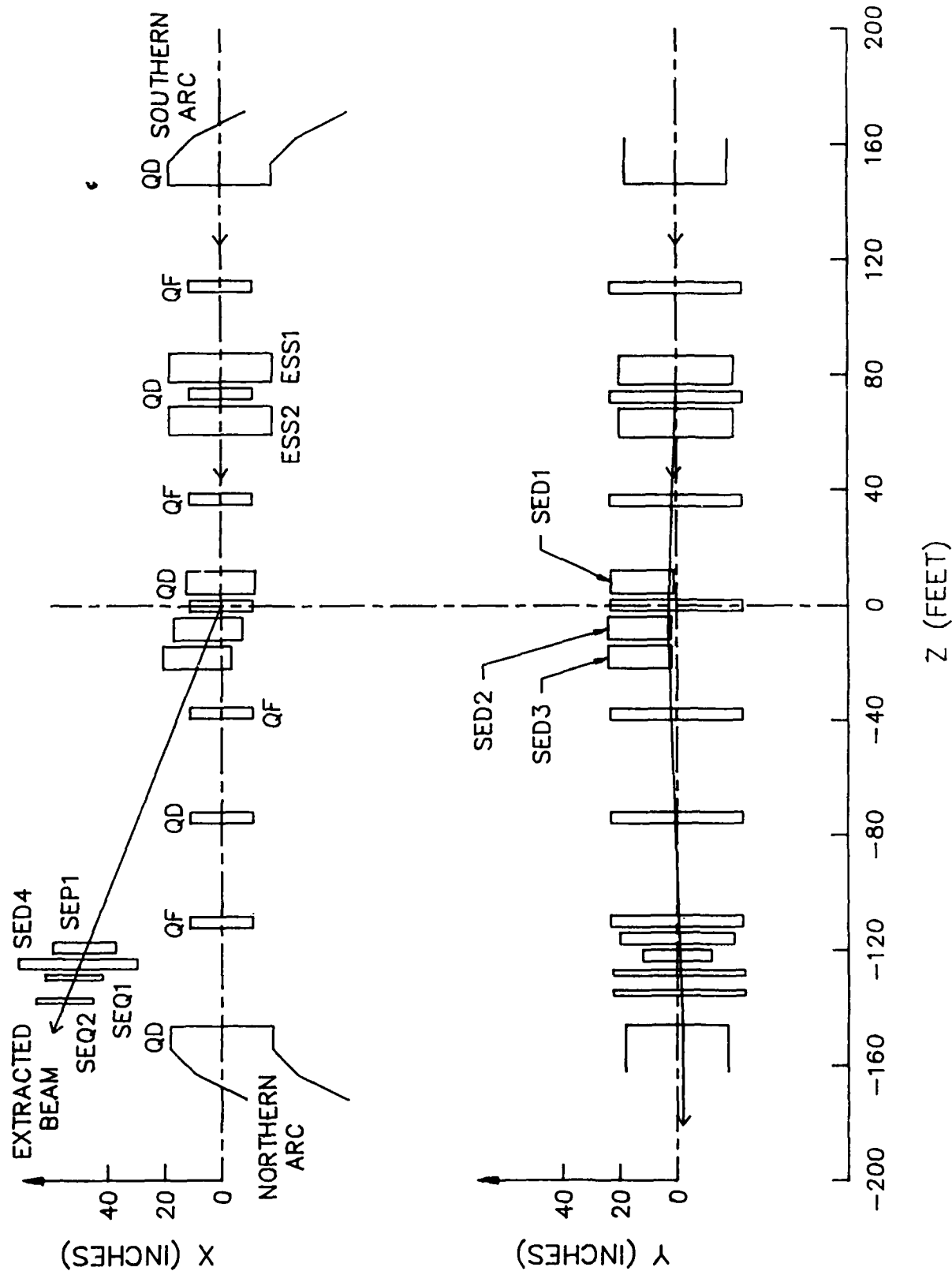
The injection kicker magnets will steer non-resonant beam left in the machine to thin Lambertsons downstream in the west straight section. The fast extraction will also be available for a fast-abort. A rise time of 100 nseconds is required with a 2  $\mu$ sec flattop. The aborted beam will pass out a channel roughly following the western straight section to an isolated beam dump.

#### F. Losses at Extraction

Losses in the present AGS extraction system have at least two components: the fraction of beam intercepted by the electrostatic septum, and the non-resonant piece which is splattered around the ring. The large  $\beta$  at the proposed extraction location improves losses by a factor of 6, the relative ratio of septum wire size to the  $\beta_{\text{max}}$  of the beam. In addition, the non-resonant beam will be dumped externally, reducing that loss by a factor  $> 10$ .

#### G. Stretcher/SEB Transfer

The extracted beam must be bent  $70^\circ$  horizontally and raised 12 feet to join the Slow Extracted Beam (SEB) channel. Table IX-3 lists the components. The  $70^\circ$  bend will be done at the stretcher elevation with a partial superconducting arc (5 cells), with the same cell spacing as in the stretcher arcs. A superconducting vertical bend of 88 mrad (2 x 1.5 meter dipoles on sides) is followed after 136 feet (center-to-center) by a warm bend to the AGS level (3 x 79 inches at 18 kgauss). As shown on Fig. IX-6, the transfer line can then be joined to the existing SEB line, in front of the electrostatic splitters which divide the beam into A, B, C and D lines. Quadrupoles are included after the Lambertsons, in the horizontal superconducting bend in the vertical-kicking region. A triplet already exists at the upstream end of the SEB line.



STRETCHER EXTRACTION EASTERN STRAIGHT SECTION

Fig. IX-5

The changes for the SEB line are slight. CD1 and CQ1 are to be replaced with a C-magnet centered at the old CQ1, bending 2.5 degrees. The pitcher CP020 will be moved upstream of the new CD1. A beam optics program has not been run on the transfer lines. Some additional elements might be required for those places where an achromatic bend is desirable.

TABLE IX-3: Stretcher/SEB Transfer Line Components, Coordinates

<u>Component</u>	<u>Flavor</u>	<u>Distance from Center of Stretcher East St. Section</u>	<u>Bend</u>	<u>Heading of Beam Component (From B10)</u>
Stretcher East st.sec.	---	---	---	195° H, 0° V
ESS1,2	Electrostatic Septa (3mx5cmx5cm)	-73'	+ 0.6 mrad	195°, 0.5 mrad V
SED1-3	3 x (4D80*2) (Thin Lambertsons)	0	-30 mrad, H	194.4° H, -5 mrad V
SEP1	7D18*3	116'	+5 mrad, V	194.4° H, 0° V
SED4	7D18*3	122'	tweak	194.4° H, 0° V
SEQ1,2	2 x (N3Q18)	136'	---	194.4° H, 0° V
SEARC	Superconducting arc (5 cells)	226.5'	-69.9° H	124.5° H, 0° V
SEP1,2	2 x (4D60*4) (Superbenders)	322'	+88 mrad, V	124.5° H, +88 mrad V
SEQ3,4	2 x (N3Q18)	334'	---	124.5° H, +88 mrad V
SEQ5	N3Q18	445'	---	124.5° H, +88 mrad V
SEP3-5	3 x (7D79*3)	458'	-88 mrad, V	124.5° H, 0° V
SEQ6	N3Q18	471'	---	124.5° H, 0° V
CD1	7C95*3	539'	-2.5°, H	122° H, 0° V

\* Distances are to center of element, along beam line.

Thin Lambertsons: 20° septum angle, 5 kilogauss in gap.

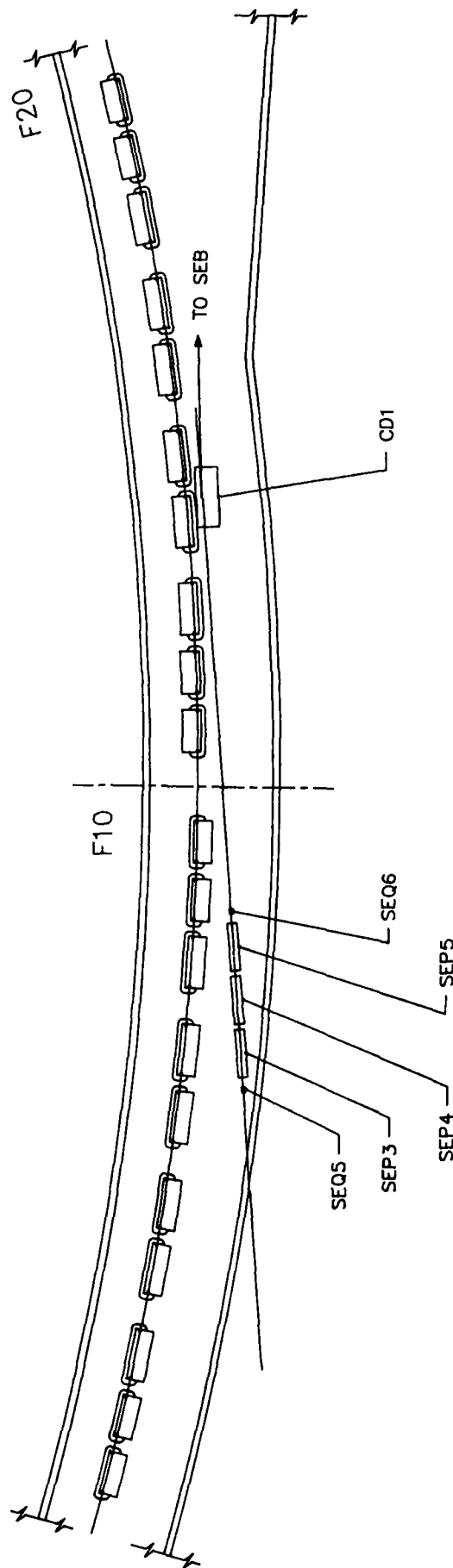


Fig. IX-6

TRANSFER LINE - STRETCHER TO SEB



## H. Instrumentation

The requirements are similar to the in-ring stretcher.

## I. Cost Estimates

Table IX-4 gives the costs for the injection, extraction and transfer line magnets and power supplies.

TABLE IX-4. Magnets and Power Supplies - Cost Estimate

<u>Magnets</u>	<u>MSTC</u>	<u>Labor</u>	<u>Total</u>	<u>Power Supplies</u>	<u>MSTC</u>	<u>Install</u>	<u>Total</u>
(14) 7D79*3	\$1,262,800	249,200	\$1,512	(14) 1500A 150V	630,000	140,000	\$770,00
(1) 2.3D79*1	30,000	9,000	39,000	(1) 1500A 150V	45,000	10,000	55,00
(3) 7D18*3	100,000	23,000	123,000	(3) 1000A 20V	15,000	30,000	45,00
(1) 7C95*3	131,000	51,800	182,800	(1) 1500A 150V	45,000	10,000	55,00
(2) 2.6D120*1.7 Kicker	107,500	60,400	167,900	} 2.66 kA 52.4kV } 38 PFN	1,140		1140,00
(1) AGS Type Kicker	53,800	30,200	84,000				
(9) 4D80*2 Lamb.	421,000	421,000	873,000	(9) 4000A 40V	360,000	90,000	450,00
(10) N3Q18	335,000	63,400	398,400	(10) 2400A 20V	96,000	100,000	196,00
(2) ES Septa	<u>278,800</u>	<u>108,800</u>	<u>387,600</u>	(2) 5 ma 15kV	<u>100,000</u>	<u>20,000</u>	<u>120,00</u>
	\$2,719,900	1,047,800	3,767,700		2,431,000	400,000	\$2,831,00

## J. RF System

As mentioned on page 43, a rf system will be included in this study. Since the bunch area of the beam from the AGS is likely to be 4 eV-sec at an intensity of  $5 \times 10^{12}$  particles/bunch, we shall require approximately 5 eV-sec bucket area for capture in the stretcher. Table IX-5 lists the rf parameters and the related impedance thresholds for collective effects.

TABLE IX-5

Part.	Stretcher	
	P	
BRHO (Tesla-meters)	100	
$\beta*\gamma$	31.9	
Atomic number	1	
$\langle Q \rangle$	1	
$N(10^9)$	5,000	
$\beta$ (inj)	0.999	
$\gamma$ (inj)	31.97	
$\epsilon_{ps} (10^{-6}\pi m^*rad)$	2.14	
$\epsilon_{psn} (10^{-6}\pi m^*rad)$	68.65	
$\eta(1/\gamma_t^{-2}\gamma^2)$	0.018	
-----		
Trev ( $10^{-6}s$ )	1.45	
-----		
RF Scenario		
(1) capture: V(volts)	16,000	
phase	0	
h	13	
area-evs/amu	5.01	
$f(syn)*2\pi$	624.8	
$\theta$	0.070	
$dE/E^{-3}$	0.54	
$dp/p^{-3}$	0.54	
$\sigma\tau(ns)$	16.46	
$\sigma L(m)$	4.93	
I(peak)(amp)	19.40	
I(av.)(amp)	6.58	
$\langle n \rangle$ microwave	7,286.5	
Threshold resistive-wall instability		
$\{Z/n\}$ (Ohm)	53.9	
$\{Z_t/n\}$ (MOhm/m)	17.6	
$\{Z\}$	6.0	} expected resistive wall impedance of steel vacuum pipe
$\{Z_t\}$ (MOhm)	0.03	
Threshold longitudinal instability		
$\{Z/n\}$ (Ohm)	8.63	

The rf system will consist of a tunable ferrite loaded, single gap cavity driven by a local push-pull power amplifiers; driven in turn, by a remotely located drive chain. It will be controlled in amplitude and frequency by an appropriate low level rf system. The low level system will be timed and phased from the AGS main ring rf system.

The system design parameters are as follows:

• Number of accelerating stations (cavities)	1
• Number of accelerating gaps	1
• Peak rf gap voltage	10 to 16 kV
• Programable range of rf voltage	1 to 17 kV
• Radio frequency at 3.5 GeV/c	7.9 MHz
• Radio frequency at 28 GeV/c	8.2 MHz
• Cavity tuning range	7 to 9 MHz
• Average beam current at $5 \times 10^{13}$ ppp	$I_{ave} = 6.5A$
• Peak beam current at $5 \times 10^{13}$ ppp	$I_{peak} = 19.5 A$
• rf pulse length	50 msec
Duty Cycle	4%

The cavity will consist of two ferrite loaded quarterwave lines driven in push-pull. It will have a single accelerating gap driven directly from the power amplifier anodes. It will be tunable over a limited frequency range by biasing the ferrite core with a conventional figure eight bias winding.

Peak ferrite dissipation will be limited to 300 milliwatts per cubic centimeter or less. For 50 ferrite rings measuring 50 cm O.D. x 30 cm I.D. x 2.5 cm thick, the peak dissipation will be about 56 kW. Average dissipation will then be less than 50 watts. Minimal forced air cooling will be adequate.

TABLE IX-6: Stretcher Rf System - Cost Estimate

<u>Item</u>	<u>Description</u>	<u>E.E.</u>	<u>M.E.</u>	<u>Des.</u>	<u>E.T.</u>	<u>M.T.</u>	<u>Costs</u>
1.	Design and build cavity (incl. structure, stand, cooling	1/2	1/4	1/2	1/2	1/2	\$125K
2.	Ferrite (50 rings @ \$1500 ea.)						75K
3.	Power amplifier-design and build	1/2			1/2	1/4	80K
4.	Driver-design and build	1/4			1/2	1/4	40K
5.	Tuning system-design and build (incl xsistor bank & P.S.)						40K
6.	Anode P.S.'s-spec. and purchase	1/4					100K
7.	Controls-design & build & timing	1/4			1/2		20K
8.	Cabling and connectors	1/4			1/2		20K
9.	Cooling		1/4			1/4	10K
10.	Instrumentation	1/2			1/2		10K
Totals		3	.5	.75	4	1-1/2	520K
Total S&P 4.25 MY							221K
Total Techs 5-1/2 MY							<u>259K</u>
TOTAL							\$1000K

## X. $\bar{p}$ OPTIONS

There are several possible  $\bar{p}$  scenarios involving the superstretchers, but only two are practical. These are described in this section, followed by a short discussion of those that won't work, and why. At the end, booster and stretcher  $\bar{p}$  options are briefly compared.

If a  $\bar{p}$  source were placed in the line from the AGS to the stretcher, the stretcher ring could be used as a  $\bar{p}$  accumulator. Stacking in the stretcher could be done on a bunch basis (boxcar), as described for protons in section IX. It is important to note at this point that the stretcher energy would be limited to between 2 GeV and 3.5 GeV. The upper limit is an artifact of the passive quench-protection system envisioned for running positives. Diodes in this system would be inactive for the  $\bar{p}$ s so the allowed stored energy is limited to what one magnet going normal can stand. The alternative requires more penetration, greater heat load, and is expensive. Energies below 2 GeV are not accessible either, due mainly to the relatively large contribution of magnetization currents in the superconductor. Variations in the eddy current would be very difficult to control.

This stretcher energy range, 2-3.5 GeV, includes the peak of  $\bar{p}$  production for 20 GeV protons, roughly 3.5 GeV. Experiments could use the  $\bar{p}$ s in this energy range by operating the stretcher in the slow spill mode, as for protons. In this mode, AGS/ $\bar{p}$  production/stretcher/SEB, the AGS cycle time would be the typical FEB cycle time, or 0.8 to 1.2 seconds. The duty factor of beam delivered to experiments would be nearly 100%.

The second possible option involves transferring the  $\bar{p}$ s back into the AGS for acceleration. An energy range of 25 MeV to 30 GeV is then available, provided vacuum is adequate at the low energy end. Extraction to the SEB line from the AGS would require a flattop, as well as switching the transfer lines from the proton arrangement. The role of the stretcher, then, would be to hold the  $\bar{p}$ s while the AGS was emptied of protons and its field reversed. This cycle time could be 3.4 seconds, including a one second flattop and four 0.56 second ramps: to 28 GeV (protons), to zero, field reversal (msec), to -28 GeV, and back to zero. The duty factor would be 1 second/3.4 seconds and the number of  $\bar{p}$ s/second would be a factor of four lower than the first option, this being the ratio of AGS cycle times for the two options.

Two other schemes were considered, involving acceleration in the stretcher or using the stretcher as a stretcher after  $\bar{p}$ s are accelerated in the AGS. The first is not feasible because of very long ramp times for the superconducting magnets and intolerable cryogenic heat loads. The AGS is a more efficient accelerator. The latter is only feasible in the energy range from 2 - 3.5 GeV, as discussed above.

The use of the stretcher as a  $\bar{p}$  accumulator can be compared to using the booster for that purpose. If we pretend, for a fleeting moment, that we have both machines and the  $\bar{p}$  option is an upgrade, the booster requires additional transfer lines and an upgrade in energy to get to 3.5 GeV. The superstretcher requires transfer line juggling and has an aperture 1/3 that of the stretcher. The booster has an rf system and ramp capability and could also be designed to reach an energy where charmonium states could be studied without accelerating in the AGS. It could also slow the  $\bar{p}$ s down for low energy experiments (Lowenstein has suggested a backward voyage through the Linac).

## **XI. SCHEDULE**

The vacuum system, RF system, conventional magnet systems, power supplies, instrumentation, and control systems can be engineered, fabrication, tested, and installed in a three year period. However, for the reasons outlined below, the S.C. magnet systems, the cryogenics, and the conventional construction will require about 1-1/2 years of effort before a 3-year period.

For the superconducting magnets, it will be necessary to design and fabricate the tooling needed for construction, as well as magnet design and materials procurement. This means about 1-1/2 years of effort before magnets are being built. The construction, testing and installation is then expected to take about 3 years (Table XI-1). Likewise, the cryogenic system will need 1-1/2 years of effort before the 1-1/2 years necessary for fabrication of the refrigerator. Installation, testing, and systems operation will probably then take another year. (Table IX-2).

The third item is the civil construction. Title I and Title II preparation will take again about 1-1/2 years and this will be followed a 2 year construction period. Beneficial occupancy can occur after 1-1/2 years of construction (Table XI-3). Table XI-4 summarizes this "critical item" schedule and consequently the overall schedule.

RATES:	NO.	REQ'D	NO.	/MONTH
DIPLOES	96		4	
QUADS	48		2	
SEXT	48		2	
CORR.	48		2	
CRYDSTATS	24		1	
CELLS	24		1	
SPOOLS	4		.3333	

69



LEGEND: EEEE = ENGINEERING  
 DDDD = DESIGN  
 PPPP = PROCUREMENT  
 FFFF = FABRICATION  
 IIII = INSTALLATION  
 TTTT = TESTING  
 QQQQ = OPERATIONS

FISCAL YEAR

70



. . . CRITICAL ITEM SCHEDULE . . .

	1987	1988	1989	1990	1991
Magnet Systems	Design →	Tooling fabric. →	Magnet fabrication Testing and installation →		
Cryogenics	Eng. & Design →	Procurement & fabrication →		Test, install, oper. →	
Conventional Facilities	Title I and II →	Conventional Construction →		B O	
Standard System			Eng. →	Procurement fabrication →	Inst. →
				↓ Beneficial Occupancy	

## XII. COST SUMMARY

In most estimates, costs for materials and fabrication have been obtained from recent projects. The labor costs include engineering and design, as well as assembly and installation. The MSTC cost includes materials and fabrication. Costs for S&P were taken as \$51K/year in 1986 dollars and Techs as \$47K/year. These are the values used in the "in-the-ring" stretcher design report.

As mentioned previously, we have taken the same costs for instrumentation and controls from the "in-the-ring" stretcher design. We also have used the same accelerator physics cost.

Table XII-1 summarizes the cost estimates and compares them to "in-the-ring" stretcher. The essential change in cost is the construction of conventional facilities.

The superconducting ring system is about a million dollars less, but the conventional facilities and transfer are about 6 million more. The net effect is a 6 million dollar increase over the previous design. However, this also includes an RF system for one million which may be optional.

TABLE XII-1: COST SUMMARY

		<u>MSTC</u>	<u>Labor</u>	<u>Total</u>
1. Ring Magnet Systems (all S.C. magnets and Power Supplies)		4,293,349 1,322,000	1,666,031 529,000	5,959,380 1,851,000
2. Cryogenic System		<u>3,740,000</u>	<u>901,000</u>	<u>4,641,000</u>
	Sub-total	* 9,355,349	3,096,031	12,451,380
	Cf. (in-the-ring)	10,749,000	2,792,000	13,541,000
3. Conventional Facilities		5,045,000	757,000	5,802,000
4. Transfer Lines (all Inj., Ext., Tsfr.)		<u>5,150,900</u>	<u>1,447,800</u>	<u>6,598,700</u>
	Sub-total	*10,195,900	2,204,800	12,400,700
	Cf. (in-the ring) }			
	}	3,696,000	2,575,000	6,271,000
	(Tsfr. + Conv.)			
5. Vacuum System		* 1,294,000	1,354,000	2,648,000
	Cf. (in-the-ring)	2,040,000	649,000	2,689,000
6. Instruments		* 945,000	868,000	1,813,000
7. Controls		* 1,747,000	1,375,000	3,122,000
8. RF System		* 520,000	480,000	1,000,000
9. Accelerator Physics		* <u>          </u>	<u>580,000</u>	<u>580,000</u>
	Total*	24,057,249	9,957,831	34,015,080
	20% Contingency			<u>6,803,016</u>
				40,818,096
	Cf. (in-the-ring)			34,800,000

Accelerator Division  
BROOKHAVEN NATIONAL LABORATORY  
Associated Universities, Inc.  
Upton, NY 11973

AGS/AD/Tech. Note No. 269

A CONCEPTUAL DESIGN FOR A VERY LOW ENERGY ANTIPROTON SOURCE

Y. Y. LEE and D. I. LOWENSTEIN

December 3, 1986

In a previous note<sup>1</sup> we raised the possibility of obtaining very low energy antiprotons of the order of 20 keV kinetic energy from the AGS. In this note we would like to outline the requirements for such a facility (or experiment) to accomplish the very low energy antiproton source.

The basic magnetic cycle of the AGS and the Booster is given in Figure 1. After injecting 1.5 GeV protons into the AGS, the magnetic field of the Booster is ramped up to 8.5 kG in order to receive 3.5 GeV/c antiprotons produced by the AGS. The antiprotons are decelerated by the Booster and then extracted to the 200 MeV linac while the AGS delivers the rest of the available protons for other experiments. The antiprotons are then decelerated in the linac to 750 keV and then to 20 keV in the RFQ linac. Figure 2 is a description of the accelerator complex.

THREE BUNCH EXTRACTION FROM THE AGS

At the end of the AGS acceleration cycle, the AGS rf voltage is raised to shorten the bunch length to a few nanoseconds before extracting three of the twelve bunches through the H10 extraction channel. This will increase the proton beam momentum spread and provide for a short antiproton bunch. The extraction channel and the beam transport should be able to accommodate the proton momentum spread. The additional equipment needed for the extraction is a ferrite kicker and power supply similar to the ones installed at H5 or E5, an extraction septum and power supply similar to the one at H10, and an AGS orbit bump and power supply.

PROTON TRANSPORT AND THE TARGET STATION

The beam transport consists of six quadrupoles, a triplet in the AGS tunnel for beam shaping and another triplet upstream of the target for focusing the beam on to the target. A special target station similar to the ones at the CERN and Fermilab antiproton facilities must be constructed because of the high intensity beams involved. A focusing element such as a lithium lens is required in order to focus the produced antiprotons into the apertures of the transport quadrupoles.

1. Y.Y. Lee, A Thought on Very Low Energy Antiprotons, BNL Acc. Div. Tech. Note No. 266 (1986).

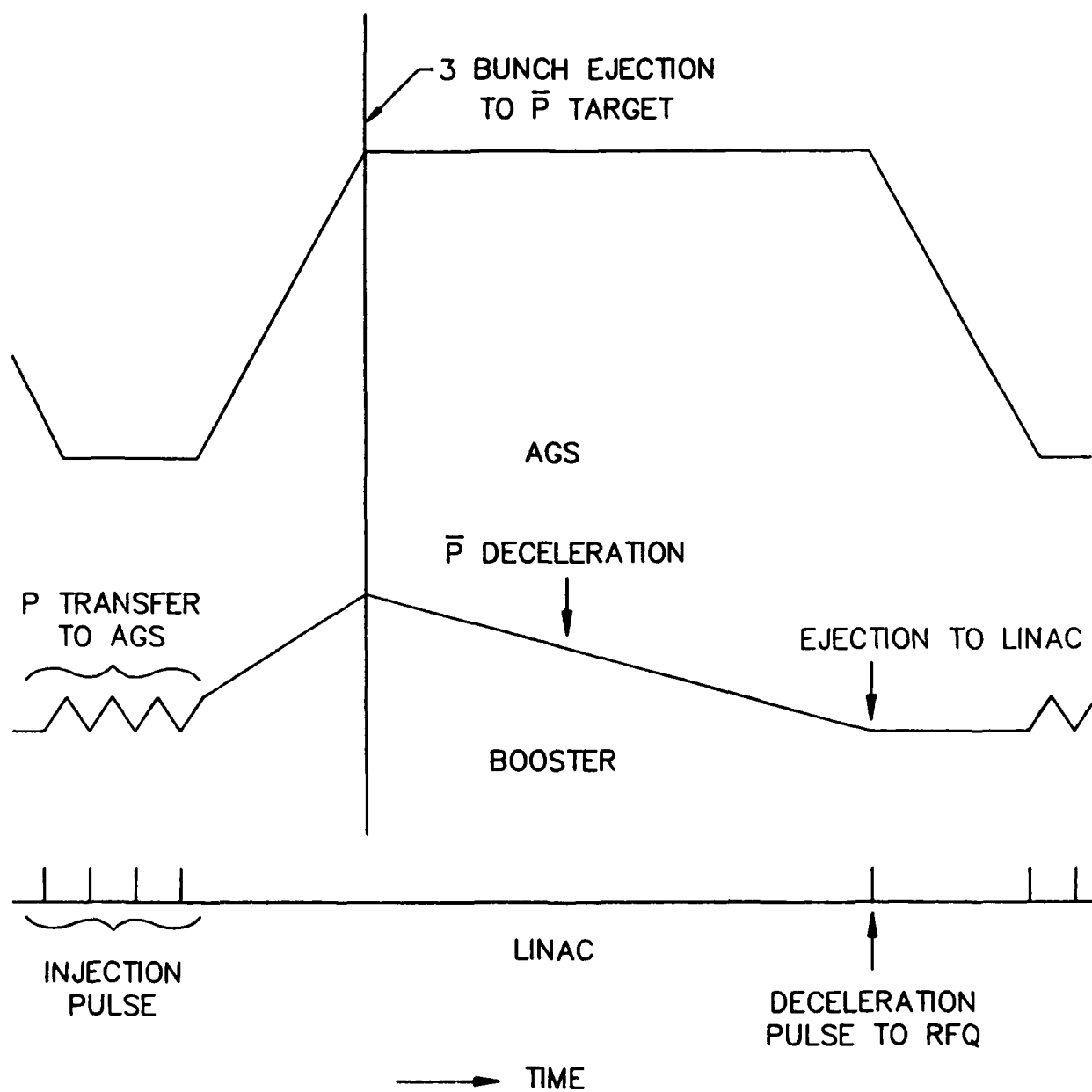


Figure 1

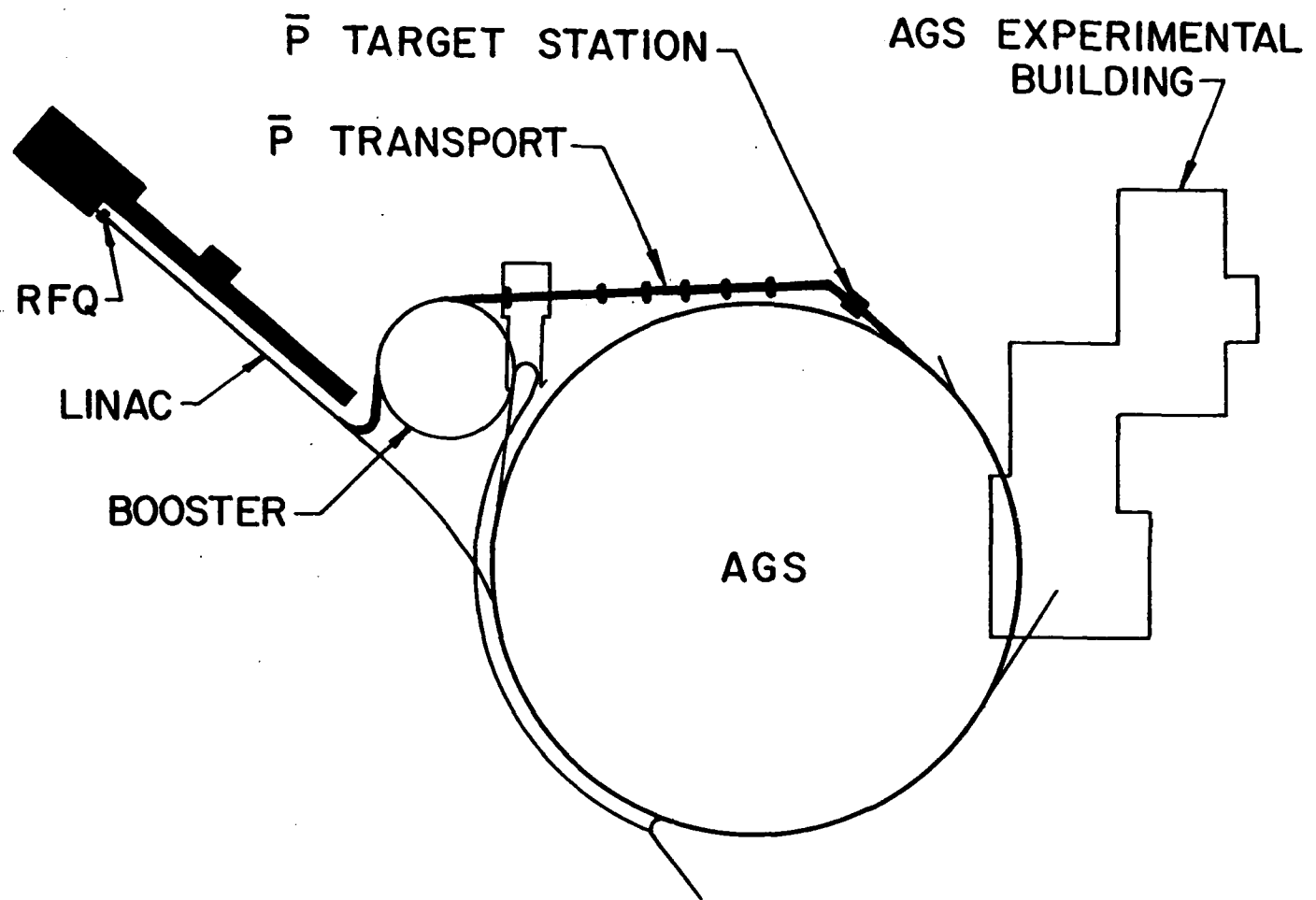


Figure 2



#### ANTI-PROTON TRANSPORT AND INJECTION INTO THE BOOSTER

Produced antiprotons will be transported to the Booster. The length of the line is approximately 150 meters and requires about 30 degrees of total bend. It requires the order of 10 quadrupoles and six 5 degree bending magnets.

Injection into the booster is accomplished by duplicating the Booster extraction septum and kickers.

#### DECELERATION IN THE BOOSTER

The antiprotons transported to the Booster will have the 50  $\pi$ -mm-mr emittance in both planes and a momentum bite of 2%. The length of the antiproton bunch is the same as the AGS proton bunch which was tailored to a few nanoseconds. By allowing the bunch to rotate in longitudinal phase space one can lengthen it to 50 nanoseconds and the antiproton momentum spread can then be reduced to a few tenths of a percent. No special equipment is needed to decelerate the beam to 200 MeV kinetic energy. One may have to install special instrumentation to detect the low intensity beam.

#### BOOSTER EXTRACTION AND TRANSPORT TO LINAC

Decelerated antiprotons can be extracted at the Booster straight section C6. A fast ferrite kicker of strength 6 kG-meter can extract 200 MeV antiprotons from the Booster. A transport system identical to the injection line but of opposite polarity can transport the antiprotons to the HEBT line of the linac. A fast kicker can inject the beam into the upstream end of the linac.

#### DECELERATION THROUGH LINAC-LEBT-RFQ-EXPERIMENT

At present we do not foresee any additional equipment required to decelerate the antiprotons through the linac and RFQ except increased sophistication in phase and amplitude controls. At the exit of the RFQ a kicker is required to deflect the decelerated antiprotons away from the regular proton channel and direct it to the detector region.

#### CONTROLS MODIFICATION

Additional sophistication is needed in the control system of the AGS, Booster and linac. Pulse-to-pulse modulation of the system is required, not only for the magnetic cycle of the machines, but also to all other systems such as rf and extraction systems.

#### COMMENTS ON THE BOOSTER POWER SUPPLY AND RF SYSTEM

At present there are two modes of Booster operation, namely fast cycling proton operation and slower cycling heavy ion operation. The proton operation needs higher voltage and lower current while heavy ion operation needs lower voltage but higher current. Power supply modules are rearranged

for each of the operations. For the proposed antiproton option, the range of antiproton deceleration current requirements forces one to use the arrangement of the heavy ion option which results in the Booster cycle period to be lengthened by a factor of two. If faster cycling of the Booster is important, one would add a set of modules to the present power supply to increase the repetition rate.

It is inefficient to bunch and decelerate in the linac unless the antiproton beam is prebunched to the linac frequency. One would add a 200 MHz rf cavity to bunch the antiprotons in the Booster. This will bring the efficiency to about 80% compared to 50% for decelerating through the linac and RFQ.

#### COMMENTS ON COOLING THE ANTIPROTONS

It has been demonstrated that one can reduce the six dimensional emittance of the beam in a synchrotron either by stochastic or electron cooling. As a proof of principle experiment the option of cooling is not compelling. In the previous note we show a factor of 350 decrease in the available antiproton flux at 200 MeV without cooling versus with cooling. We have not estimated the additional costs of introducing stochastic cooling but refer the reader to the copious literature from both CERN and Fermilab.

#### APPROXIMATE COST

We estimate the order of magnitude costs to carry out a test of the scheme. The estimate is scaled from either existing AGS equipment costs or scaled from the Booster proposal. We used a rule of thumb number of about \$150/kilowatt for the power supply estimates. We summarize them in Table I.

TABLE I  
(cost in thousands)

I. EXTRACTION FROM AGS-----		360.
FERRITE KICKER	50.	
POWER SUPPLY	50.	
EXTRACTION SEPTUM	100.	
POWER SUPPLY	100.	
ORBIT BUMP	10.	
POWER SUPPLY	50.	
II. TARGET STATION AND PROTON TRANSPORT-----		1070.
QUADRUPOLES (6)	240.	
POWER SUPPLIES	180.	
TARGET STATION AND LI LENS	650.	

TABLE I - continued

III. P-BAR TRANSPORT AND BOOSTER INJECTION-----		1750.
TRANSPORT TUNNEL(450 FT)	450.	
QUADRUPOLES (10)	400.	
POWER SUPPLIES	300.	
DIPOLES ( 5)	200.	
POWER SUPPLIES	100.	
INJECTION SEPTUM	100.	
POWER SUPPLY	100.	
FAST KICKER	50.	
POWER SUPPLY	50.	
IV. BOOSTER EXTRACTION AND TRANSPORT TO LINAC-----		1010.
EXTRACTION KICKER	100.	
POWER SUPPLY	100.	
QUADRUPOLES (15)	150.	
POWER SUPPLIES	250.	
DIPOLES ( 8)	160.	
POWER SUPPLY	150.	
KICKER	50.	
POWER SUPPLY	50.	
V. INSTRUMENTATION AND CONTROLS-----		500.
VI. CHANGES IN BOOSTER TUNNEL AND BUILDING 914-----		100.
VII. BOOSTER POWER SUPPLY ADDITION-----		1000.
VIII. 200 MHz CAVITY SYSTEM-----		<u>450.</u>
SUBTOTAL-----		6240.
EDIA(@15%)		940.
CONTINGENCY(@20%)		1440.
TOTAL		<u><u>8620.</u></u>

BNL 52082  
AGS/EP&S 87-1  
UC-28  
(Particle Accelerators and  
High-Voltage Machines — TIC-4500)

**PROCEEDINGS  
OF THE  
1986 SUMMER WORKSHOP  
ON ANTIPROTON BEAMS IN THE 2-10 GeV/c RANGE**

**D. Lazarus, Editor**

**May 7, 1987**

**AGS DEPARTMENT**

**BROOKHAVEN NATIONAL LABORATORY  
ASSOCIATED UNIVERSITIES, INC.  
UPTON, LONG ISLAND, NEW YORK 11973**

**UNDER CONTRACT NO. DE-AC02-76CH00018 WITH THE  
UNITED STATES DEPARTMENT OF ENERGY**

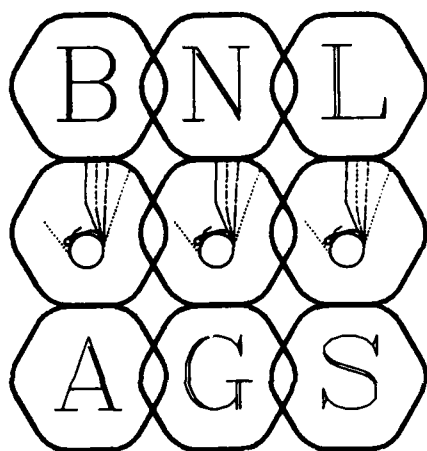
. . .      Table of Contents      . . .

---

<u>Section</u>	<u>Title</u>	<u>Page</u>
1	Introduction. . . . .	1
2	C' Target and 1 km Beam . . . . .	5
3	Summary of Long $\bar{p}$ Beams in the D and D/U Lines. . . . .	9
4	Antiproton Beams from the Booster . . . . .	15
5	Conclusions . . . . .	20

Appendix

1	Antiproton Production Spectra . . . . .	23
2	A Time Separated $\bar{p}$ Beam . . . . .	26
3	General Remarks on Antiproton Beams . . . . .	44
4	Beam Momentum Resolution. . . . .	49
5	High Field Properties of the AGS Booster Dipole Magnet . . . . .	51
6	Very Low Energy Antiprotons . . . . .	59
7	Overview of Booster $\bar{p}$ Potential . . . . .	62
8	Details of Cost Estimates . . . . .	65



PROCEEDINGS OF THE 1986  
SUMMER WORKSHOP ON  
ANTIPROTON BEAMS  
IN THE 2-10 GeV/c RANGE

---

*B.E. Bonner • Rice University*

*H.N. Brown • Brookhaven National Laboratory*

*G. Bunce • Brookhaven National Laboratory*

*A.S. Carroll • Brookhaven National Laboratory*

*G. Danby • Brookhaven National Laboratory*

*H.W.J. Foelsche • Brookhaven National Laboratory*

*J.W. Glenn, III • Brookhaven National Laboratory*

*J. Jackson • Brookhaven National Laboratory*

*T.E. Kalogeropoulos • Syracuse University*

*D.M. Lazarus • Brookhaven National Laboratory*

*D.M. Lee • Los Alamos National Laboratory*

*Y.Y. Lee • Brookhaven National Laboratory*

*D.I. Lowenstein • Brookhaven National Laboratory*

*G.S. Mutchler • Rice University*

*D.C. Peaslee • University of Maryland*

*A.F. Pendzick • Brookhaven National Laboratory*

*L.S. Pinsky • University of Houston*

*H. Poth • Karlsruhe University*

*D.K. Robinson • Case Western Reserve University*

- v -

## A B S T R A C T

The possibilities for building a facility for the formation spectroscopy of "charmonium" and the study of "exotics" at the AGS with high intensity antiproton beams of good resolution and enhanced purity are explored. The performance potential of a number of long beams and the AGS booster are evaluated and costs are estimated. Fluxes of several  $10^7$  antiprotons per pulse with purities of 5% to 99% are possible with conventional long beams. A similar total antiproton flux would be available with the Booster with no beam contamination. This could effectively be enhanced by two orders of magnitude by reducing the momentum spread in order to scan very narrow (less than 1 MeV) resonances. The maximum momentum attainable with the present Booster magnet design is 5.6 GeV/c which only reaches the  $\chi_0(3415)$  charmonium state. Modifications are possible which would raise the maximum momentum to 6.3 GeV/c to include all states up to and including  $\eta'_c(3590)$  in its range. The performance potential for this physics at the AGS is found to compare favorably with that at other laboratories with more antiprotons delivered annually, running in the post-Booster era, than at FNAL or Super-Lear with ACOL under typical scheduling conditions. A high resolution purified source of antiprotons in the 2-10 GeV/c range at BNL would cost \$3.0M - \$4.1M including an experimental hall.

#### ACKNOWLEDGEMENT

*The authors would like to express their gratitude  
to Ms. Joan Depken and Mr. Rippie Bouman  
for their excellent assistance in preparing these proceedings.*





## 1. INTRODUCTION

Since 1980 there have been several proposals to establish the existence of charmonium states not accessible to formation at electron positron colliders, and to determine their masses and widths. Those states with quantum numbers other than  $J^P = 1^-$  -- like the  $\eta_c$ ,  $\chi_0$ ,  $\chi_1$ ,  $\chi_2$ ,  $\eta_c'$  and the  $^1P_1$  -- can be formed in antiproton-proton collisions. They are of interest because their masses and widths can be calculated from QCD-inspired potentials and a non-relativistic Schroedinger equation with a relatively high degree of confidence, thus providing one of the few quantitative tests of the theory. Gluonic degrees of freedom may lead to additional states beside those derived from simple potentials. The initial proposals SPSC/P81-12 at the CERN SPS, E763 at the AGS, R704 at the ISR, and E792 at the AGS were respectively not approved, withdrawn, approved and run for a limited period (three weeks), and not approved.

The SPS experiment using a one kilometer long beam and a high resolution spectrometer would have been capable of yielding a mass resolution of 300 KeV for the  $\chi$  states with an antiproton flux of  $3 \times 10^6$ /pulse and  $\pi/p = 4.1$  by virtue of the long flight path.

Experiment 763 (LBL/Mt. Holyoke/BNL) was proposed at Brookhaven in 1980 and withdrawn following measurements of the antiproton flux in the Medium Energy Separated Beam. The measured fluxes were 85,000  $\bar{p}$  per  $10^{12}$  protons on target at 3.7 and 6.0 GeV/c. Pion contamination was at the 3:4 and 8:1 level in the two cases. These fluxes were a factor of 3 below those anticipated in the proposal and an order of magnitude less than expectations for R704 at the ISR.

Experiment R704 finally ran as sole user of antiprotons in the ISR with a hydrogen gas jet; in the three week period it was able to obtain data indicating the presence of  $\chi_1$ ,  $\chi_2$  and the  $^1P_1$  states and to make crude measurements of the widths. The experiment would have been a success had it not been decided to terminate ISR operations. As a result the experiment obtained 30, 50, and 5 events for the respective states above with a mass resolution of about 2 MeV.

Experiment 792, a proposal similar to the SPS experiment, was submitted to the AGS in 1984. In addition to purification by pion decay over a long flight path, a novel feature was put forward in which the beam would be slowly extracted from the AGS while maintaining the rf

AD-A207 482

POTENTIAL FOR A NEAR TERM VERY LOW ENERGY ANTIPROTON  
SOURCE AT BROOKHAVEN NATIONAL LABORATORY(U) AIR FORCE  
ASTRONAUTICS LAB EDWARDS AFB CA G D NORDLEY APR 89

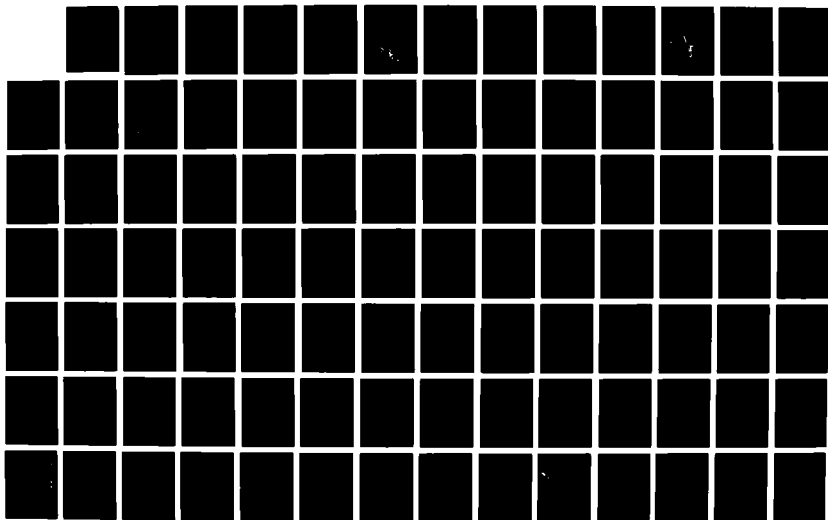
2/3

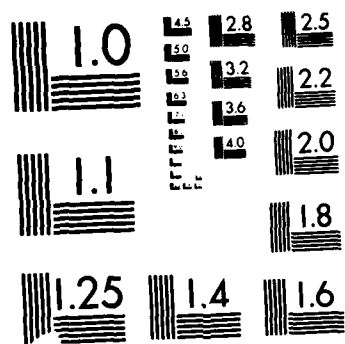
UNCLASSIFIED

AFAL-SR-89-001

F/G 20/7

NL





RESOLUTION TEST CHART  
 NATIONAL BUREAU OF STANDARDS-1963-A

bunch structure intact; a total separation of antiprotons and pions in their time of arrival could be made over the long flight path.<sup>1</sup> Although the physics was considered admirable by the Program Committee, the proposal was not approved because of the high cost of the target station, beam, high resolution spectrometer and remote experimental area.

In 1985 some members of the R704 groups plus new collaborators proposed Fermilab E760, an upgraded version of the ISR experiment to run in the Fermilab Antiproton Accumulator during Tevatron fixed target running periods. Improvement by a factor of 5 in intensity and 4 to 5 in detector solid angle was anticipated. The mass resolution in the  $X_1$ ,  $X_2$  region would be 300 KeV. This is to be compared with a resolution of 20 MeV obtained in radiative  $J/\psi$  decays by the Crystal Ball collaboration and 2 MeV in R704. Experiment 760 may suffer technical difficulties in decelerating the antiproton beam in the accumulator to the  $\eta_c$ , and  $J/\psi$  (an important energy calibration point), but the basic goals can be met. A more serious restriction is the inability to analyze and identify all products of the antiproton-proton interactions over the full solid angle, which is imposed by limited access to and space available in the accumulator ring. This is especially true for the more difficult parts of the experiment where the background may be large or cross section small, as in  $\eta_c$ ,  $^1D_2$ , or  $^3D_2$  states.

The sizable community of physicists active in this field held a workshop at Fermilab in April, 1986 and the proceedings<sup>2</sup> provide an excellent summary of the physics potential in this area. Ideally this physics program could best be carried out with the cooled antiproton beam extracted from the Fermilab accumulator and transported to a large solid angle magnetic spectrometer facility providing good particle identification along with good segmentation. In view of the high priority of Tevatron collider experiments CDF and  $D\bar{0}$ , this is thought to be unlikely.

Because of the great interest in this area of physics and the lack of adequate facilities for this research it was decided to explore the possibilities for a dedicated facility to produce a high intensity purified antiproton beam in the 2-10 GeV/c range at Brookhaven. A workshop was held on August 18-22, 1986, at the AGS Department; several possible options were evaluated, and the results are presented in the following sections.

A new antiproton beam at the AGS should span the range from 2 to 10 GeV/c for the following reasons, in order of ascending momentum:

1. It should connect to the upper momentum of LEAR (2 GeV/c).
2. It should cover the charmonium region.
3. It should reach the  $\Lambda_c \bar{\Lambda}_c$  threshold.

The invariant masses of the states in question are given in Table 1-1, along with the corresponding  $\bar{p}$  beam momenta required for their formation.

Table 1-1. Charmonium and Hyperon-Antihyperon Masses and Beam Momenta for Formation

Channel	$s^{1/2}$ (MeV)	$p(\text{beam})(\text{MeV}/c)$
$\Sigma^+ - \bar{\Sigma}^+$	2379	1854
$\Sigma^0 - \bar{\Sigma}^0$	2385	1871
$\Sigma^- - \bar{\Sigma}^-$	2395	1899
$\Xi^0 - \bar{\Xi}^0$	2630	2582
$\Xi^- - \bar{\Xi}^-$	2643	2621
$\eta_c$	2980	3689
$J/\psi$	3097	4066
$\Omega^- - \bar{\Omega}^-$	3345	4936
$\chi_0$	3415	5192
$\chi_1$	3511	5552
$^1P_1$	3525	5607
$\chi_2$	3556	5724
$\eta'_c$	3590	5860
$D^+ - \bar{D}^-$	3739	6444
$^3D_1$	3772	6580
$^3D_2 / ^1D_2$	(3852/3860)*	6910/6940*
$\Lambda_c - \bar{\Lambda}_c$	4562	10109
$\Sigma_c - \bar{\Sigma}_c$	4900	11819

\* Predicted

A variety of particle studies is accessible to  $\bar{p}$  beams in this energy range: ordinary hadron pairs and their excited states--already observed in  $e^+e^-$  collisions<sup>3</sup>--will be much more copious here. Extension of Regge trajectories is facilitated by high initial thresholds, which  $\bar{p}p$  provides; and the precise momentum control will enable angular analysis to separate out individual states. Exotics such as the U(3.1) should be readily observed,<sup>4</sup> representing a broad field of study if their existence can be established. There is, in addition, the possibility of charm production in both boson and baryon hosts, but that is the most extreme goal. Although charm may be the most glamorous topic, it may ultimately prove less significant for  $\bar{p}p$  pursuit than the larger bulk of other studies outlined above.

As a reference standard the yield of antiprotons measured at CERN has been used.<sup>5</sup> Corrected to AGS operating conditions, this becomes

$$Y = 1.2 \times 10^{-6} \bar{p} \text{ (2 msr \% interacting proton)}^{-1} \quad (1.1)$$

at 5 GeV/c. Equation (1.1) agrees with the Sanford-Wang semiempirical calculation.<sup>6</sup>

For comparison of the various options below, the standard antiproton flux is assumed:

$$F = f Y \Delta \Omega \Delta p/p = 4.0 \times 10^{-6} \bar{p} \text{ (beam proton)}^{-1} \quad (1.2)$$

where  $f \approx 1/3$  is the fraction of beam protons that interact in the target. For the long beam line options the standard assumption is  $\Delta \Omega = 5$  msr,  $\Delta p/p = .04$ , which is consistent with the prototype long antiproton beam design of H.N. Brown.<sup>7</sup> The acceptance determined for the booster is  $\Delta \Omega = 40$  msr,  $\Delta p/p = .02$ . In order to capture such a large solid angle from the antiproton production target, a lithium lens would be employed with chromatic aberrations that reduce the effective beam proton fraction to  $f \approx 1/9$ . The lithium lens might also enhance  $F$  in other options but is most attractive in the booster option where one would not have to deal with the corresponding increase in pion flux: cf. Table 3-1.

#### References

1. AGS Experiment 626, T. Kalogeropoulos et al.
2. Proceedings of the First Workshop on Antimatter Physics at Low Energy, April 10-12, 1986. Fermi National Accelerator Laboratory.
3. ARGUS Collaboration, Phys. Lett. 183B, 419 (1987).
4. M. Bourquin et al., Phys. Lett. 172B, 113 (1986).
5. See Appendix 1 for further details.
6. J.R. Sanford and C.L. Wang, BNL 11749 (May, 1979).
7. Included here as Appendix 2.

## 2. C' TARGET AND 1 KM BEAM

T. Kalogeropoulos, Group Leader  
B. Bonner                      G. Mutchler  
H. Brown                      A. Pendzick  
D. Lee                         K. Robinson

### I. Introduction

The primary objective of this group was to reduce the cost of the one kilometer antiproton beam in AGS proposal E792, which is shown in Fig. 2-1. We find that a suitably redesigned beam can be built for about \$2.0M plus \$0.8M for an experimental area. The cost of the experimental area can be reduced by locating it adjacent to the RHIC open area. This reduces the beam length to 800 meters. These costs do not include the high resolution spectrometer.

### II. Beam Characteristics

Table 2-1 summarizes the beam characteristics. All distributions relevant to the beam in E792 apply here. An achievable time-of-flight resolution of  $\delta t = 100$  psec is assumed. Advantages of this beam design include the following:

1. Compatibility with the SEB program.
2. The muon g-2 ring can be fed from this beam with pion or muon injection.\*
3. Construction can start immediately.
4. It does not interfere with RHIC.

A disadvantage is the sacrifice of the LESBII.

Table 2-1. C' BEAM CHARACTERISTICS

Momentum range:	2-11 GeV/c
Momentum bite $\Delta p/p$ :	.04
Angular acceptance $\Delta\Omega$ :	5 msr
Maximum $\bar{p}$ flux $(10^{13} \text{ beam prot.})^{-1}$ :	$4 \times 10^7$
Length (meters):	1000 (800)
Purity $\pi^-/\bar{p}$ (5 GeV/c):	7:2 (7:1)
$\bar{p}$ production target location:	C' target moved upstream 6 m
$\bar{p}$ experiment location:	stand-alone hall (RHIC-dependent hall)

\* The muon g-2 experiment has been sited elsewhere since the conclusion of the workshop.



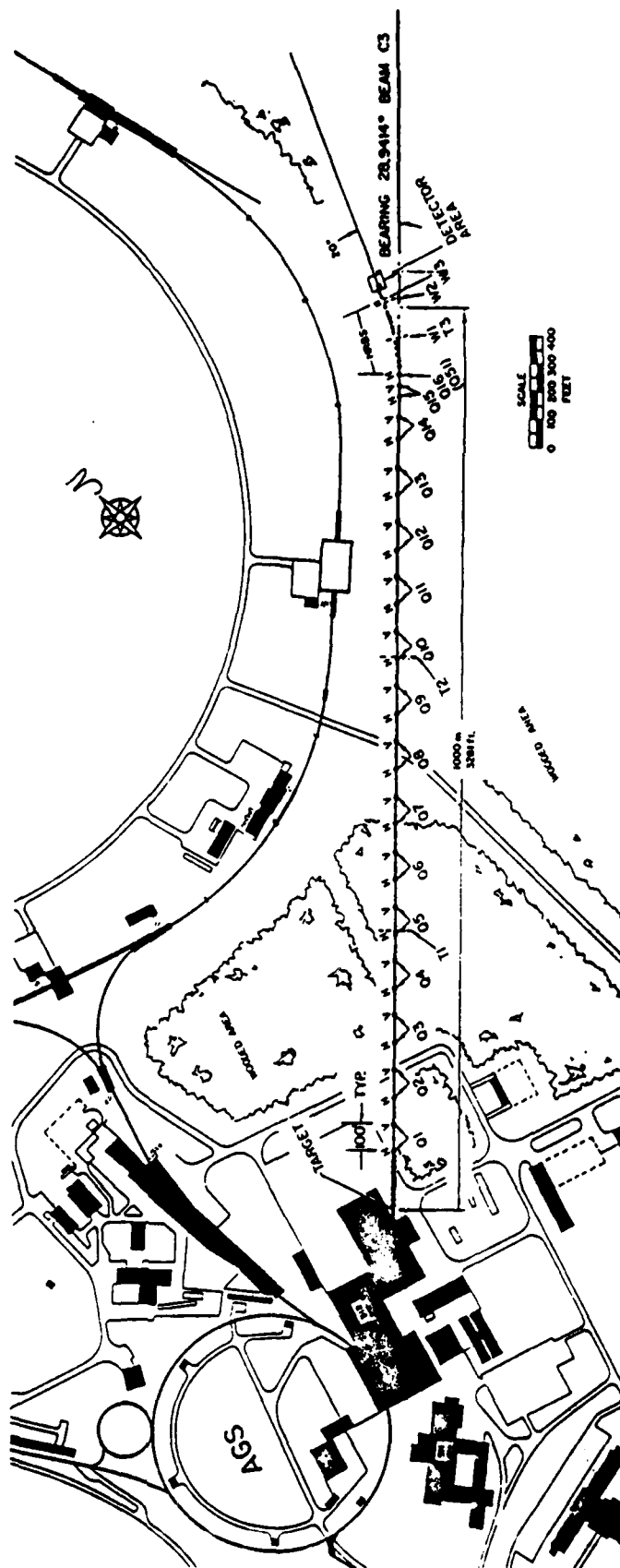


Fig. 2-1. Antiproton C' Line Option

### III. Discussion

#### 1. Front Region

In the E792 design the LESBII was unaffected. New shielding and a difficult construction area resulted in \$4.0M as a cost estimate. The present recommendation moves the C' target upstream and places the front end (which selects momentum and dumps the primary proton beam) inside the building where all utilities, a crane and the shielding of LESBII are available. In this case the cost is brought down to \$825K.

The estimate of \$825K includes the cost of 5 quadrupoles at \$40K each and 5 dipoles (18D72 or equivalent) at \$95K each. This front end for the beam will select momentum bites down to  $\pm 0.3\%$ . The 11 GeV/c momentum covers production of  $\Lambda_c \bar{\Lambda}_c$  and  $\Sigma_c \bar{\Sigma}_c$  pairs. The dogleg configuration presented in E792 is preferred; another configuration with two dipoles discussed in H. Brown's report (Appendix 2) is also possible and less expensive, but the minimum momentum bite is  $\pm 1\%$ . Such a large minimum is likely to limit the effective luminosity of experiments on narrow charmonium states.

#### 2. Transport Region

The original cost estimate of the beam FODO transport was \$1832K. This estimate was made with the beam being built above ground. The cost reduces to \$1323K if the beam is trenched in at the AGS beam height.

#### 3. Experimental Area

An experimental area 40'W x 60'L x 30'H can be built at a cost of \$755K. The cost can be reduced if this area is close to the RHIC "Open Area" experimental hall where electrical utilities and cooling water are available. In this case the beam length would be 800 meters, and the cost of the experimental area is \$430K. This will, in addition, produce a 20% reduction in the cost of the transport.

#### 4. High Resolution Beam Spectrometer (HRBS)

The HRBS allows tagging of antiprotons with a resolution  $\Delta p/p = 2 \times 10^{-4}$  with resultant  $\bar{p}p$  center-of-mass resolution of about 300 KeV in

the charmonium region. Such resolution is necessary in order to measure widths of narrow ( $\lesssim 1\text{-}2\text{ MeV}$ ) states and to reduce associated background. The original cost estimate for this spectrometer amounted to \$1660K, half of which was the cost for new 18D72 dipoles or their equivalent.

Considering the Fermilab jet target accumulator experiment (E760) with an expected resolution of 300 KeV/c and the absence of background in  $\bar{p}p \rightarrow \gamma + J/\psi$  as observed in ISR Experiment R705, the group concluded that the spectrometer is highly desirable. Every effort should be made, moreover, to see whether magnets can be made available rather than relax the resolution and install the HRBS later. It will be more expensive as an add-on.

#### 5. Other Options

The group considered bending the beam by  $180^\circ$  halfway downstream and bringing it back to the LESBII experimental hall. The cost of the  $180^\circ$  bend has been estimated to be about \$2.0M. Such a configuration is attractive and offers the possibility of making a storage ring. Because of the cost it has not been pursued further.

#### IV. Cost Summary

Table 2-2 summarizes the costs of this option. A more detailed breakdown is presented in Appendix 8.

Table 2-2. COST SUMMARY - C' LINE OPTION

	Cost (K\$)	Labor (MW)
Proton transport and target region	825	447
Beam transport	1323	627
Experimental area - 1000m	755	25
(800m)	(430)	(25)
TOTAL	2903	1099
	(2578)	(1099)
High Resolution Beam Spectrometer (HRBS) 1070		300

### 3. SUMMARY OF LONG $\bar{p}$ BEAM IN THE D AND D/U LINES

H. Poth, Group Leader  
H. Brown  
J. W. Glenn, III  
H. Foelsche  
D. Lowenstein  
A. Pendzick

#### I. Introduction

This group considered the following possible approaches to a long, decay purified antiproton beam. Their locations are shown in Fig. 3-1.

##### 1. Option U

The production target is installed in the U-line between the 8° and the 10° bends.<sup>1</sup> The captured antiprotons are transported through the RHIC transfer line into the injection area in the RHIC tunnel, deflected upwards to exit the tunnel at ground level, and transported to a new experimental hall next to the compressor building. Requirements include:

- i. Installation of a slow extraction system for the U-line from the AGS.
- ii. Bypass of the neutrino production target.
- iii. Deflection out of the RHIC injection section,  $\bar{p}$  transport to the experimental hall.
- iv. Cut in the transfer tunnel for shielding.

##### 2. Option D/U

The production target is installed in the D-line as far upstream as possible.. From there the  $\bar{p}$  beam is bent 30° into the AGS tunnel and transported to the U-line with which it is merged shortly behind the U-line extraction point from the AGS at H10. The rest is equivalent to the previous option. This lengthens the beam by about 200 meters. Requirements include:

- i. Beam transport from the production area to the RHIC transfer line.
- ii. Deflection out of the RHIC injection section,  $\bar{p}$  beam transport to the experimental hall.

### 3. Option D/(g-2) \*

Here a production target in the D-line is also used as a pion production target for the muon g-2 experiment. Downstream of the target and the first quadrupoles is a switch magnet that serves either the g-2 ring or the  $\bar{p}$  beam. From the switch magnet there follows a straight  $\bar{p}$  beam transport to the injection section of RHIC, where a separate experimental hall is needed.

### 4. Option D/(g-2)' \*

The same front end as for D/(g-2) is followed by an additional 20° bend at the end of the parking area. This directs the beam to the RHIC wide angle hall, which is used as the experimental hall for  $\bar{p}$  experiments. Requirements include beams transport from the production target to the experimental hall.

## II. Beam Characteristics

The  $\bar{p}$  beams of this section are listed in Table 3-1. The acceptance of the U-line is restricted; this is slightly ameliorated when the U-target station is used because of better beam focus. As one can see from the table, the beam properties do not differ very much. Whatever option is considered, the requirements for the following items are practically invariant:

1. Proton beam focus on the production target.
2.  $\bar{p}$  production target and shielding.
3.  $\bar{p}$  capture into transfer line.
4. Experimental hall.

Further remarks on the features of conventional antiproton beams can be found in Appendix 3.

## III. Discussion

One should note the importance of small beam emittance if one wants to momentum analyze the antiproton beam or use a long target of small diameter. Moreover, low emittance facilitates the use of a beam separator. The

\* The muon g-2 experiment has been sited elsewhere since the conclusion of the workshop.

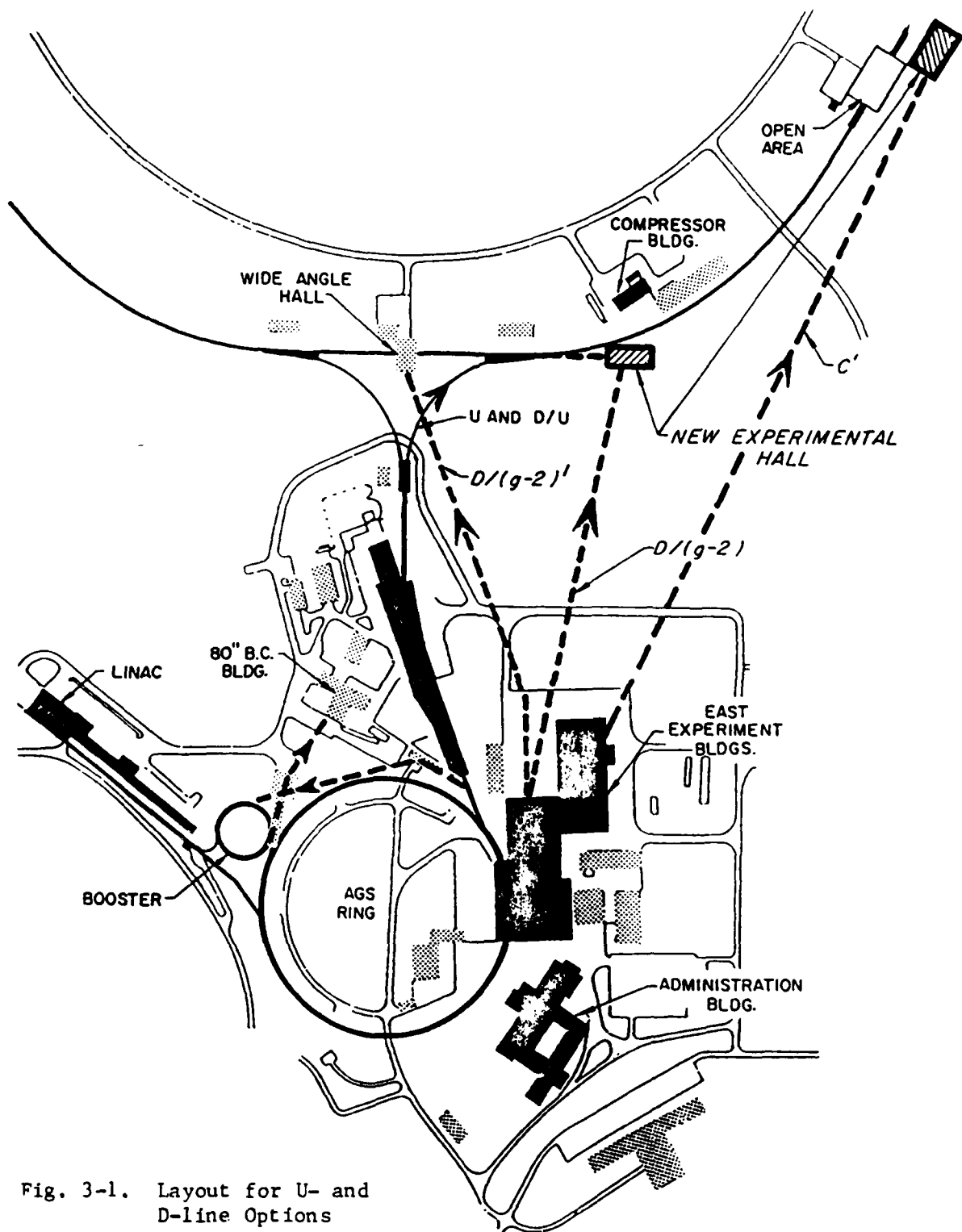


Fig. 3-1. Layout for U- and D-line Options

Table 3-1. U AND D LINE BEAM CHARACTERISTICS

	Options:	<u>U-line</u>	<u>D/U line</u>	<u>D/(g-2)</u>	<u>D/(g-2)*</u>
Momentum range (GeV/c):		2 - 10	2 - 10	2 - 10	2 - 10
Momentum bite $\Delta p/p$ :		.02	.02	.04	.04
Angular acceptance $\Delta\Omega$ (msr):		*1.7	*0.8	**7	**7
Maximum $\bar{p}$ flux ( $10^{13}$ beam prot.) <sup>-1</sup> :		$0.7 \times 10^7$	$0.3 \times 10^7$	$5 \times 10^7$	$5 \times 10^7$
Purity $\pi^-/\bar{p}$ (5 GeV/c):		14:1	7:1	21:1	14:1
Length (meters):		500	700	600	650
$\bar{p}$ production location:		U target	D target	D target	D target
$\bar{p}$ experiment location:		New hall near RHIC compressor building - - - -			
					RHIC wide angle hall

\* Special restrictions of U-line, combined with improved focus at U production target.

\*\* To fill the angular acceptance of 20 msr will require a lithium lens, which introduces a chromatic aberration loss factor of about 1/3: hence a net effective solid angle of  $20 \times (1/3) \approx 7$  msr. See Appendix 6 for the same considerations applied to the booster option.

beam length is of importance mostly at higher momenta, since for a length below 1 km, the decay purification is not very good and the  $\pi^- \bar{p}$  flight time difference does not allow an effective separation. At 4 GeV/c and below, however, a beam length of 600m should suffice.

From experimental considerations, it is apparent that we should examine in more detail how to get rid of other negative particles (electrons, muons, pions) in the beam. They cause high accidental rates in detectors, in particular beam time-of-flight counters, and ultimately limit the rate at which an experiment can run. Not all possibilities were checked in detail, but there are essentially three ways to achieve greater purity of  $\bar{p}$  beams:

1. A fast kicker near the end of the beam line.
2. An rf separated beam using one separator.
3. A two rf separator beam.

The first two methods require bunched extraction from the AGS. While a fast kicker could do the job in a long line (perhaps by installing it at the vertical bend in the RHIC injection station for options U and D/U), the use of rf separators would render a long antiproton beam unnecessary. The use of two rf separators at high frequency -- e.g., 2.9 GHz -- with slow extraction of a debunched beam would be compatible with the rest of the program. This would avoid the poor duty cycle that would result with bunching at the AGS frequency. This possibility should be considered in the future in more detail.

With respect to the future extension of a long antiproton beam line, options U, D/U, and D/(g-2)' provide the possibility of injecting the antiproton beam into RHIC and transporting it to any desired experimental area. Hence the beam length can be extended considerably. What might be even more interesting in this respect is the possible "loan" of a sophisticated RHIC detector for an antiproton experiment.

In summary, none of the options has an outstanding advantage over the others, and different criteria have to be found to select the right option. Cost and compatibility with the rest of the program are most important.



#### IV. Cost Summaries

Table 3-2 contains cost summaries for the various options in comparative form. A more detailed breakdown is presented in Appendix 8.

#### References

1. H. Poth, "A New Approach to a Pure Antiproton Beam at GeV Energies", BNL EP&S Tech. Note 110 (May 1985); also presented at Brookhaven HEDG meeting in April 1986.

Table 3-2. COST SUMMARIES - LONG P BEAM STUDIES

Options:	U-line		D/U-line		D/(g-2)		D/(g-2)'	
	Cost (K\$)	Labor (MW)	Cost (K\$)	Labor (MW)	Cost (K\$)	Labor (MW)	Cost (K\$)	Labor (MW)
Extraction system	500	186						
Proton transport	155	83	190	26	190	62	190	62
Target region	1105	113	650	228	275	119	275	119
Beam transport	1130	364	1865	656	724	309	1348	486
Experimental area	<u>455</u>	<u>25</u>	<u>455</u>	<u>25</u>	<u>455</u>	<u>25</u>	—	—
Totals	<u>3345</u>	<u>771</u>	<u>3160</u>	<u>935</u>	<u>1644</u>	<u>515</u>	<u>1813</u>	<u>667</u>

#### 4. ANTIPROTON BEAMS FROM THE BOOSTER

A.S. Carroll, Group Leader  
 Y.Y. Lee  
 D.C. Peaslee  
 A.L. Pendzick  
 L.S. Pinsky

##### I. Introduction

The concept is outlined in Fig. 4-1. In each AGS cycle the booster is filled with protons and operates normally, ejecting into the AGS. After acceleration in the AGS, fast extraction of 3 rf beam bunches occurs at H10 into the U-line where they are focused on an antiproton production target. The remaining 9 AGS bunches are available for other purposes. The antiprotons are collected by a lithium lens and transported at 4 GeV/c, near peak production, to the booster where they are injected through the proton extraction channel, running in reverse direction around the booster. They are then extracted in one straight section with a moderately thick septum tangent to the AGS and transported directly to the 80-inch bubble chamber complex, which serves as an experimental area.\* The extraction and transport occurs during the AGS spill. The booster is then ready to accept the next charge of protons at the usual repetition rate.

##### II. Beam Characteristics

Table 4-1 summarizes the beam characteristics which are further explained in the following paragraphs.

The booster magnet system as presently designed can reach an antiproton momentum of 5.2 GeV/c at 12.7 kg corresponding to a center-of-mass energy in  $\bar{p}p$  collisions of  $s^{1/2} = 3.42$  GeV. This would allow formation of  $\eta_c(2980)$ ,  $J/\psi(3100)$ , and  $\chi_0(3415)$  but nothing higher in the hidden charm sequence. A more desirable limit physically is  $s^{1/2} = 3.70$  GeV, corresponding to a  $\bar{p}$  momentum of 6.3 GeV/c, which would allow production of  $\psi'(3685)$ ,  $\eta_c'(3590)$  and all the  $\chi$  states. More detailed studies in Appendix 5 address the feasibility of such an extension in momentum range.

\* The 80-inch bubble chamber building has been chosen as the Experimental Hall for the muon g-2 experiment since the time of the workshop.

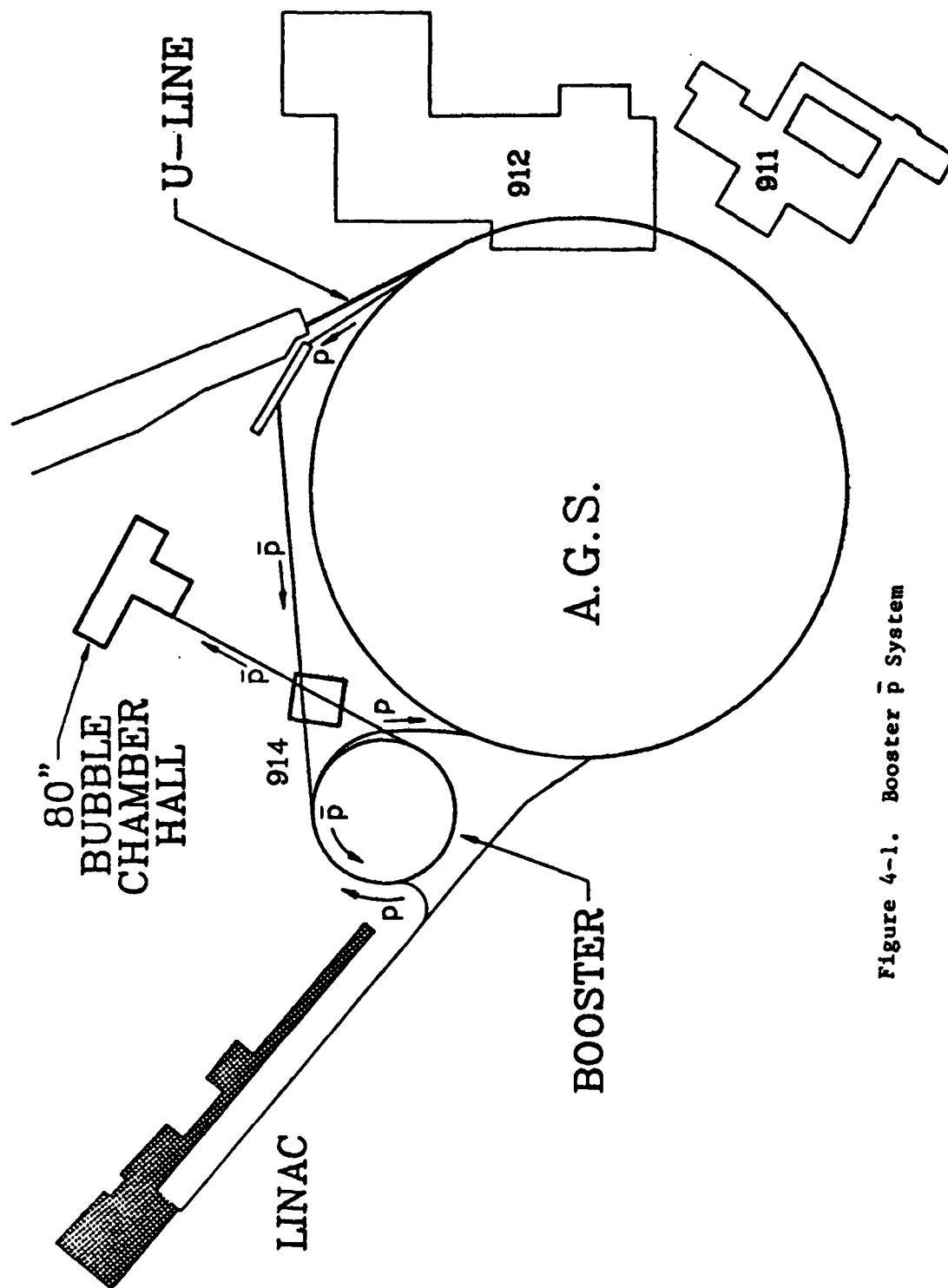


Figure 4-1. Booster  $\bar{p}$  System

Table 4-1. BOOSTER ANTIPROTON BEAM CHARACTERISTICS

Momentum range:	0.65 - 5.2 GeV/c
Momentum acceptance $\Delta p/p$ :	.02
Angular acceptance:	40 msr
Maximum $\bar{p}$ flux ( $10^{13}$ beam prot.) <sup>-1</sup> :	$4 \times 10^7$
Purity $\pi^-/\bar{p}$ (all momenta):	0:1
Length (meters):	(not relevant)
$\bar{p}$ production target location:	U-line target
Experimental Area:	80" bubble chamber bldg. *

The momentum spread of  $\pm 1\%$  delivered from the  $\bar{p}$  production target can be reduced to  $\sim 10^{-4}$  by debunching, and further by phase displacement acceleration during extraction. It is important to note that this procedure compresses the  $\Delta p$  of the total  $\bar{p}$  flux without loss of particles; a double advantage results--wide  $\Delta p$  for search and scan, narrow  $\Delta p$  for study of a resonance already located.

The purity of the extracted  $\bar{p}$  beam is essentially perfect, since the booster ring functions as an extremely long beam line with very large dispersion.

The muon g-2 experiment can use the same target and experimental area. Since both  $\bar{p}$ 's in the booster and g-2 require fast extraction and there are no slow extraction requirements in the U-line, the compatibility may be better than in other lines such as C' and D where experiments requiring slow extraction are also mounted.

The availability of antiprotons from this system must wait on completion and commissioning of the booster. Under ideal conditions this could occur as early as 1990, but it seems more realistic to allow early 1991 as the initial date likely for antiproton experiments. Of course the target and direct beam line to the experimental area can be built at once and used for antiproton and muon g-2 studies.

The cost estimate for 5.2 GeV/c antiprotons is detailed in Table 4-2 and includes all necessary modifications to the booster itself, as well as the extra costs of going to 6.3 GeV/c.

\* The 80" Bubble Chamber building has been chosen for the muon g-2 experimental area since the conclusion of the Workshop. An extension to this building would provide an ideal experimental area at low cost by utilizing existing services.

### III. Discussion

#### 1. Advantages

The specifications above already display some of the advantages of this concept, but it may be worthwhile to recount a more complete list:

- i. Pure  $\bar{p}$  beam with no muon halo.
- ii. High flux,  $\bar{p}$ 's always taken at production maximum.
- iii. High resolution ( $10^{-4}$ ) without additional means such as HRBS.
- iv. Momentum compression with existing booster rf.
- v. Continuously tunable momentum.
- vi. Well equipped experimental hall immediately available.\*
- vii. Compatible with AGS slowly extracted beam (SEB) operation.
- viii. Nearly ideal compatibility with muon g-2 experiment.
- ix. Very flat spill, booster acts as  $\bar{p}$  stretcher.
- x.  $\bar{d}$  beams available without modification.
- xi. Very low momentum antiprotons also possible (cf. Appendix 6).

#### 2. Disadvantages

The principal drawbacks of this scheme are as follows:

- i. The time before availability is approximately 4 years.
- ii. The maximum momentum  $\bar{p} \lesssim 5.2$  GeV/c with the present booster design.

If the present concept appears viable, it will be necessary to make immediate plans for adapting the booster as described, in order to incorporate the needed changes in construction.

### IV. Cost Summary

The cost summary in Table 4-2 assumes the use of the present H10 extraction system and of all shielding in the proton target area already provided for the muon g-2 experiment, as well as the same target. If it should not prove possible to use the same target, the booster option must

\* The 80-inch bubble chamber building has been chosen as the Experimental Hall for the muon g-2 experiment since the time of the workshop.

include the cost of a primary target station, which is included as a contingency. If, however, the preferred extraction for g-2 is at I-10 then locating there would effect savings in the  $\bar{p}$  transport line and bending magnets.\* A more detailed breakdown is presented in Appendix 8.

The preliminary cost estimate of \$3.6M is on the same order as any other scheme that produces  $\bar{p}$  beams of comparable flux, purity, resolution and controllability.

Table 4-2. COST SUMMARY - BOOSTER OPTION

	Cost (K\$)	Labor (MW)
Target region	945	123
50° bend and $\bar{p}$ transport to booster	1016	378
Booster magnet modifications to reach 6.3 GeV/c**	990	284
Transport to 80" bubble chamber	626	175
Experimental area	<u>430</u>	<u>25</u>
TOTAL	<u>4107</u>	<u>985</u>

\* I-10 has been chosen for extraction to a target for the muon g-2 experiment since the conclusion of the workshop.

\*\* The 80" Bubble Chamber building has been chosen for the muon g-2 experimental area since the conclusion of the Workshop. An extension to this building would provide an experimental area at low cost by utilizing existing services.

## 5. CONCLUSIONS

The highest performance option for a purified intense antiproton beam at the AGS would clearly be the booster option if not for the limited momentum range. The ability to vary the momentum spread is a unique and powerful tool for formation spectroscopy. Once a given state has been located in a scan with a relatively large momentum bite e.g.  $\frac{\Delta p}{p} = .02$ , the bite could then be reduced to scan an object of width less than 1 MeV. This amounts to an increase in effective luminosity by the same two orders of magnitude. This would not be possible in the long beam options. Unfortunately the top momentum of 6.3 GeV/c would not permit formation of the  $^1D_2$  and  $^3D_2$  states. The economic and political aspects of further modifying the booster design at this stage would weigh heavily on this option.

The long flight path beams are in general not terribly different from one another in performance or cost. The most attractive is the beam from the C' target area to a new area adjacent to the RHIC Open Experimental Area. It is the longest beam and would deliver antiprotons to a "bargain" experimental hall, which would obtain power and water from the Open Area Hall. The other long beam options suffer somewhat in their shorter lengths and compromises with other installations such as the neutrino area and RHIC injection and experimental areas.

The high resolution spectrometer would be necessary for any of these beam line options to be competitive in the measurement of widths of charmonium states. At best, time-of-flight can yield resolutions approaching 2 MeV in the center-of-mass, even if one ignores the very high rates in the beam counter hodoscopes due to more than  $10^8$  beam pions per spill.

The momentum resolution is plotted as a function of momentum, for each of the beams under consideration, in Fig. 5-1. A similar plot for the center-of-mass resolution is given in Fig. 5-2.

Table 5-1 compares costs of all the schemes considered here.

Table 5-1. OVERALL COST SUMMARY

	Cost (M\$)	Labor (MW)
C' Option	2.90	1099
(with inexpensive hall)	(2.58)	(1099)
U-line Option	3.16	771
D/U-line Option	2.60	757
D/(g-2) Option	1.64	515
D/(g-2)' Option	1.81	667
High Resolution Beam Spectrometer for above	1.07	300
Booster Option	4.11	985

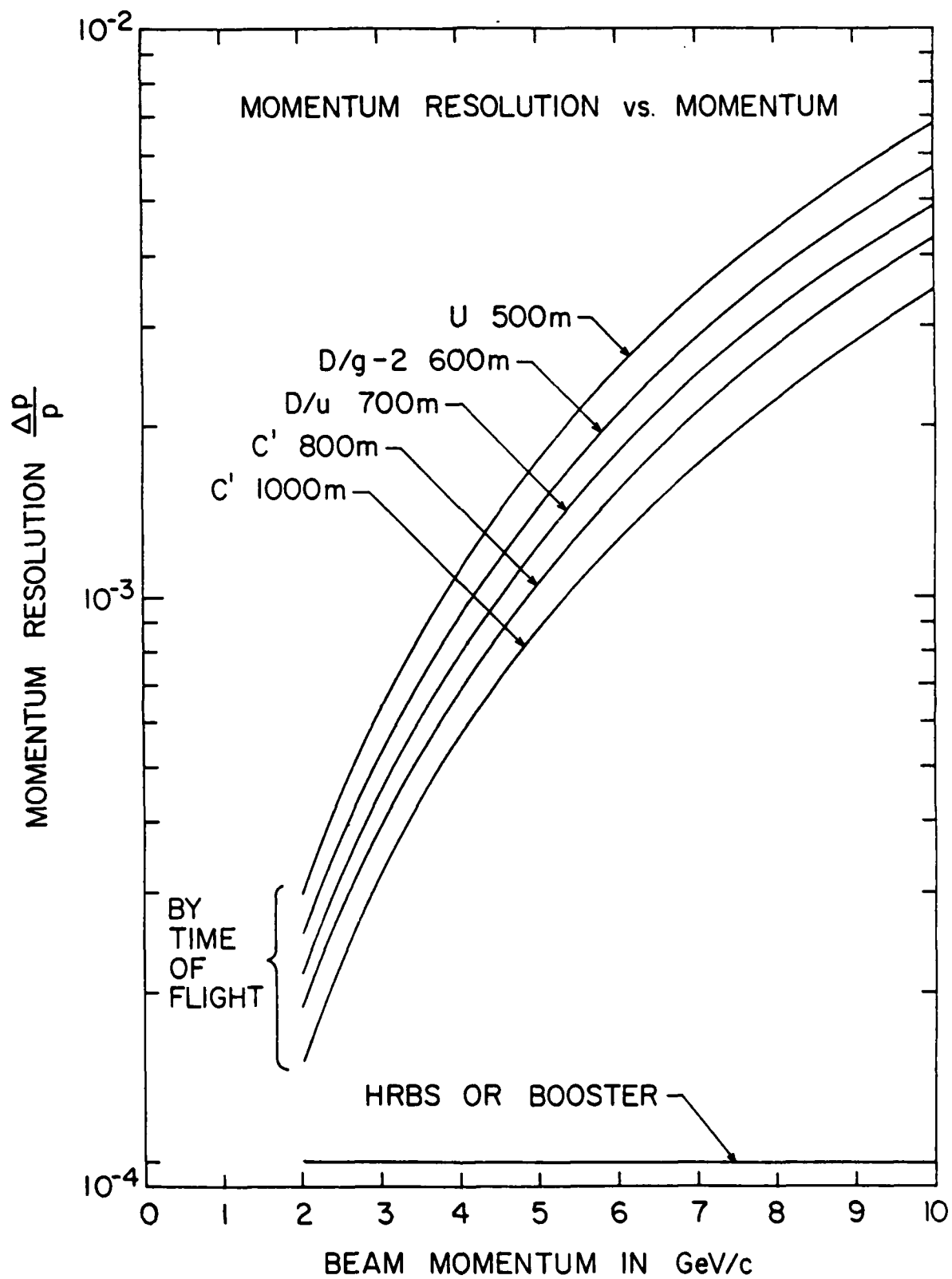


Fig. 5-1. Momentum resolution for the various beam options.



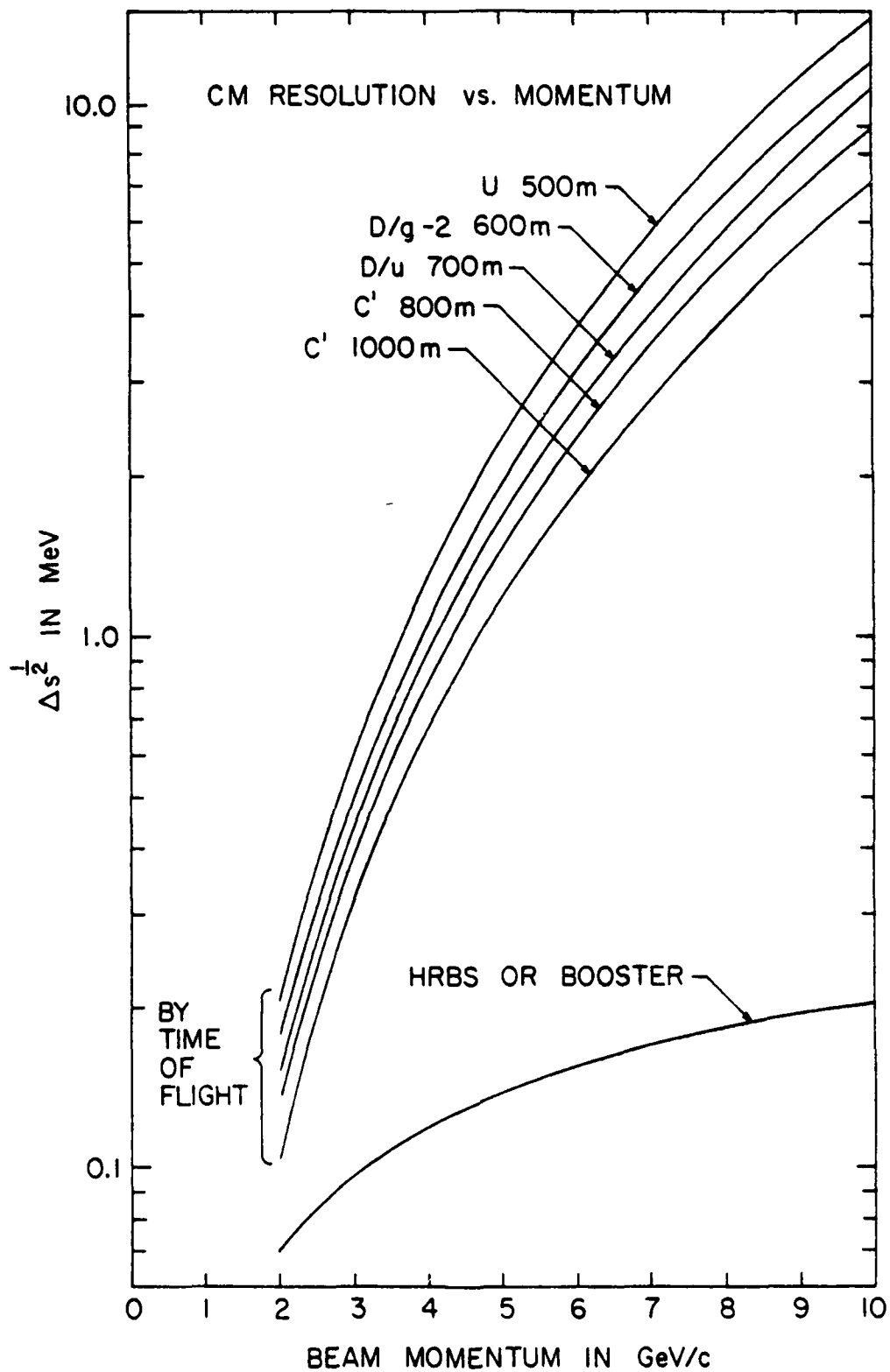


Fig. 5-2. Center-of-mass resolution for the various options.

## APPENDIX 1. Antiproton Production Spectra

D. M. Lazarus

### I. CERN Results

The antiproton production originally assumed<sup>1</sup> in the design of the CERN Antiproton Accumulator (AA) was  $d\sigma_0 = 2.46 \pm 0.42 \times 10^{-2} \bar{p}$  (sr GeV/c interacting proton)<sup>-1</sup> based on measurements<sup>2</sup> with 23 GeV/c protons on a Pb target on a supposed spectral maximum for antiprotons of 4 GeV/c. The antiproton flux measured at the AA was a factor 3-4 lower than anticipated.<sup>3</sup> The production cross section was accordingly reduced by a factor of 2. The numerical value for the yield is then

$$\begin{aligned} Y &= 2 \times 10^{-2} \times 4 \times d\sigma \\ &= 0.98 \pm 0.17 \times 10^{-6} \bar{p} \text{ (2 msr \% -interacting proton)}^{-1}. \end{aligned} \quad (\text{A1.1})$$

for production of 4 GeV/c antiprotons by 23 GeV/c protons.

To scale to AGS operating conditions, we use the Sanford-Wang formula<sup>4</sup> for the increase of primary energy to 28.3 GeV, and to account for peak production momentum of 5 GeV/c instead of 4 GeV/c. Thus,

$$Y_A = 1.2 \pm 0.2 \times 10^{-6} \text{ (2 msr \% interacting protons)}^{-1} \quad (\text{A1.2})$$

which appears as Eq. (1.1) in the text. No correction for target material is made.

### II. Sanford-Wang Formulas

The yield predicted by Sanford-Wang formulas for antiproton production<sup>4</sup> from 28.3 GeV protons on Be is shown in Fig. A1-1, averaged over two different solid angles about 0°: 5 msr and 40 msr. The first is appropriate to long beam line options, the second to the booster. The 5 msr curve has a broad maximum between  $\bar{p}$  momenta of 5 and 6 GeV/c at  $Y = 1.3 \times 10^{-6}$ , the 40 msr curve peaks at 4-5 GeV/c with a maximum  $Y = 0.9 \times 10^{-6}$ . The difference arises from greater weighting of wide-angle production in the second case.

To convert to anticipated  $\bar{p}$  flux, we assume  $f = 1/3$  as the fraction of beam protons that interact in the production target. Hence for beam

line options with  $\Delta\Omega = 5$  msr and  $\Delta p/p = .04$  the peak flux is

$$\begin{aligned} F &= f Y \Delta\Omega \Delta p/p = (1/3) \times 1.2 \times 10^{-6} \times 5 \times 2 \\ &= 4 \times 10^{-6} \bar{p} \text{ (beam proton)}^{-1} \end{aligned} \quad (\text{A1.3})$$

For the booster option, chromatic aberrations in the lithium lens induce a further reduction in  $f$  by a factor 3: namely,  $f = 1/9$ . Then with  $\Delta\Omega = 40$  msr and  $\Delta p/p = .02$  the peak flux becomes

$$F = (1/9) \times 0.9 \times 10^{-6} \times 40 \times 1 = 4 \times 10^{-6} \bar{p} \text{ (beam proton)}^{-1} \quad (\text{A1.4})$$

This is the same number as in Eq. (A1.3) and is adopted in Eq. (1.2) of the text.

### III. AGS Medium Energy Separated Beam (MESB)

The MESB<sup>5</sup> at the Brookhaven AGS has a calculated acceptance of  $\Delta\Omega \Delta p/p = 0.3 \times 6 = 0.9$  msr % and a production angle of  $3^\circ$ . At both 3.7 and 6 GeV/c the Sanford-Wang prediction is  $2 \times 10^5 \bar{p}$  ( $10^{12}$  beam protons)<sup>-1</sup>. The measured values<sup>6</sup> are  $0.9 \times 10^5$  and  $.85 \times 10^5$  with  $\pi/p \approx 3:4$  and  $8:1$

ratios respectively. This flux is more than a factor 2 lower than expected. It is possible that the mass slit and momentum jaws were not adjusted to full beam acceptance because of the high degree of pion contamination.

#### References

1. "Design Study of a Proton-Antiproton Colliding Beam Facility," CERN/PS/AA/78-3.
2. D. Dekkers et al., Phys. Rev. 137, B962 (1965).
3. E. Jones et al., IEEE Trans. Nuc. Sci. 30, 2778 (1983).
4. J.R. Sanford and C.L. Wang, BNL 11479 (May, 1967).
5. C.T. Murphy and J.D. Fox, BNL 18627 (January, 1974).
6. Brookhaven E763 internal memorandum (March, 1981).

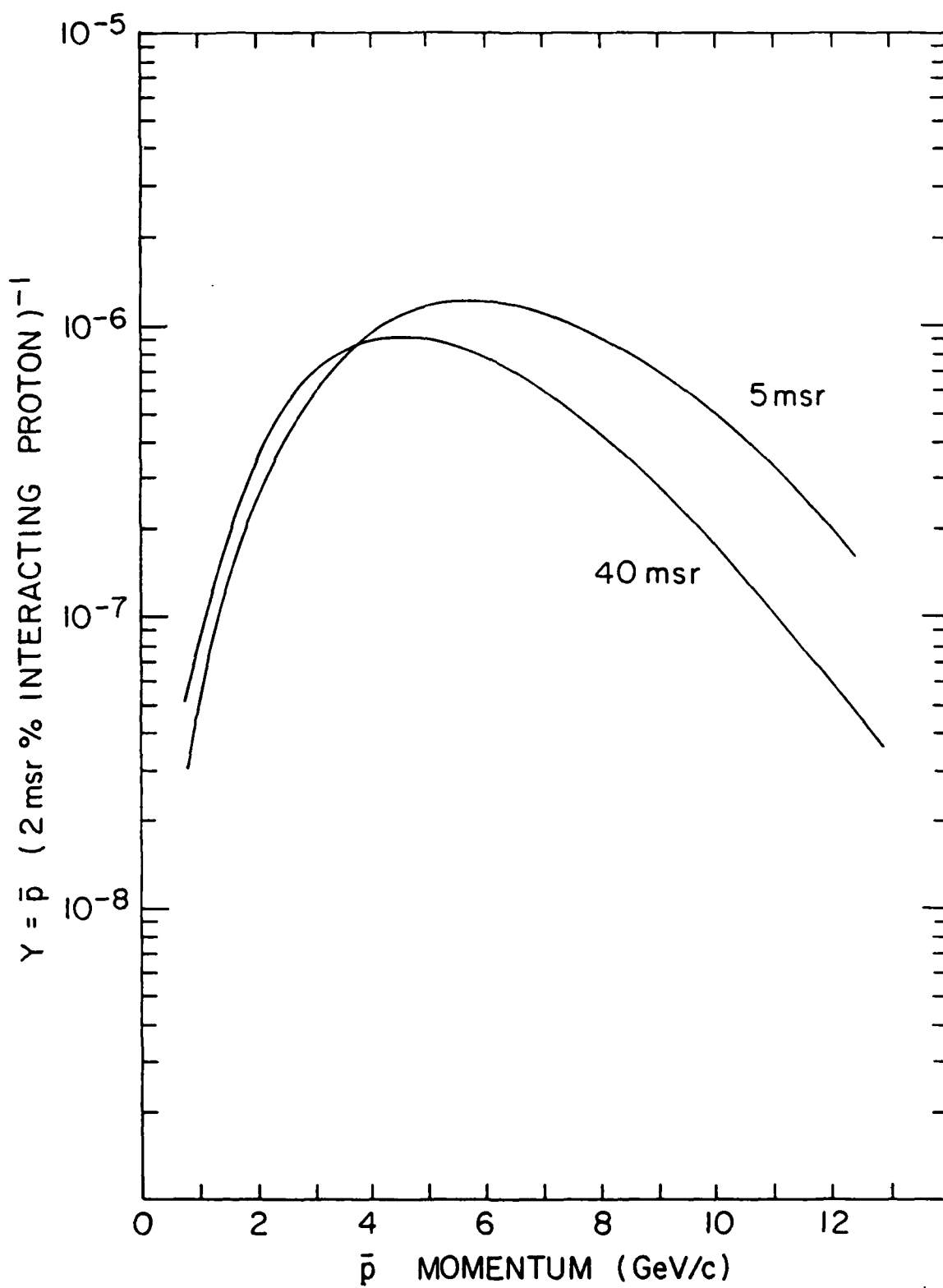


Fig. A1.1. Antiproton yield for 28.3 GeV/c protons on Be

APPENDIX 2. A Time Separated  $\bar{p}$  Beam

H. N. Brown

Accelerator Department

BROOKHAVEN NATIONAL LABORATORY  
Associated Universities, Inc.

EP&S DIVISION TECHNICAL NOTE

NO. 90

H. Brown

June 2, 1980

A TIME SEPARATED  $\bar{p}$  BEAM

This was originally issued as BNL EP&S Division Technical Note No. 90, June 1, 1980. It is reproduced here in its original form.

## A Time Separated $\bar{p}$ Beam

### I. Introduction

In 1974, Fainberg and Kalogeropoulos<sup>1</sup> measured the time structure of a resonant extracted beam from the AGS with the RF kept on to maintain tight bunching. The external pulses were found to be unexpectedly narrow (FWHM = 2.4 nsec after correction for counter resolution). An explanation for this and some pertinent comments were put forth by Barton<sup>2</sup> in a subsequent report.

The original motivation for the study was to examine the extent to which single counter time of flight (TOF) measurements would be feasible, making it possible to measure velocities of neutral secondary particles from a target.<sup>3</sup> The encouraging result led later to a proposal by Kalogeropoulos<sup>4</sup> to use the tightly bunched protons to produce a secondary time separated beam (TSB) of anti-protons, i.e., a beam with a long flight path over which the lower velocity particles ( $\bar{p}$ 's) separate longitudinally from the more numerous fast particles ( $\pi$ 's) so that the  $\bar{p}$  interactions can be studied independently by suitably gated detectors.

### II. TOF Characteristics

For a given beam length  $L$ , there are various momenta  $p$  at which the  $\bar{p}$  TOF is equal to the  $\pi^-$  TOF plus an integral number of AGS bunch periods:

$$t_{\bar{p}} = t_{\pi} + n T$$

i.e.,  $\bar{p}$ 's of these flight times are overlapped by the intense  $\pi^-$  bursts from later bunches striking the target. If the effective  $\pi^-$  pulse width is  $\pm \delta$ , then there are overlap bands given by

$$\Delta(p, L) \equiv (t_{\bar{p}} - t_{\pi}) = n T \pm \delta \quad (1)$$

within which beam particles are unusable and the experimental detectors are to be vetoed. For  $n = 0$ , only  $\Delta = +\delta$  has significance. The function  $\Delta$  is:

$$\begin{aligned}\Delta(p, L) &= \frac{L}{c} \left( \frac{1}{\beta_{\bar{p}}} - \frac{1}{\beta_{\pi^+}} \right) = \frac{L}{c} \left( \frac{E_{\bar{p}} - E_{\pi}}{pc} \right) \\ &= \tau \left[ \sqrt{1 + \left( \frac{m_{\bar{p}} c}{p} \right)^2} - \sqrt{1 + \left( \frac{m_{\pi} c}{p} \right)^2} \right] \left\{ \tau = \frac{L}{c} \right\}\end{aligned}\quad (2)$$

and the inverse of this is

$$\begin{aligned}\frac{a^2 c^2}{p^2} &= \frac{\Delta}{\tau} \left[ \frac{\Delta}{\tau} \frac{b^2}{a^2} + 2 \sqrt{1 + \left( \frac{\Delta}{\tau} \right)^2 \left( \frac{m_{\bar{p}} m_{\pi}}{a^2} \right)^2} \right] \\ \left\{ a^2 &= (m_{\bar{p}}^2 - m_{\pi}^2) > 0, b^2 = (m_{\bar{p}}^2 + m_{\pi}^2), \tau = \frac{L}{c} \right\}\end{aligned}\quad (3)$$

Fainberg and Kalogeropoulos<sup>1</sup> show that the AGS bunch may be adjusted so that, including the resolving time of their detecting circuit, the proton density falls off as  $e^{-\frac{t}{\tau_B}}$ , where  $\tau_B = 3.7$  nsec, on either side of bunch center. Using their detector as a practical example, and taking the position that we want the overlapping  $\pi^-$  intensity to be down by a factor of  $r = 10^3$ , we would set

$$\delta = \tau_B (\ln r) = 25.6 \text{ n sec.} \quad (4)$$

in Equation (1).

To the extent that the pion decay helps to purify the beam, the overlap bands would tend to become narrower with increasing decay length  $L$ . If one could effectively remove the resultant muons at the end of the beam, then in such an ideal case the overlap band widths would taper to zero, and remain so, where

$$e^{-\frac{L}{c\tau_{\pi}} - \frac{m_{\pi} c}{p}} \ll \frac{1}{r} \left\{ \tau_{\pi} = \text{pion lifetime} \right\}$$

Equation (4) would be replaced by

$$\delta = \tau_B \left[ \ln r - \frac{L}{c\tau_\pi} - \frac{m_\pi c}{p} \right] \geq 0 \quad (5)$$

Substituting this in Equation (1), the overlap bands may be calculated from (2) or (3). They are shown in Fig. 1. Without the pion decay, each overlap band would have an approximately uniform width on the log-log plot.

### III. The Long Transport Section

Since Fig. 1 indicates that a TSB will be hundreds of meters in length, an economical optical system must be designed to transport a large phase space over a long distance. Given the 28 eight inch aperture quadrupoles that we will obtain from SREL, this is not a difficult problem, in principal, since a simple alternating gradient channel (AGC) can accept a relatively large transverse phase space over a substantial momentum band, say  $\pm 10\%$  or more. A plot of the betatron oscillation function  $\beta_{\max}$  (at the center of a focussing quad) versus quadrupole focal strength exhibits a very broad minimum; i.e., the acceptance  $E = \pi \frac{a^2}{\beta_{\max}}$  varies slowly over a wide range of momenta. This behaviour is illustrated in Fig. 2, which is drawn for the case of thin lenses (a good approximation for the channels of interest here). We see that if the quads are spaced by a distance  $\ell$  on centers,  $\beta_{\max}/\ell \doteq 3.35$ . Hence, the acceptance in the initially focussing plane is

$$E_f = \pi \frac{a^2}{3.35\ell}$$

where  $a$  = quad aperture radius.

In the other plane, there is more variation in the aspect ratios of the (upright) admittance ellipses, but nevertheless, over  $\pm 10\%$  in momentum, the common area accepted is still about 90% of  $E_f$ .

The total transverse acceptance of the AGC is then

$$E_f E_d \doteq (.9) \left( \frac{\pi}{3.35} \right)^2 \frac{a^4}{\ell^2}$$



If the source has semi-widths of  $w_x$  and  $w_y$  and emits into semi-angles  $\Delta x'$  and  $\Delta y'$ , then equating source emittance to channel admittance, we have

$$(\pi w_x \Delta x') (\pi w_y \Delta y') = E_f E_d = (.9) \frac{\pi^2}{(3.35)^2} \left( \frac{a^2}{\ell} \right)^2$$

The accepted solid angle is therefore:

$$\Delta \Omega = \pi \Delta x' \Delta y' = \frac{.9\pi}{(3.35)^2} \left( \frac{a^2}{w_x w_y} \right) \left( \frac{a}{\ell} \right)^2 \quad (7)$$

As an example, suppose we distribute the 30 quads over 300 meters, then  $\ell = 400''$  while  $a = 3.75''$ . A typical AGS target corresponds to  $w_x w_y = 0.1'' \times 0.05''$ . This leads to  $\Delta \Omega = 62$  mster which, multiplied by a momentum band of  $\pm 10\%$  or so, would mean a very substantial acceptance. The catch is encountered in trying to perform the emittance match implicit in Eq.(7) over a wide momentum range; the actual acceptance realized is much smaller. This problem will be discussed further in Section V.

As pointed out by Kalogeropoulos, the TSB momentum range need not be restricted to the range between the  $n = 0$  and  $n = 1$  boundaries of Fig. 1. The  $n = 1$  and  $n = 2$  overlap bands are separated by about  $\Delta p/p = \pm 15\%$ , while  $\Delta p/p = \pm 9\%$  is the  $n = 2$  to  $n = 3$  separation. Thus, if the transport system is arranged to select momentum bites less than these amounts, the beam may be used at momenta below the  $n = 1$  overlap band.

#### IV. Momentum Selection

A unit cell with a phase shift of  $\pi/2$  lies near the broad minimum in  $\beta_{\max}$ . Selecting this phase shift for the AGC allows one to neatly embed two equal bend dipoles early in the lattice, separated by  $\Delta \Psi = \pi$ , with a  $\Delta p$  defining slit at  $\Delta \Psi = \pi/2$ . The remainder of the channel is then approximately adispersive. The momentum recombination is not exact, of course, due to the chromatic aberration in the quads. The effect of the residual dispersion was observed in the particle loss pattern, downstream of the dipoles, in the Monte Carlo calculations of Section VII.

A bend in the beam line is also imperative to prevent an intense proton beam from entering the AGC. The proton separation can also be aided by employing a non-zero ( $0.5^\circ$ - $1.0^\circ$ )  $\bar{p}$  production angle. After the proton beam separates from the negative TSB, it can be dumped in a beam stop or, at some expense, deflected out to another target location.

In section II, it was remarked that pion decay could help to purify the beam if the resulting muons could be removed. This could be largely accomplished by means of another momentum defining section, at the end of the AGC, similar to the one just described. Such a section has not been included in the examples below because it is quite likely that some users will wish to have an even higher resolution arrangement for the purpose of measuring individual incoming particle momenta. The details of such a beam spectrometer will be experiment dependent and have not been studied carefully as yet.

#### V. The Entrance Doublet

In Section III, it was mentioned that it is difficult to effect an exact match over a wide momentum band from a small, large solid angle source into an AGC with large aperture and small angular spread. Monte Carlo beam traces were performed to determine how many  $\bar{p}$ 's could be captured in the channel's acceptance. An exact matching (at  $p = p_0$ ) arrangement of three or four suitably placed quads (with apertures arbitrarily large) was found to exhibit very severe chromatic aberration. The overall emittance into the acceptance of the quad channel was less than that from a simple doublet focussed for a point to parallel condition in both planes. ( $H_{22} = V_{22} = 0$ ). Consequently, such a doublet was chosen as the basic objective lens for the system.

An attempt was made to correct the chromatic aberration of the objective doublet by inserting sextupoles and additional dipoles in the first 4 cells ( $\Delta Y = 2\pi$ ) of the transport channel. This approach was suggested by a method

devised by K. Brown<sup>5</sup> to eliminate the 2nd order chromatic (momentum-dependent) terms in a curved AG lattice. Using the program TRANSPORT,<sup>6</sup> it was possible to make various  $(\delta p \delta \xi_T)$  terms of the second order transformation matrix go to zero or, alternatively, to minimize the effects of these terms on an ellipsoid representing the  $\bar{p}$  emittance. Although the method works very nicely for the chromatic aberration arising in the lattice itself, it did not seem to be effective in reducing the chromatic effect of the objective doublet, which is the dominant source in this case. In fact, all the "solutions" obtained for the sextupole scheme led to lower fluxes, eventually transported through the remainder of the channel, then were obtained with no sextupoles and only two bends for momentum selection-recombination. In addition, a "gentler" match, combining the quads in the first two cells of the AGC with the doublet, was also tried, again with inferior results.

For given maximum pole tip fields and apertures, the optimum doublet configuration depends on momentum, with longer quads required for higher momenta. In an attempt to approximate the optimum doublet over a range of momenta, the front ends of the example beams described here have four quadrupoles at the front end. The scheme then, is to use Q1 and Q2 as the collecting doublet at the lowest momenta, with Q3 and Q4 set to some "neutral" condition. ("Neutral" is hazily defined as some set of fields which tends to minimize spreading of the p beam before it enters the quad channel. This point hasn't been investigated yet, and so, in the example beams described, the fields were set to zero.) For intermediate momenta, the first element of the doublet would be (Q1,Q2) together, with Q3 being the second element and with Q4 off. The highest momenta would require the doublet to be (Q1,Q2,Q3), Q4. This works out fairly well since, for the point to parallel condition, the first element of this doublet must be considerably stronger than the second.

## VI. Spot Focus at Experiment

The final beam spot is formed simply by adding another doublet at the end of the AGC. Since the beam emittance is largest in the vertical plane, the final doublet element was chosen to be vertically focussing for the example beams discussed in the next section. The same doublet was used for both examples for simplicity. It gives a convenient spot size in both cases. The final beam length and momentum range chosen, and experimental needs, would lead to a closer optimization of this doublet.

## VII. Example Beams

In order to illustrate the range of possibilities, two AGC examples have been chosen, one with quads spaced 400" on centers and one with them 1200" on centers. Table I lists some pertinent data for the two examples. A conception of the layout of the shorter beam is shown in Fig. 3.

The fourth objective lens, Q4, is horizontally focussing and incorporates the function of the first half quad ( $\frac{1}{2}$ QH1) of the AGC. Similarly, the last AGC quad ( $\frac{1}{2}$ QH16) is included in the 8Q32 which also forms Q5 of the spot focussing doublet. The AGC quads QV1, QH2, and QV2 have 12" apertures to allow for the momentum dispersion in those two cells. Consequently, the 15 cells of the AGC utilize just 26 distinct quads of the 8Q16 or 8Q24 varieties and 3 of the 12Q30 or 12Q40 varieties.

The acceptances ( $\Delta\Omega\Delta p/p$ ) for these two examples, derived from Monte Carlo ray tracing, are illustrated in Figures 4 and 5. In each figure, the continuous curve for the "Optimum Doublet" is derived using two quads operating at maximum pole tip field (assumed to be 3.6 kG/inch x 4.0 inch = 14.4 kG) whose lengths are set differently at each momentum to produce the point to parallel condition desired. The real, fixed length quads employed as described in Section V, produce the stepped acceptances shown. Naturally, on each step, the gradients increase proportionally with p until the maximum

(3.6 kG/inch) is reached, at which point one must step down and use the next longer quad combination. Corresponding  $\bar{p}$  yields, calculated from the Sanford-Wang production formula,<sup>7</sup> are shown in Fig. 6. The formula is not reliable below  $\sim 2.0$  GeV/c.

#### VIII. Alignment and Other Constraints

One must be careful in positioning the quadrupoles in a long alternating gradient channel. For the limited number of cells chosen, 15, the tolerances are stringent but not overly severe. If all quads are randomly positioned with the same rms error,  $\delta_{\text{rms}}$ , then the rms phase space (x,x' say) displacement of the beam axis at the end of the AGC ( $\frac{1}{2}$ QH16) is on a very nearly upright ellipse with amplitudes

$$\begin{aligned}\delta x_{\text{rms}} &= 14.7 \delta_{\text{rms}} \\ \delta x'_{\text{rms}} &= 4.31 (\delta_{\text{rms}}/\ell)\end{aligned}$$

where  $\ell$  is the center to center quad spacing.

If all quads are misaligned in the appropriate phase by an amount  $\pm \delta$ , then the maximum beam displacements at the end of the AGC are:

$$\begin{pmatrix} \delta x_{\text{max}} \\ \delta x' \end{pmatrix} = \begin{pmatrix} 59.8 \delta \\ 11.7 \delta/\ell \end{pmatrix} \quad \{\text{for max } \delta x\}$$

or

$$\begin{pmatrix} \delta x \\ \delta x'_{\text{max}} \end{pmatrix} = \begin{pmatrix} 40.0 \delta \\ 17.5 \delta/\ell \end{pmatrix} \quad \{\text{for max } \delta x'\}$$

The vertical effects at the center of the last vertically focussing quad would be slightly smaller.

Hence, if  $\delta_{\text{rms}} = 0.02''$ , the rms displacement near the end of the AGC would be about  $0.3''$  or 8% of the aperture and we would begin to notice a loss of flux. An unfortunate in-phase error of  $\pm 0.02''$  could lead to a  $1.2''$  excursion.

Finally, one should note that, from the presently envisaged "D" target position, it is 490 meters to the ISABELLE ring. The long example beam, 924 m, would have to include a vertical rise of perhaps 2 meters in order to be able to pass the TSB beam pipe over the ISABELLE ring tunnel. The AGC quad spacing would have to be tailored to span the cross-over point. Beyond that, to the north, one would have to cope with the recharge basin. There would undoubtedly be a number of other problems. The longest TSB, allowing for an experimental area and muon stop, that could be installed without serious interaction with ISABELLE would be about 450 meters long. Any TSB over  $\sim 200$  m in length will have to make a cut up to  $\sim 18$  feet deep in the hill lying between 5th Avenue and the ISA. It may be preferable to translate the TSB elevation. For instance, two  $2^\circ$  pitching magnets could provide a 10 foot rise over 4 unit cells ( $\Delta\psi = 2\pi$ ), leaving the beam dispersion-free thereafter. There would be some beam loss between the pitchers, but this could be minimized by placing them near horizontally focussing quads.

## References

1. A. Fainberg and T. Kalogeropoulos, "The AGS Beam Structure", Accelerator Dept. Informal Report BNL-18938, May 6, 1974.
2. M.Q. Barton, "Some Comments on AGS Bunch Areas", Accelerator Dept. Informal Report, BNL-19076, July 17, 1974.
3. T. Brando, A. Fainberg, T. E. Kalogeropoulos, D. N. Michael, G. S. Tzanakos, "Observation of Low Energy Anti-neutrons in a Time Separated Neutral Beam at the AGS", Dept. of Physics, Syracuse University (to be published).
4. Private Communication and Letter of Intent.
5. Private Communication.
6. K.L. Brown, F. Rothacker, D.C. Carey, Ch. Iselin, "Transport - A Computer Program for Designing Charged Particle Beam Transport Systems", SLAC-91, Rev. 2, May 1977.
7. J. R. Sanford and C. L. Wang, "Empirical Formulas for Particle Production in P-Be Collisions Between 10 and 35 GeV/c", Accelerator Department AGS Internal Report JRS/CLW-2, May 1, 1967.

TABLE I: EXAMPLE BEAMS

Overall Length:	314 m	924 m
Objective Lenses:	3 ea-8Q24	3 ea-8Q32
	1 ea-8Q32	1 ea-8Q48
AGC Lattice:	15 cells	15 cells
	400" on Centers	1200" on Centers
AGC Quads:	26 ea-8Q26 (or 8Q24)	26 ea-8Q16(24)
	3 ea-12Q30 (or 12Q40)	3 ea-12Q30(40)
Dipole Bends:	2 ea-18D36, 2° each	2 ea-18D36, 2/3° each
Spot Focus:	1 ea-8Q32	1 ea-8Q32
	1 ea-8Q48	1 ea-8Q48
Spot: RMS Widths	.44"H x .17" V	.18"H x .08"V
Base Widths	2.4"H x 0.8"V	1.2"H x 0.7"V
Separable p	~ 1.5 - 4.2 GeV/c	~ 2.7 - 7.8 GeV/c
	~ 1.0 - 1.1 GeV/c	~ 1.8 - 2.15 GeV/c
	~ 0.8 GeV/c	~ 1.47 GeV/c
Acceptances: $\Delta\Omega\Delta p/p$	1.47 msr	0.35 msr
	0.72 msr	0.26 msr
	0.42 msr	0.16 msr



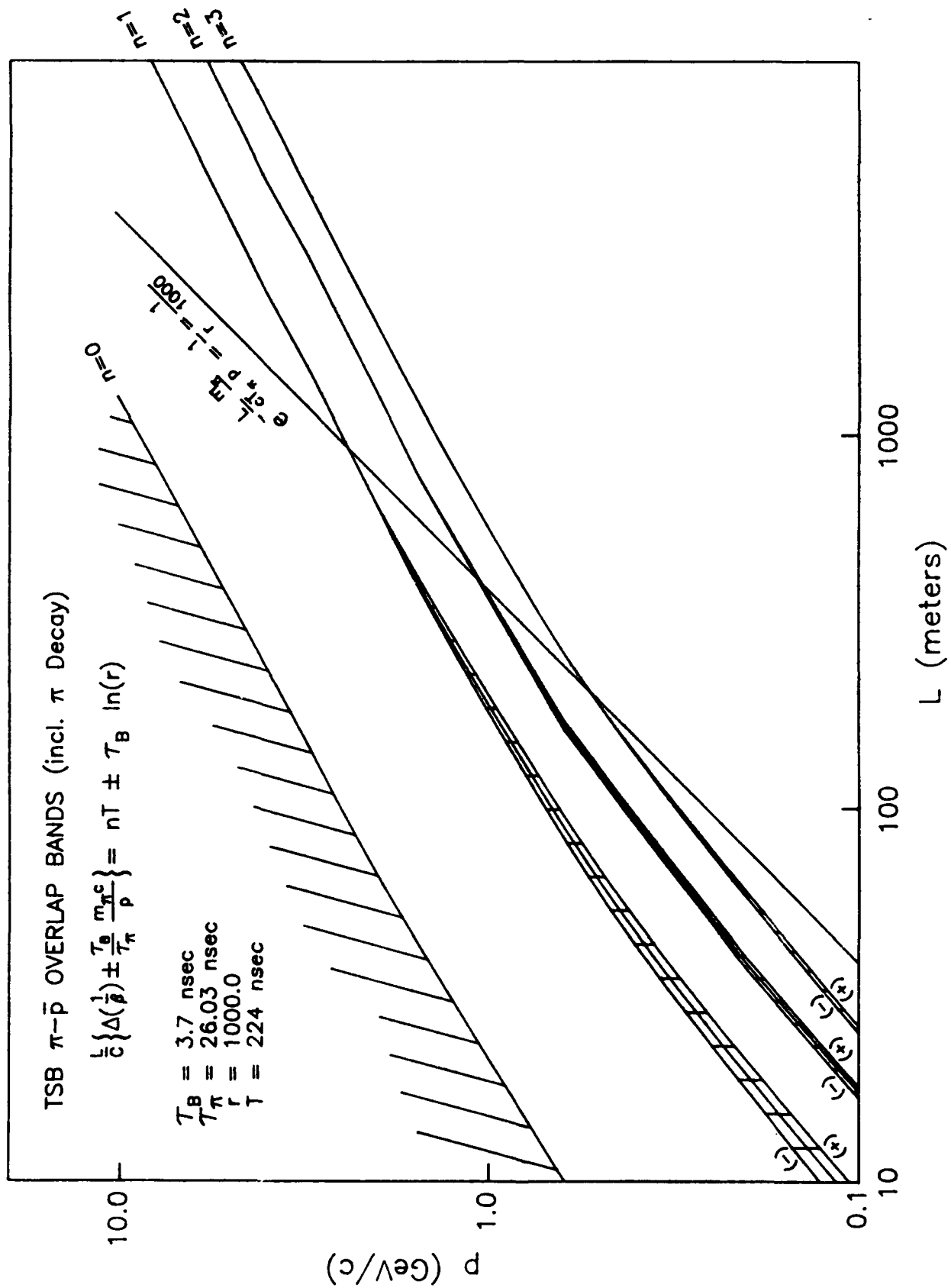


Fig. 1.  $\pi$ - $\bar{p}$  Overlap Bands

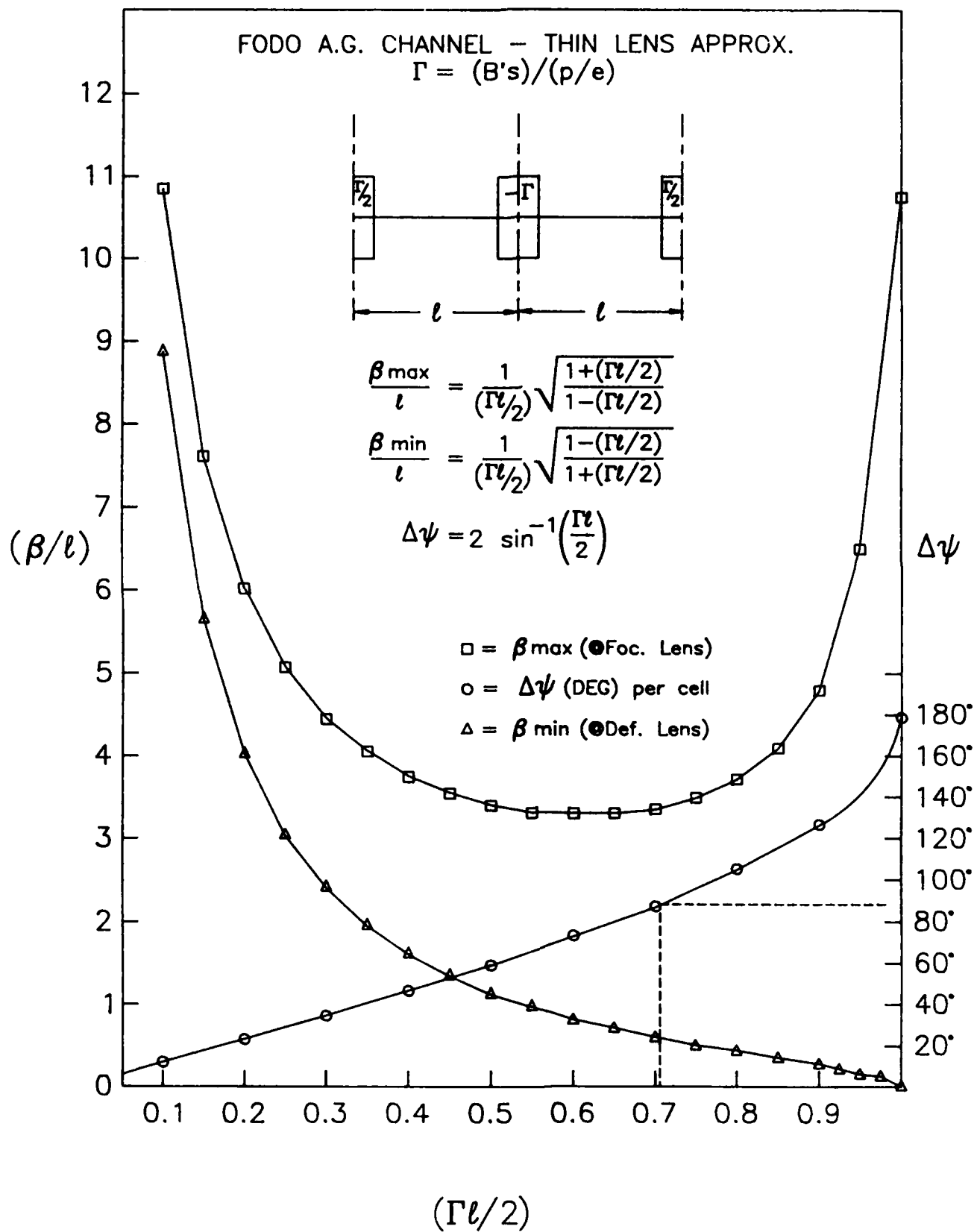


Fig. 2. AGC Parameters 125

Fig. 3. Plan Drawing of 314 m TSB

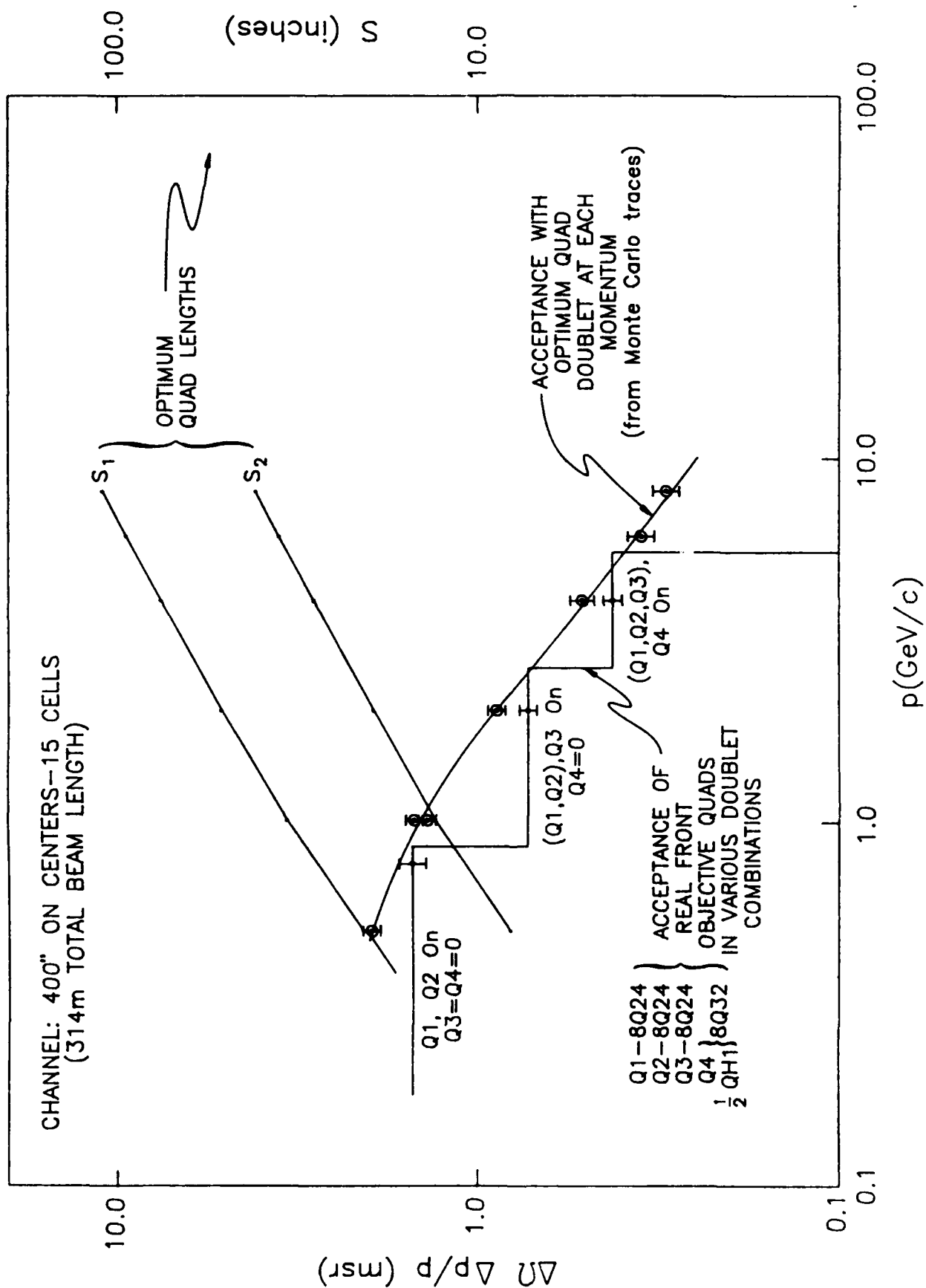


Fig. 4. Acceptances for 314 m TSB

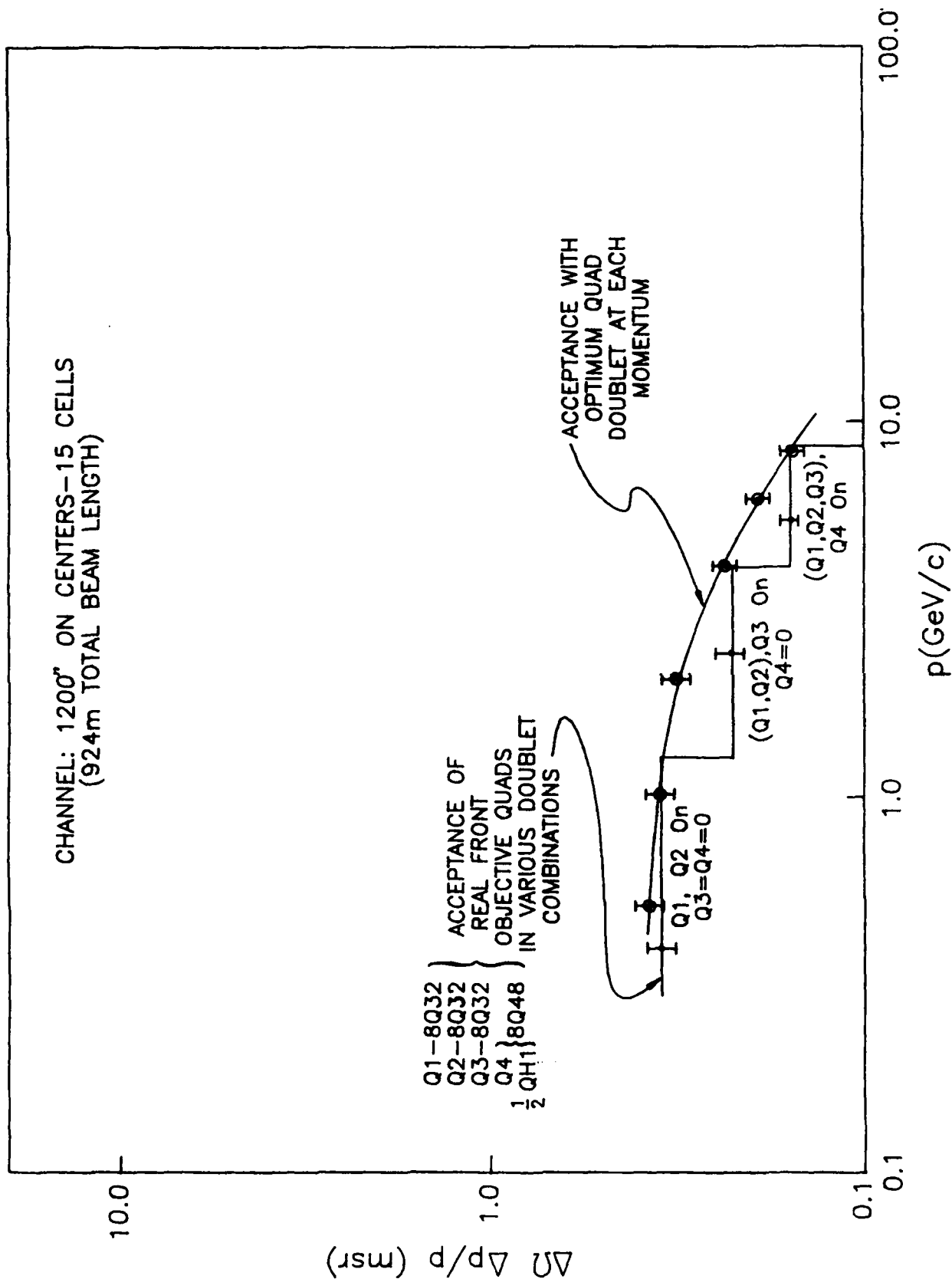


Fig. 5. Acceptances of 924 m TSB

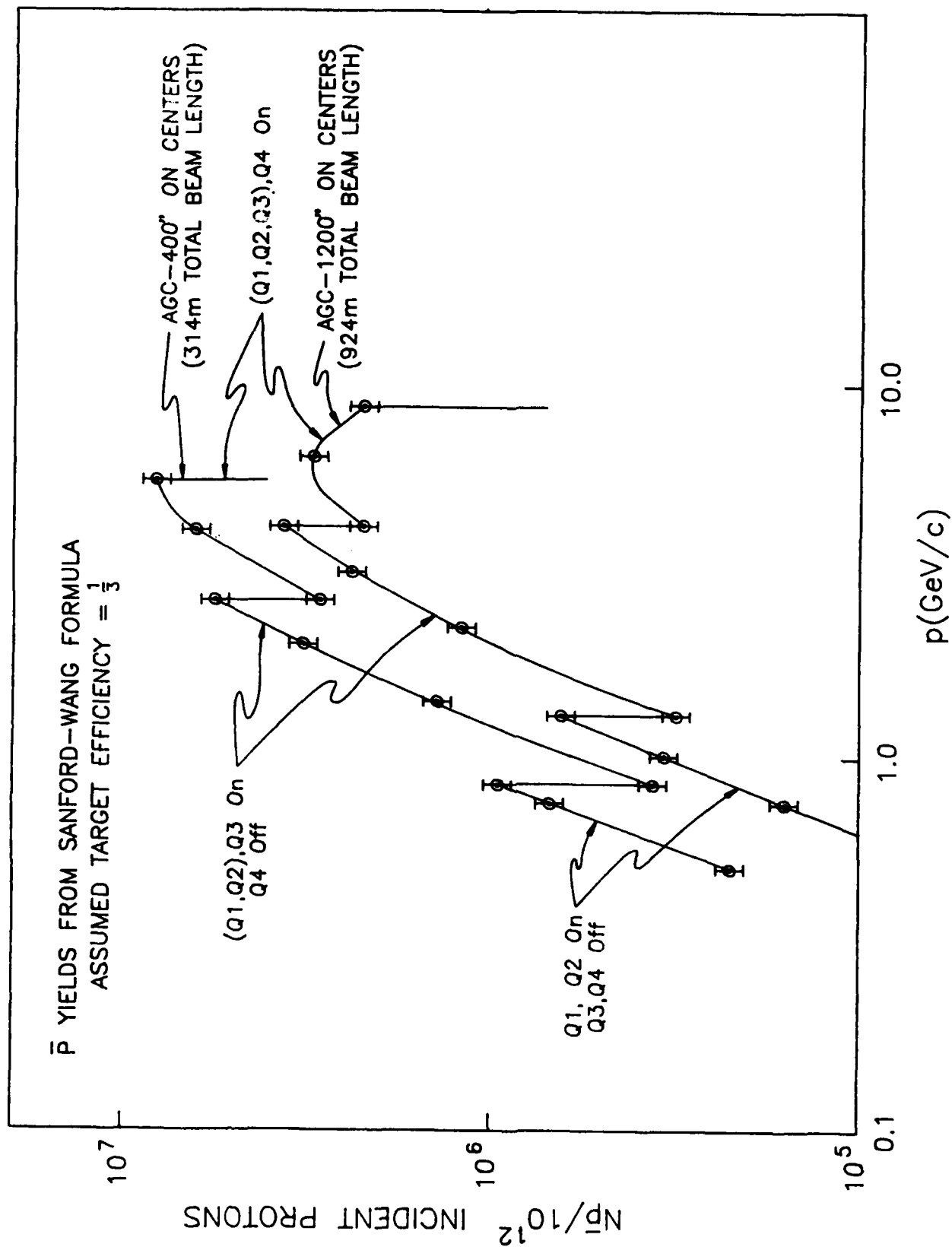


Fig. 6. Calculated Antiproton Yields

### APPENDIX 3. General Remarks on Antiproton Beams

H. Poth

#### I. Beam Momentum Spread vs CMS Resolution

The momentum resolution ( $\Delta p/p$ ) of the  $\bar{p}$  beam incident on a hydrogen target is related to the center-of-mass resolution by

$$\Delta s^{1/2}/s^{1/2} = 0.5 \times (1 - 1/\gamma) \times \Delta p/p \quad (A3.1)$$

where  $s^{1/2}$  is the center-of-mass energy. A beam resolution of 0.1% at 5.2 GeV/c ( $\gamma = 5.63$ ) gives, for instance, a mass resolution of 0.04%, which corresponds to 1.4 MeV at the  $\chi_0$  mass.  $s^{1/2}$  is plotted as a function of  $\bar{p}$  momentum for  $\frac{\Delta p}{p} = 10^{-4} - 10^{-2}$  in Fig. A3-1.

#### II. Beam Momentum Resolution

The momentum resolution of each beam is determined by its longitudinal acceptance (momentum bite) unless a momentum analysis is done. This can be performed in two ways:

1. Time-of-flight (TOF) measurements.
2. Beam spectrometry.

The momentum resolution achievable through a TOF measurement is

$$\frac{\Delta p}{p} = 0.3 \beta \gamma^2 \frac{\Delta t}{L} = 0.3 \left( \frac{p}{m} \right) \left[ 1 + \left( \frac{p}{m} \right)^2 \right]^{1/2} \frac{\Delta t}{L} \quad (A3.2)$$

where  $\Delta t$  is the time-of-flight resolution of the counter system in ns and  $L$  is the flight path in meters. For a beam of 0.8 km length and fast detectors with  $\Delta t = 0.1$  ns, the momentum resolution at 2.5 GeV/c ( $\gamma = 2.85$ ) becomes  $\Delta p/p = 3 \times 10^{-4}$ , which corresponds to a cms resolution of the order of 250 KeV but at 5 GeV/c it would only be 1.4 MeV resulting from a momentum resolution of  $10^{-3}$ .

High energy spectrometers achieve typical resolving powers of  $10^{-4}$  or better at a momenta below 1 GeV/c. It might be possible to obtain similar values with a beam spectrometer by having a large dispersion by a suitable bend and a spatial resolution of 1 mm., e.g. a beam of 4% momentum spread dispersed over 40 cm. This ignores its finite emittance whose effect is discussed in Appendix 4.

### III. Energy Loss in Target

Minimum ionizing particles lose 4.12 MeV per g/cm<sup>2</sup> in liquid hydrogen. The energy loss  $\Delta T$  in the target can be related to cms resolution  $\Delta s^{1/2}$  by

$$\begin{aligned}\Delta s^{1/2} \text{ (MeV)} &= m s^{-1/2} (\Delta T) = 938 \times s^{-1/2} \times (4.12 \times 0.0709 d) \\ &= 274 d(\text{cm})/s^{1/2}(\text{MeV})\end{aligned}\quad (\text{A3.3})$$

where  $m$  is the mass of proton or antiproton and  $d$  is the target length. Thus, a mass resolution of 1 MeV at the  $\chi_0$  mass of  $s^{1/2} = 3415$  MeV corresponds to 12.5 cm of liquid hydrogen of density 0.0709 g/cm<sup>3</sup>.

From the above considerations it is concluded that experiments aiming at a mass resolution of 1 MeV in the range under discussion should be possible with a beam momentum analysis of  $10^{-3}$  and vertex reconstruction to a few centimeters.

### IV. Beam Purity

If no particular measures are taken, the purity of the  $\bar{p}$  beam depends entirely on the length of the beam and its bends. The number of pions remaining after a given flight path  $L$  can be approximated by

$$N_{\pi}(L) \approx N_{\pi}(0) \exp(-17.9 L/p) \quad (\text{A3.4})$$

Here  $L$  is to be taken in km and the beam momentum  $p$  in GeV/c. A beam of 0.8 km length therefore has a  $\bar{p}$  purification factor (pion rejection factor) of 60 at 3.5 GeV/c but only 4 at 10 GeV/c. Figure A3-2 gives the ratio of Eq. (A3.4) to  $\bar{p}$  flux for beam lengths of interest. Without a highly dispersive bend such as the high resolution beam spectrometer, beam counters will still be subject to high muon rates.

### V. Achievable Luminosity

The luminosity with an external beam and an external target can be calculated:

$$L = F R \rho d N_0 / A \quad (\text{A3.5})$$



where  $F$  is the flux of  $\bar{p}$  per incident proton,  $R$  is the flux of incident protons,  $\rho$  is the density of the  $\bar{p}$  target,  $N$  is Avogadro's number,  $A$  the atomic weight of the target material and  $d$  the target length. A 56 cm long target of liquid hydrogen has an area density of about  $4 \text{ g/cm}^2$ . Upon insertion of  $F$  from Eq. (1.2) and assumption of  $R = 10^{12}/\text{sec}$  at the present AGS, the achievable luminosity at the  $\bar{p}$  production maximum becomes  $L = 5 \times 10^{30} (\text{cm}^2 \text{ sec})^{-1}$ . The total  $\bar{p}p$  cross section at 5-6 GeV/c is about 60 mb: hence a reaction rate of about 300,000 per second in the target, out of which one must filter a specific reaction of interest (e.g., charmonium production).

The above luminosity is comparable to what is anticipated for E760 at Fermilab. The present luminosity will be lower at other momenta, however, due to falloff in the  $\bar{p}$  production rate.

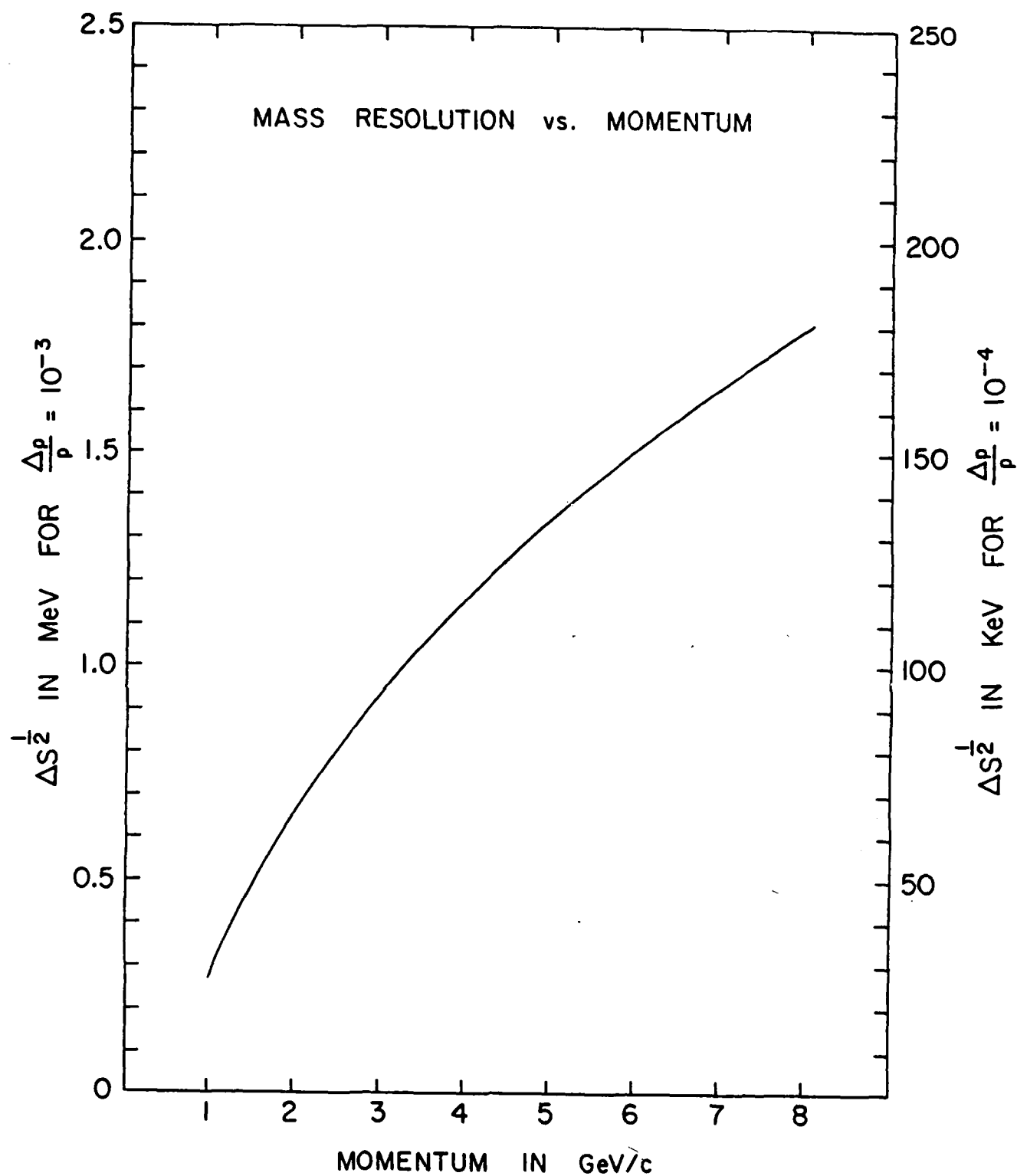


Fig. A3-1. cms Mass Resolution vs.  $\bar{p}$  Momentum

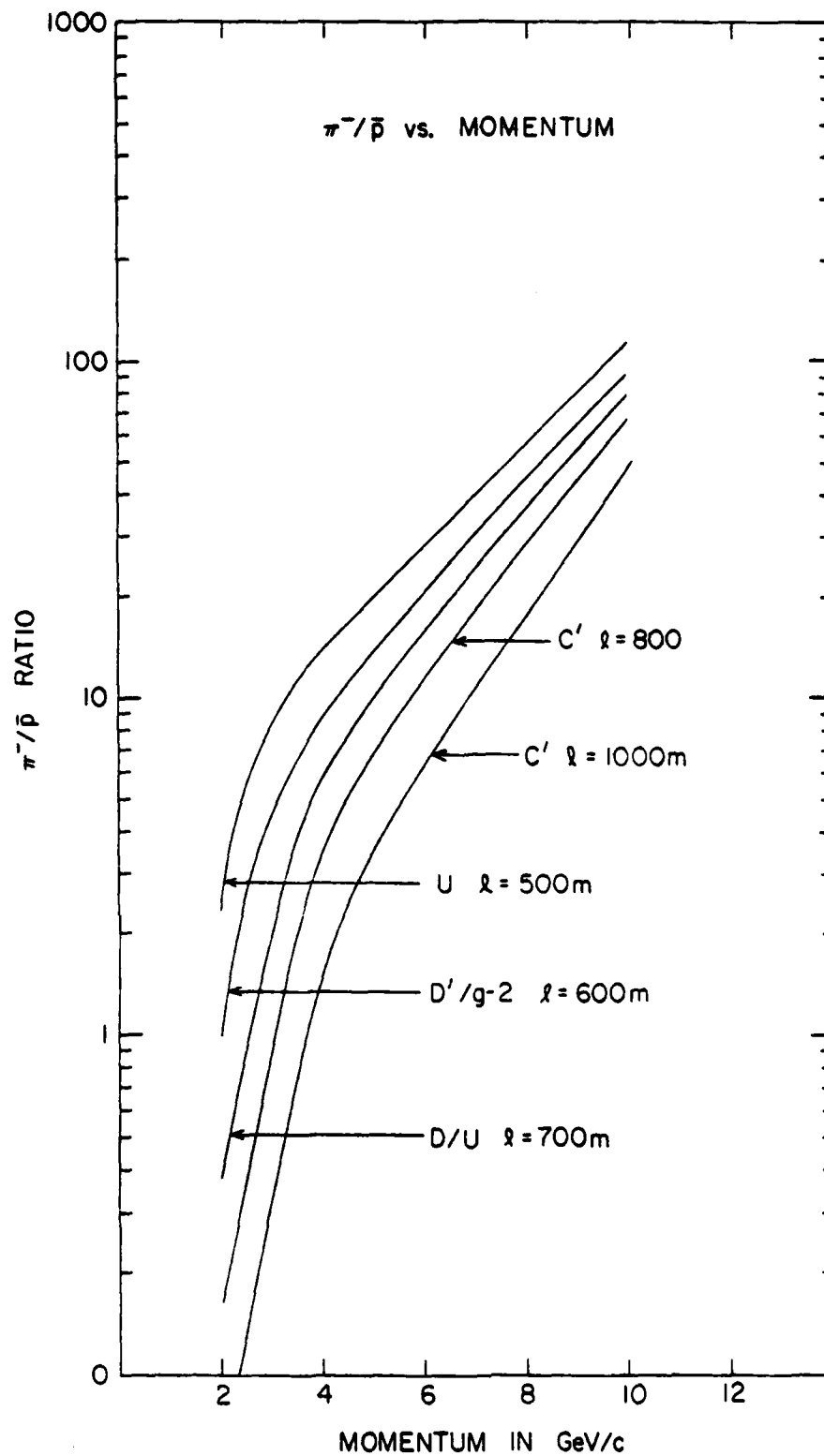


Fig. A3-2. Purity of Various  $\bar{p}$  Beams

#### APPENDIX 4. Beam Momentum Resolution

J.W. Glenn, III

The momentum resolution of a beam obviously depends on the analyzing bend angle and less obviously on the emittance of the beam and the size of the focusing elements before the momentum defining elements, since it depends on the spot size as well as the dispersion.

Assume a system that has the analyzing bend at the focusing elements which create the spot at the momentum defining elements (more complex systems can be approximated by this). The resolution  $R$  (where larger  $R$  implies poorer resolution) is defined as:

$$R = \frac{X}{\frac{dX}{\Delta p/p}} \quad (A4.1)$$

where  $X$  is the beam half-size and the dispersion  $\frac{dX}{dp/p}$  is the change in beam position per fractional change in momentum. But

$$\frac{dX}{\Delta p/p} = L\alpha \quad (A4.2)$$

where  $L$  is the length of drift after a bend of  $\alpha$  radians. The minimum size obtainable after drift  $L$  is

$$X = L\epsilon/Y \quad (A4.3)$$

where  $\epsilon$  is the emittance of the beam and  $Y$  the beam half-size at the start of the drift (limited by quadrupole aperture). Thus,

$$R = \frac{L \epsilon/Y}{L \alpha} = \frac{\epsilon}{\alpha Y} \quad (A4.4)$$

The length drops out: a large drift implying a large spot, also a large dispersion.

In the decay purified antiproton beam leading into the RHIC injection area, a  $7.5^\circ$  vertical bend with a 12Q30 and 6RQ24 vertically focused doublet has been suggested. The vertical aperture of 24" in the 6RQ24 combined with an emittance of 6 mm-mrad gives a resolution of  $1.5 \times 10^{-4}$ . Any degradation in emittance--e.g., gas and window scattering

after the emittance defining elements--degrades the resolution, as will any spot size increase due to field errors in the focusing elements.

It should be noted that the emittance of the beam is proportional to the production target size, i.e. the proton beam spot, and the angles accepted in the secondary beam line. Thus, the larger the target, the poorer the resolution; and the larger the angle accepted, and hence the higher the intensity, the poorer the resolution. To optimize the resolution, the production target should be placed where the smallest proton beam would be available.

## APPENDIX 5. High Field Properties of the AGS Booster Dipole Magnet

G. T. Danby and J. W. Jackson

The booster dipole high field properties are of interest in determining the highest energy to be available for various possible booster modes of operation. This in principle can include applications not originally planned for: antiprotons, for example.

### 1. Original design choices<sup>1</sup>

- a. Rapid acceleration for multiple pulse injection (up to 10 Hz) into the AGS for high proton current operation required a magnet design with minimum stored energy consistent with aperture requirements.
- b. High intensity proton operation, as well as the function of accumulating many turns of polarized protons, required a large aperture with excellent field properties from injection up to intermediate fields.
- c. Heavy ion acceleration required slow acceleration, 1/2 second rise time, up to 12 kG. This has recently been raised to 12.7 kG. The highest field is related to optimum stripping efficiencies of heavy ions in transit from the booster to the AGS.
- d. The pole width chosen was the minimum required to give the necessary injection good field aperture, extending essentially over the entire vacuum pipe.
- e. The narrow pole with commensurately small cross section yoke return, wrapped around tight fitting coils located above and below the high field region, provides the low stored energy.
- f. As 12 kG is approached, sextupole effects begin to grow very slowly, producing only  $\Delta B/B_0 = 10^{-4}$  at  $r = 1$  inch. This was a design specification.
- g. Above 12 kG dipolar saturation commences because of the small iron cross section. Aberrations in the field quality--sextupole, etc.--grow very slowly, however, if the magnet is excited above its maximum design field.

---

<sup>1</sup> Accumulator/Booster Proposal for the AGS, BNL 32949-R, February 1984.

- h. Saturation is predominantly sextupolar: Operation of lattice correction sextupoles can to first order cancel the effect of this aberration for larger apertures if desired, or for higher field operation.

2. Possible use of the booster as an antiproton storage ring

- a. Antiprotons produced at an AGS target station at the optimum production energy could be injected into the booster.
- b. They could be stored, or accelerated/decelerated prior to storage.
- c. As an alternative to acceleration, production could occur at non-optimum production energy, and storage carried out without acceleration.
- d. Strong interest was expressed in the possible operation of the booster as a storage ring up to 6.5 GeV/c, i.e., 25% higher energy than its design value. This is in order to reach interesting  $\bar{p}p$  resonances. This is clearly the hardest question.

3. Discussion of low energy  $\bar{p}$  possibilities

- a. The excellent low field properties of the booster magnets is very helpful to low field storage possibilities.
- b. Antiprotons might be decelerated to low energies and transferred to a small ring or "bottle."
- c. The large number of free straight sections available might accommodate cooling apparatus at low energies where cooling is most efficient.
- d. A cooled beam might then be accelerated to higher energies with higher beam intensity.

Comment: The above possibilities seem to be permitted from a magnetic point of view. Quantities of low frequency rf, beam cooling, etc., are at this point just speculation but appear worth pursuing.

#### 4. Discussion of high energy $\bar{p}$ possibilities

We now turn to the high field computer dipole magnet study, which is the "meat" of this report.

Figure A5-1 shows the field deviation  $\Delta B/B_0$  on the horizontal mid-plane (HMP). Note that these results were computed for 100% steel packing factor and for a decarburized iron permeability table. If the packing factor was 95%, for example, the saturation aberration shown would occur at 5% lower central field than computed. This is illustrated in brackets in Fig. A5-1.

Table A5-1 lists the multipole content of the field as a function of dipole field. The multipoles are expressed as parts in  $10^4$  of the dipole at a radius of 1.5 inches. The signs correspond to the coordinates (r, y = +1.5 in., 0 in.). Note that the multipoles are also tabulated for 100% packing factor. For a packing factor of 95%, for example, the multipoles listed at 15 kG will occur at  $15 \times 95\% = 14.25$  kG. It can be seen that for 15 kG operation, assuming the lattice sextupoles roughly compensate for the  $b_2$  saturation, the residual 10-pole aberration is  $\sim 3 \times 10^{-4} \Delta B/B_0$  at  $r = 1.5$  in. This corresponds to a roughly circular good field region.

In summary, from an acceptable field aberration point of view, the magnets can be powered significantly above the design field of 12.7 kG. Their actual performance will depend on the steel properties: chemistry (permeability), thickness of laminations, thickness of insulating layer and compression of laminations. These will soon be much better known for the actual production magnet steel.

As far as aberrations are concerned, silicon steel should behave as well as decarburized iron, since it normally outperforms soft iron below 16 kG. As a result, a small packing factor correction to the multipoles tabulated from the computer results for 100% packing factor is credible.



The "bad news" is shown in Fig. A5-2, which gives the dipolar saturation. The "ampfac" is the increase in  $I/B$  due to finite permeability, plotted versus aperture field  $B$ . For example, the increased current at  $B = 15$  kG is 18% above that which would be required for  $\mu = \infty$  and for 100 packing factor. Note that the alternate horizontal scale of  $B$  (below the computed scale) which corresponds to 95% packing factor with decarburized iron.

Silicon steel will also effectively displace the curve in a similar manner, since it has inferior permeability properties at very high fields (*i.e.*, in the iron flux returns of the magnet). This dipolar saturation is dominated by the narrow poles and flux returns: saturation being designed to commence at 12 kG.

Table 5-2 lists the currents corresponding to various fields with 100% packing factor and also with 95% packing factor. The 95% values are likely to be reasonably close to the actual  $I/B$  magnet performance. This is roughly sufficient to allow for both the actual packing factor and a contribution from the reduced performance of silicon steel.

These computations will be repeated with the final steel laminated magnet properties when available.

5. Is very high field operation practical?

This is not easily answered (note that 6.5 GeV/c requires 15.77 kG).

- a. The dipole magnet power required is about 70 KW per unit, or roughly 3 MW for all dipoles.
- b. For quite slow cycling or dc operation the power supply required is not excessive.
- c. The quadrupoles have not been considered at this time, but if a problem occurred, they could always be operated at a lower tune.
- d. Bussing and connections would have to be designed for significantly higher power than originally considered ( $\sim 2x$ ). Water flow capability would have to be suitably increased.
- e. Larger fringing fields would occur. This would have to be considered in locating other apparatus that might be field sensitive.

- f. In conclusion, more study is required if this option is to be considered seriously.

A policy decision would have to be made to keep high energy  $\bar{p}$ 's in mind during the booster final design phase. Extra work would be required just to find out whether or not to build in this option. It appears too big a perturbation to try to consider only as an "afterthought."

Table A5-1. BOOSTER DIPOLE FIELD QUALITY

$B_0$ (kG)		$b_2$	$b_4$	$b_6$	$b_8$
$f=95\%$	$f=100\%$				
	1.6	+ 0.04	+0.02	0.00	-0.00
	5.0	- 0.14	+0.02	0.00	-0.00
7.6	8.0	- 0.27	-0.01	-0.00	-0.00
	9.0	- 0.43	-0.07	-0.02	-0.01
9.5	10.0	- 0.71	-0.19	-0.03	-0.01
	11.0	- 1.23	-0.39	-0.09	-0.01
11.4	12.0	- 2.35	-0.81	-0.17	-0.02
	12.5	- 3.30	-1.16	-0.20	-0.02
	13.0	- 4.58	-1.56	-0.22	-0.02
13.3	14.0	- 8.15	-2.37	-0.19	-0.04
	14.5	-10.43	-2.74	-0.17	-0.08
14.25	15.0	-13.03	-3.05	-0.20	-0.09
14.7	15.5	-15.96*	-3.38	-0.27	-0.10

Multipoles expressed in units of  $10^{-4}$  at  $R = 1.5$  inc.,  $Y = 0$  in.

\* Note that this value corresponds to a sextupole magnet of 6 in. diameter, 4 in. length, and a pole tip field of 2.5 kGauss.

Table A5-2. BOOSTER DIPOLE - CURRENT REQUIREMENTS

$B_o$ (kG)	AMFACC	$I$ (kA)	
		f=100%	f=95%
2.4356	1.0	1.000	1.050
5.0	1.0046	2.062	2.165
8.0	1.0054	3.302	3.467
9.0	1.0062	3.718	3.904
10.0	1.0078	4.138	4.345
11.0	1.0019	4.570	4.799
12.0	1.0267	5.058	5.311
13.0	1.0610	5.663	5.946
14.0	1.1116	6.390	6.710
15.0	1.1795	7.264	7.627
15.5	1.2213	7.772	8.161



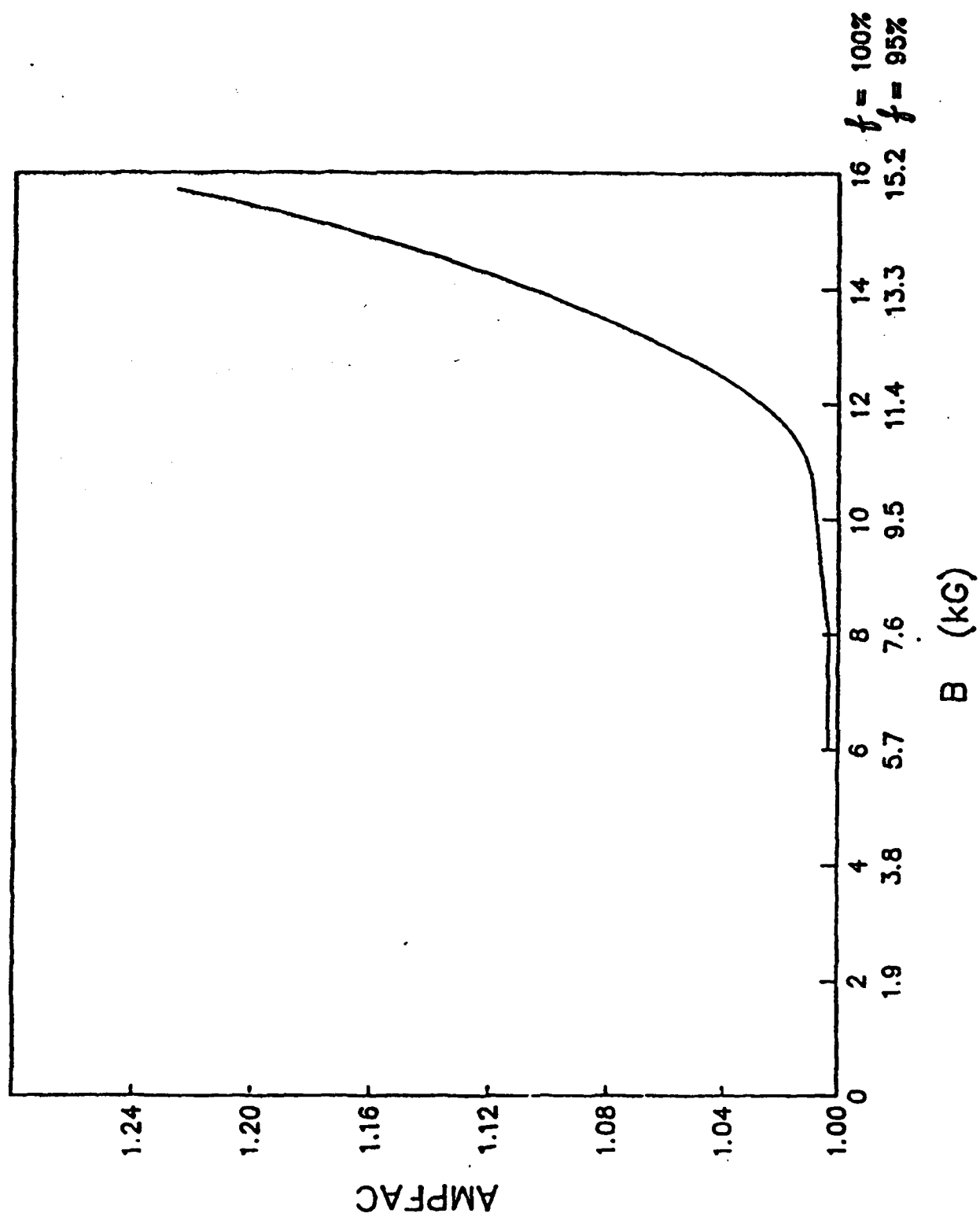


Fig. A5-2. Booster Dipole AMPFAC vs. Central Field

## APPENDIX 6. Very Low Energy Antiprotons

Y.Y. Lee

### 1. Introduction

It has been proposed<sup>1</sup> that the AGS Booster<sup>2</sup> be used as a time stretcher/purifier for antiprotons of momentum .65 to 5.2 GeV/c. The lower limit corresponds to the linac output of 200 MeV kinetic energy. In this note we should like to extend the idea to very low energy antiprotons at tens of KeV kinetic energy.

A brief description of the system has been given in Section 4 of the text. Once the antiprotons are injected and captured in the booster, one can either accelerate or decelerate them. After deceleration to 200 MeV kinetic energy, they can be further decelerated through the linac and an RFQ (radio frequency quadrupole) preinjector down to the ion source energy.

### 2. Antiprotons without cooling

Assuming the standard yield of antiprotons in Eq. (1.1),  $Y = 10^{-6} \bar{p}$  (2 mrs % interacting proton)<sup>-1</sup>, one can estimate the number of antiprotons that can be accumulated in the booster acceptance of 50 mm-mr and 2% momentum bite. Realistically the AGS proton beam at 28.4 GeV/c can be focused down to 1 mm spot size, and therefore the angular acceptance one can expect in each dimension would be  $50 \text{ mm-mr} / 0.5 \text{ mm} = 100 \text{ mr}$  with the solid angle subtended being 40 msr.

Because of the finite length of the target, the collection efficiency would be reduced further. For a 10 cm long target particle production studies show that only 1/3 of the particles fall into the usable phase space. The corresponding  $\bar{p}$  flux is given in Eq. (1.2), which we express as follows:

$$N_{\bar{p}} = 4.0 \times 10^{-6} N_p \quad (\text{A6.1})$$

where  $N_p$  ( $N_{\bar{p}}$ ) is the number of incident protons (usable antiprotons).

The post booster AGS will accelerate  $.5 \times 10^{13}$  protons/bucket, and if one uses 3 of those buckets for  $\bar{p}$  production per cycle,

$$\begin{aligned} N_{\bar{p}} &= 4 \times 10^{-6} \times 1.5 \times 10^{13} \\ &= 6 \times 10^7 \bar{p}/\text{pulse} \end{aligned} \quad (\text{A6.2})$$

at 4 GeV/c, the transport momentum of the antiprotons into the booster.

If one decelerates the collected antiprotons, assuming the rf system has enough debunching to take care of the antiproton beam energy spread, i.e., reduce the energy spread while making the bunch long, then the betatron phase space decreases as  $1/p^2$ . Deceleration in the booster to momentum  $p$  leads to a flux reduction by a factor  $(p/4 \text{ GeV/c})^2$ . The normalized emittance of the collected beam at 4 GeV/c is 213 mm-mr, and this emittance will be trimmed through the deceleration process. The normalized acceptance of the booster at 200 MeV linac energy is 34.3 mm-mr. Figure A6-1 shows the resultant antiproton intensity as a function of final decelerated kinetic energy in the booster.

### 3. Deceleration through the linac

The decelerated antiprotons can be extracted near the booster injection channel and transported through either the injection transport system with its dipoles reversed or through a separate transport system to the 200 MeV end of the linac. They are then decelerated to a kinetic energy of 750 GeV at the "entrance" of linac tank 1. The acceptance of the system is dominated by the normalized admittance<sup>3</sup> at the 750 KeV point of 10 mm-mr. Thus, one will lose beam intensity through the 200 MeV linac by a factor of  $(10/34.3)^2 = .085$  and by an additional factor of 2 due to beam bunching inefficiency. As a result  $0.7 \times 10^5$  antiprotons will survive to 750 KeV. The antiprotons can be further decelerated through the RFQ preinjector to energies of 20 KeV.

### 4. Effect of cooling

If one could cool the antiprotons to less than 10 mm-mr normalized to 14.6 mm-mr at 200 MeV energy, theoretically half the  $6 \times 10^7$  antiprotons collected at 4 GeV/c could be decelerated to 750 KeV and then to 20 KeV.

### References

1. A.S. Carroll, Y.Y. Lee, D.C. Peaslee, and L.S. Pinsky, to be published.
2. AGS Booster conceptual design report, BNL 34989R (1985).
3. G.W. Wheeler et al., Particle Accelerators 9, No. 1/2, (1979).

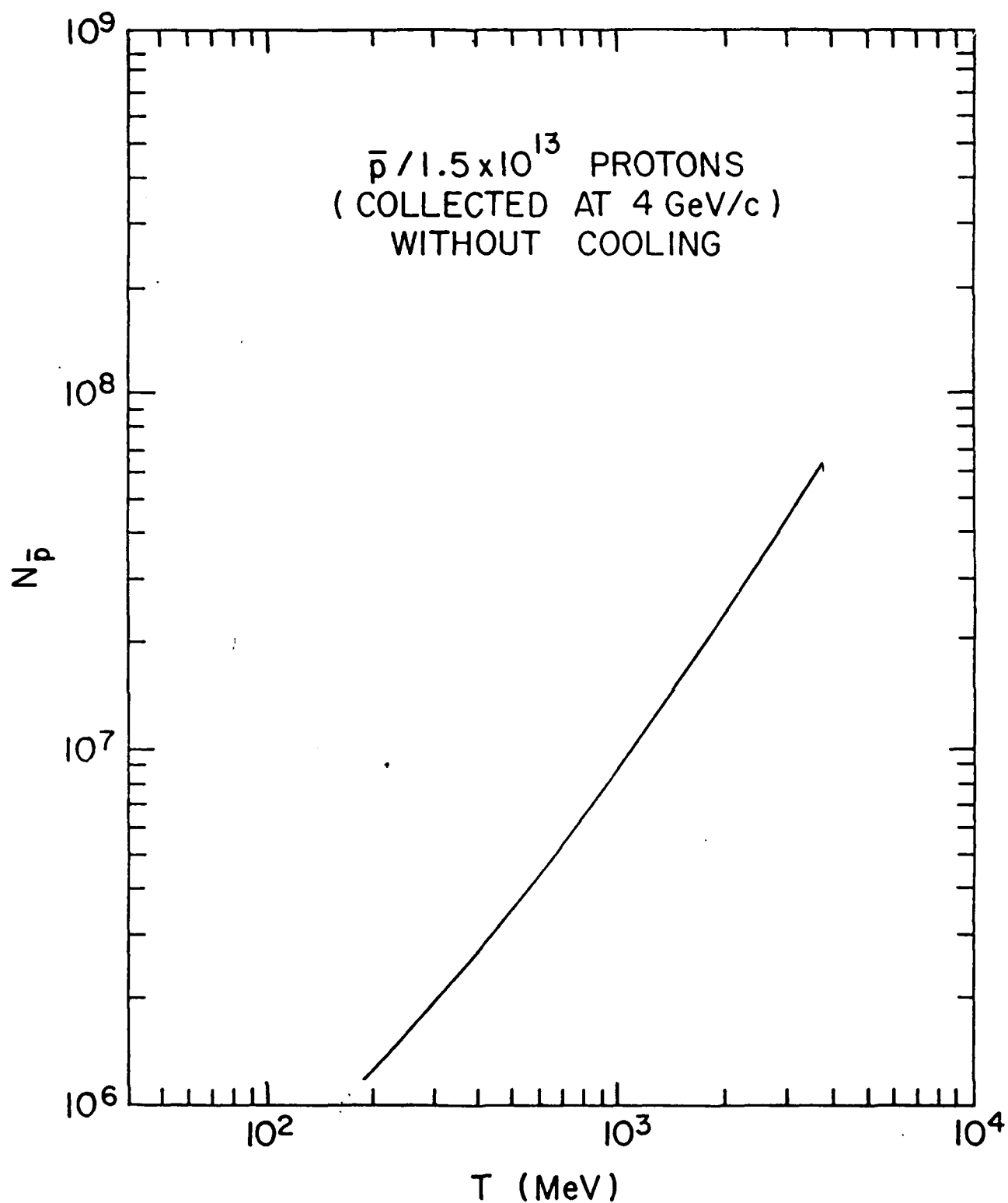


Fig. A6-1. Intensity of Decelerated Antiprotons



## APPENDIX 7. Overview of Booster $\bar{p}$ Potential

D.C. Peaslee

### I. Introduction

The accompanying studies describe a specific arrangement whereby the proposed AGS Booster can be employed in a parasitic mode to provide an external beam of 2-6 GeV/c antiprotons whenever the AGS operates in the slowly extracted beam mode and is not running polarized protons or heavy ions. This possibility of continuous production, combined with the favorable operating record established by the AGS, can provide an antiproton source unmatched by any other in that momentum range. This conclusion, at first perhaps surprising, is documented below.

### II. Continuous parasitic mode: $\bar{p}$ yield

According to Appendix 6 the post-booster AGS will accelerate in every cycle 12 buckets of  $0.5 \times 10^{13}$  protons each, of which 3 are extracted to produce antiprotons while the other 9 buckets are available for the rest of the program. The result is  $6 \times 10^7 \bar{p}$  pulse, which must be ejected from the booster each cycle of about 2.5 seconds. Typical AGS performance is some  $10^3$  pulses/hr for about  $10^2$  hr/week when the SEB program is running, a total of around  $10^5$  pulses/week. The SEB program of the AGS approaches 20 weeks' running time in a normal year. Thus the potential antiproton yield is of order

$$Y(\text{Booster}) \approx 10^{14} \bar{p}/\text{year} \quad (\text{A7.1})$$

### III. Comparative yield at LEAR

Typical operation at LEAR to-date has consisted<sup>1</sup> of stacking  $3 \times 10^9$  antiprotons every 75 minutes, corresponding to  $6 \times 10^{10} \bar{p}/\text{day}$ . This beam has been provided to experiments<sup>2</sup> about 30 days/yr during the 3 years that LEAR has operated. Thus a  $\bar{p}$  yield of

$$Y(\text{LEAR}) = 2 \times 10^{12} \bar{p}/\text{year} \quad (\text{A7.2})$$

has been available.

A new antiproton source (ACOL) is expected to operate at LEAR in 1987 with an order of magnitude improvement<sup>3</sup> in daily intensity to  $10^{12}$   $\bar{p}$ /day, but at no expected increase<sup>2</sup> in duty cycle over 30 days/years; thus,

$$Y(\text{ACOL}) = 3 \times 10^{13} \bar{p}/\text{year} \quad (\text{A7.3})$$

It appears that because of its parasitic rather than exclusive operating mode, the expected annual antiproton yield from the Booster is almost 2 orders of magnitude greater than  $Y(\text{LEAR})$  and a factor of at least 3 greater than at LEAR after ACOL.

Section 4 of the text indicates that the booster option will be continuously tunable to any desired momenta between about 0.7 and 5.2 GeV/c without modification. There appears to be no technical barrier to increasing that upper limit to around 6.5 GeV/c (Appendix 5); what would be needed is some incremental design study. If we extrapolate to 7 GeV/c, the equivalent of super-LEAR would be available, again with the increase of yield represented by Eq. (A7.1) over (A7.2).

#### IV. Comparative yield at FINAL: E760

The accumulator at FNAL can be used as an antiproton source in conjunction with an internal gas jet target, as in the recently approved experiment E760. The accumulator is designed<sup>4</sup> to stack  $4 \times 10^{11}$  antiprotons in 4 hours at a momentum of 8.9 GeV/c. During Tevatron collider operation the accumulator will not be available for other purposes. On the other hand, during fixed target running the accumulator could be operated parasitically with perhaps a 50% duty cycle: i.e., stacking about  $2 \times 10^{11}$  antiprotons every 4 hours or some  $10^{12}$   $\bar{p}$ /day at 8.9 GeV/c.

Decelerating these antiprotons to arbitrary momenta for experiments with a gas jet target will be difficult because the accumulator was designed as a fixed-energy machine. Losses must be expected; going to the top of the charmonium spectrum at around 7 GeV/c implies a reduction of at least  $(7/8.9)^2$  to around  $6 \times 10^{11}$   $\bar{p}$ /day. This yield is on the same order as ACOL: if FNAL provides only 30 days/year of antiprotons for the internal target, as at CERN, the effective yield for E760 will be a factor of 3 less than  $Y(\text{Booster})$ . Of course, there is no previous operating experience at FNAL on which to base estimates, but the importance of high-energy needs vis-a-vis fixed target operation is likely to be no less than at CERN for the foreseeable future.

## V. Effective luminosity

The effective luminosity of the booster antiproton system may be estimated in a most favorable case as follows: Assume a liquid  $H_2$  target some 2-3 meters long, of order the nuclear mean free path, with detectors arranged along its length to pinpoint the interaction vertex. Then  $6 \times 10^7 \bar{p}/\text{pulse} = 2 \times 10^7 \bar{p}/\text{second}$  translates to an effective luminosity

$$L = 10^{32}/\text{cm}^2 \text{ sec} \quad (\text{A7.4})$$

This is a full order of magnitude greater than for ACOL or E760, but of course refers to a scan over the 50-100 MeV range of energy loss in the target. While this would be adequate for ordinary hadron resonances, the special narrowness of some charmonium states would impose a reduction on Eq. (A7.4), back to  $L' \lesssim 10^{31}/\text{cm}^2 \text{ sec}$ . This is comparable to the luminosity expected for E760; there still remains the advantage in expected annual duty cycle of the AGS over FNAL for low energy antiproton operations.

## VI. Tunability

The booster cycle described in Section 4 of the text is able to deliver antiprotons at any momentum within its range, even though they are injected at 4 GeV/c. The booster momentum range neatly covers the gap between LEAR ( $\lesssim 2 \text{ GeV}/c$ ) and E760 (down from 8.9 GeV/c with difficulty, say to 6.5-7 GeV/c). This intermediate momentum range encompasses not only a number of charmonium states but many more resonances of u, d, s quarks and antiquarks, representing a great extension of light hadron spectroscopy.<sup>5</sup> In addition, recent candidate for exotic states have appeared--e.g., the  $f(2.2)$  and  $U(3.1)$ , and more are to be expected in this region.

The great flexibility of the booster antiproton arrangement can be seen by noting that it could readily carry out practically the entire program envisioned in the recent Fermilab workshop on antimatter physics at low energies.<sup>6</sup>

## References

1. P. Lefevre, D. Mohl, and D.J. Simon, Ref. 6, p.69.
2. B.E. Bonner and L.S. Pinsky, Ref. 6, p. 457.
3. R. Landua, Ref. 6, p. 36.
4. P.A. Rapidis, Ref. 6, p. 84.
5. D.C. Peaslee, EP&S Division Tech. Note 107, BNL (May, 1984).
6. Proc. 1st Workshop on Antimatter Physics at Low Energy, Fermi National Accelerator Laboratory (April, 1986).

# APPENDIX 8

## Details of Cost Estimates

### A. Pendzick

#### C' Option

<u>Proton Transport</u>	<u>Cost (K\$)</u>	<u>Labor (MW)</u>
New C3D2:	80	13
Relocate C3P2, C3QS, C3Q9 & C3P3	15	52
Relocate C' Target Station		10
Remove LESB II		32
 <u>Target Region</u>		
Q1 - Q5 magnets & PS available	150	155
D1 - D5 magnets & PS available	475	155
Power, water, shielding available from LESB II		
Instrumentation	30	20
Vacuum	75	10
Building available from GPP	—	—
Total	<u>825</u>	<u>447</u>

Cost Estimates (continued)

	<u>Cost (K\$)</u>	<u>Labor (MW)</u>
-		
p beam transport:		
Q1 - Q6 (doublets) AGS 8Q24 magnets and PS available	24	156
Q7 - Q15 (doublets) SREL 8Q24 magnets available	36	234
Water Q1 - Q6 from EEBA Q7 - Q15 air cooled	75	--
D1 - D7 Trim dipoles	105	21
Power supplies 2 - 300V x 100A 7 - 20V x 500A	80 70	10 14
Housing (30)	150	
Slabs 30	45	
Power 30	30	30
Tray, signals, power feed	125	50
Instrumentation	100	30
Vacuum	100	32
Security + 6000' fence	83	20
Magnet & PS hookup materials	100	--
Final focus at target: 3 quadrupoles	<u>200</u>	<u>30</u>
Total	1323	627

Experimental area:		<u>Cost*</u> <u>(K\$)</u>
Building 40' x 60' x 30'	180	180
5-ton crane	25	25
Power 2-1/2 MW (new) (extended from the open area)	250	50

\*

C' line terminates at 800m near RHIC Open Area. (Four O'Clock Hall)

	<u>Cost (K\$)</u>	<u>Labor (MW)</u>	<u>Cost* (K\$)</u>
Domestic water and cooling tower (extended from RHIC open area)	175		50
Sprinklers, fire detection, etc.	75		75
Telephones, signals, etc.	<u>50</u>	<u>25</u>	<u>50</u>
Totals	755	25	430
GRAND TOTALS	2,903	1,099	2,578
High Resolution Beam Spectrometer**	1,070	300	1,070

---

\* C' line terminates at 800m near RHIC Open Area (Four O'Clock Hall)

\*\* Assuming quadrupoles are available.

U-Line Option

	<u>Cost (K\$)</u>	<u>Labor (MW)</u>
Slow Extraction from AGS:	<u>500</u>	<u>186</u>
Proton transport in U-line:		
UQ10 available	15	13
UQ11 available	15	13
UQ12 (N3Q48)	95	31
Trim Doublet	30	26
Water, power, power supplies available	—	—
Total	155	83
Target Region:		
Shielding - 1650 tons concrete	495	--
200 tons steel @ 500/	100	--
Civil contracts	225	--
U-Target and instrumentation	35	10
Q1	95	31
Q2	30	31
D1	95	31
Vacuum	<u>30</u>	<u>10</u>
Total	1105	113
$\bar{p}$ beam transport		
To RHIC injection area (not part of this estimate)		
Vertical bends: 2 - 3X12D75	190	62
200' beam transport: 7 - 4" quads	280	217
Power supplies - 2	80	10
Tunnel extension 100'	200	
Trays, signals, power	75	25

	<u>Cost (K\$)</u>	<u>Labor (MW)</u>
Magnet and PS hookup materials	35	
Vacuum	30	10
Instrumentation	20	10
Quad houses and slabs - 3	20	
Final focus at target - 3 quads	<u>200</u>	<u>30</u>
Total	1130	364

Experimental area:

Power and water come from the RHIC  
compressor room at an additional cost  
of \$25K.

	<u>455</u>	<u>25</u>
GRAND TOTAL	<u>3345</u>	<u>771</u>



D/U Option - Transfer to "U" Line

	<u>Cost (K\$)</u>	<u>Labor (MW)</u>
Proton Transport:		
New DQ5	95	13
New DQ6	<u>95</u>	<u>13</u>
Total	190	26
Target Region:		
"D" Target	35	10
Q1	95	31
Q2	30	31
D1 - D4	380	124
Beam port through ring wall	35	12
Water, power and power supplies available		
Vacuum	50	10
Instrumentation	<u>25</u>	<u>10</u>
Total	650	228
$\bar{p}$ beam transport:		
200' to 4-1/2° bend in U-line: 7 quads	280	217
Match to 4-1/4° bend: 2 - 18D36	190	62
New UD1	95	31
To RHIC injection area (not part of this estimate)		
Vertical bends: 2 - 3X12D72	190	62
200' beam transport: y - 4" quads	280	217
Power supplies - 5	200	
100' tunnel extension	200	
Tray, signals, power	75	25

	<u>Cost (K\$)</u>	<u>Labor (MW)</u>
Magnet & power supply hookup materials	65	
Vacuum	50	20
Instrumentation	20	10
Quad houses and slabs - 3	20	
Final focus at target 3 quads	<u>200</u>	<u>30</u>
Total	1,865	656
Experimental area:		
Power and cooling water come from the RHIC compressor room at additional cost of \$24K	<u>455</u>	<u>25</u>
GRAND TOTAL	<u><u>3,160</u></u>	<u><u>935</u></u>

D/g-2 Option

	<u>Cost (K\$)</u>	<u>Labor (MW)</u>
Proton transport:		
New D110	95	31
New DQ11	<u>95</u>	<u>31</u>
Total	190	62
Target region:		
"D" target	35	10
Q1	95	31
D1	95	31
Power, water, shielding available		
Vacuum	25	6
Instrumentation	<u>25</u>	<u>10</u>
Total	275	119
$\bar{p}$ beam transport:		
1400' like C' option $\frac{1400}{3000} \times 1123K$	524	279
Final focus at target - 3 quads	<u>200</u>	<u>30</u>
Total	724	309
Experimental area:		
Same as 800m variant of C' option except power and water come from RHIC compressor room at an additional cost of \$25K	<u>455</u>	<u>25</u>
GRAND TOTAL	<u>1644</u>	<u>515</u>

D/(g-2)' Option

	<u>Cost</u> <u>(K\$)</u>	<u>Labor</u> <u>(MW)</u>
Proton transport:		
Same as above for D/(g-2)	190	62
Target region:		
Same as above for D/(g-2)	275	119
$\bar{p}$ beam transport:		
1625' at C' option rate	608	324
20° bend - 4 dipoles and PS	540	132
Final focus at target - 3 quads	<u>200</u>	<u>30</u>
Total	<u>1348</u>	<u>486</u>
GRAND TOTAL	<u>1813</u>	<u>667</u>

Booster Option

	<u>Cost (K\$)</u>	<u>Labor (MW)</u>
Target region:		
Lithium lens		
D1	250	?
Q1	95	31
Q2	95	31
Power supplies available		
Shielding - 900t concrete	270	
Vacuum	30	20
Instrumentation and target station	35	10
Power and water relocation	<u>75</u>	<u>      </u>
Total	945	123
$\bar{p}$ transport to booster:		
50° bend: 4 - 18D72	380	124
416' beam transport at C' rate	156	83
Quad dipoles to match into booster - 5	200	155.
Power supplies - 8	<u>280</u>	<u>16</u>
Total	1016	378
Booster modifications:		
Ejection line (30')	90	12
Ejection equipment	175	60
Booster tunnel modifications:		
New HI line	50	16
Widen 1/6 of existing tunnel	75	10
Booster magnet modifications to reach 6.3 GeV/c	<u>600</u>	<u>186</u>
Total	990	284

	<u>Cost (K\$)</u>	<u>Labor (MW)</u>
Transport to 80" bubble chamber building:		
416' beam transport at C' rate	156	83
Dipoles and PS - 2	270	62
Final focus at target - 3 quads	<u>200</u>	<u>30</u>
Total	626	175
Experimental area:		
80" Bubble Chamber addition building 40' x 60' x 30'	180	
Extend 40-ton crane range	25	
Power (2.5 MW)g-2)	50	
Domestic Water	50	
Sprinklers, fire detection etc.	75	
Telephones, signals, etc.	<u>50</u>	<u>25</u>
Total	430	25
GRAND TOTAL	<u>4107</u>	<u>985</u>



Accelerator Division  
Alternating Gradient Synchrotron Department  
BROOKHAVEN NATIONAL LABORATORY  
Associated Universities, Inc.  
Upton, New York 11973

Accelerator Division  
Technical Note

AGS/AD/Tech. Note No. 278

TRAPPING DECELERATED ANTI-PROTONS

A. Hershcovitch and Y.Y. Lee

March 26, 1987

Introduction

There have been thoughts<sup>1,2</sup> of using the AGS, as well as its Booster, Linac, and RFQ, to decelerate AGS produced 3.5 GeV/c anti-protons to energies as low as 20 keV. Without cooling,<sup>1</sup> during each AGS cycle as many as  $10^5$   $\bar{p}$ 's can survive this deceleration process. The trapping of these antiprotons in a relatively inexpensive gated electrostatic trap (aka, Penning trap) is under consideration in this note. An examination of the maximum capability of such a trap reveals that its storage capability far exceeds any conceivable  $\bar{p}$  supply. Nevertheless,  $\bar{p}$  accumulation in such a trap is rapid and with series addition of traps, the total number of stored antiprotons can exceed those of present day storage rings.

The Trap

Gated electrostatic traps have been used in basic plasma physics experiments<sup>3</sup> to study single species plasmas. Although these traps have been in use for well over 20 years,<sup>4</sup> it was not until some instabilities were understood and suppressed to enable researchers to achieve remarkable densities of both electron beams and electron gases<sup>3</sup> for periods of  $10^4$  sec. In a gated electrostatic trap, charged particles are combined radially by a uniform solenoidal magnetic field and axially by two electrodes biased to a voltage which is high enough to repel the stored particles. The bias on the electrodes can be reduced by pulses to enable particles to enter or to exit the trap, hence, the electrodes function as gates. Beams of antiprotons can be trapped using the following processes: before low energy  $\bar{p}$ 's exit the RFQ, the voltage on the gate closer to it is lowered to enable entry into the trap. The antiprotons are reflected at the opposite gate, and the potential on the entry gate is raised just as the leading antiprotons return to it. This results in trapped antiprotons with which experiments can be performed.



In the absence of instabilities under ultra-high vacuum conditions ( $10^{-10}$  Torr or better), the maximum density of trapped particles is determined by equilibrium conditions of such a non-neutral plasma (in such a high vacuum space charge neutralization can be neglected). This equilibrium state can be investigated using the equation of motion of a trapped particle, i.e., the equilibrium of a single charged particle.

For an antiproton in such a  $\bar{p}$  plasma column to be in equilibrium, the radially outward centrifugal and electric forces acting on this antiproton must be balanced by the radial inward magnetic force. In the case of a uniform axial magnetic field and an axially symmetric electric field (neglecting the small diamagnetic correction due to the rotation of  $\bar{p}$ 's), the equation of motion of a  $\bar{p}$  in equilibrium describing a circular orbit is

$$-\frac{mv_{\theta}^2}{r} = -qE(r) - qv_{\theta}B \quad (1)$$

where  $B$  is the magnetic field,  $q$  and  $m$  designate charge and mass respectively,  $v_{\theta}$  is the azimuthal velocity of the antiproton and  $E(r)$  is the radial electric field which can be determined from Poisson's equation (in cylindrical coordinates)

$$\frac{1}{r} \frac{\partial}{\partial r} r E(r) = -4\pi qn(r). \quad (2)$$

If we assume constant density profile, i.e.,  $n(r) \equiv n$  for  $0 < r < R$  and  $n(r) = 0$  for  $r > R$ , Equation (2) can be integrated to yield

$$E(r) = \frac{-r4\pi qn}{2} \quad \text{for } 0 < r < R$$

or, in terms of the plasma frequency  $\omega_p^2 \equiv \frac{4\pi nq^2}{m}$  this equation becomes

$$E(r) = -\frac{m}{2q} \omega_p^2 r \quad (3)$$

Experimental evidence indicates that the density profile in such a trap is "bell" shaped rather than a square profile. There are functions which are quite suitable to describe such a profile, one of which

( $J_0(r)$  - ordinary Bessel function of the first kind) was used by the author to analyze a gated electron trap. However, since a more accurate analysis introduces only a small numerical correction to Equation (3), which is not important to our analysis, a square density profile is used throughout this note. Introducing the angular velocity  $\omega = v_\theta^2/r$  in Equation (1), substituting for  $E(r)$  from Equation (3) into Equation (1), and using the definition of the cyclotron frequency  $\Omega \equiv qB/m$ , Equation (1) can be written as

$$-\omega^2 = \frac{\omega p^2}{2} - \omega \Omega. \quad (4)$$

Solving Equation (4) for  $\omega$ , in order to find the range of parameters for which equilibrium exists, we obtain

$$\omega = \frac{\Omega}{2} \left[ 1 \pm \left( 1 - \frac{2\omega^2}{\Omega^2} \right)^{0.5} \right] \quad (5)$$

From Equation (5), it becomes obvious that the density limit of a trap is given by the condition

$$\frac{2\omega^2}{\Omega^2} = 1. \quad (6)$$

In the case of a beam drifting along B, this limit is known as Brillouin flow. The plasma (antiproton) column at this density limit is rotating at  $\Omega/2$ . Basically, at this limit, the repulsive electrostatic forces (as measured by  $\omega^2$ ) are balanced by the restoring magnetic forces (as measured by  $\Omega^2$ ).

In a trap with a magnetic field of 10T, the maximum density of trapped antiprotons that can be stored (using Equation (6)) is  $2.63 \times 10^{11} \text{ p/cm}^3$ . In a 1-meter long,  $1 \text{ cm}^2$  cross section, trap,  $2.63 \times 10^{13}$  p's can be stored. These numbers exceed any conceivable source of antiprotons by orders of magnitude. There are factors that reduce the limit set by Equation (6). These are due to instabilities, however, experiments with electrons proved that these instabilities can be stabilized.<sup>3</sup> Also, the electron densities reached in these experiments<sup>3</sup> were well over 10% of the limits set in Equation (6). Since the

AGS system can produce only  $10^5 \bar{p}$ /pulse, we consider a 1T trap. Such a trap is inexpensive, and it can store up to  $2.6 \times 10^9 \bar{p}/\text{cm}^3$ , i.e., a 1-meter long trap would have stored  $10^6 \bar{p}$  pulses if they could have been delivered within a storage time. The storage time is determined by collisions with the background gas in absence of instabilities, hence the requirement of an ultra-high vacuum. A  $10^4$  sec confinement time was observed at a pressure of  $10^{-10}$  Torr for low energy ( $\sim$  eV) electrons.

### Trap Loading

A possible way to enhance the target thickness of such a  $\bar{p}$  trap is to accumulate as many antiproton pulses as possible, by injecting successively higher energy antiprotons. Consequently, the voltage on the gates needs to be increased accordingly. The number of  $\bar{p}$  pulses that can be accumulated is a function of three parameters: (1)  $\bar{p}$  confinement time, (2) the increment by which the gate potential is increased, (3) the maximum voltage on the gates.

The  $\bar{p}$  storage time is most probably dominated by scattering due to collisions with background gas molecules rather than annihilation, since calculated annihilation cross sections<sup>5</sup> decreases very rapidly at energies above 10 eV. Elastic scattering cross sections for  $\bar{p} - \text{N}_2$  collisions for antiprotons with energies of 10's of keV's should be similar to those of electrons having the same relative velocity, since  $p - \text{N}_2$  collisions at these energies are dominated by charge exchange. Although electron confinement times (half-life) approaching  $10^4$  sec (2.8 hours) have been observed in gated electron traps,<sup>3</sup>  $\bar{p}$  storage time will be somewhat lower since an antiproton in a trap will spend some time at low velocities at the turning points. This factor may lead to some non-negligible annihilations. Nevertheless, it is reasonable to expect a  $\bar{p}$  storage time of about two hours.

Incremental increases of the gate voltages should be much larger than the energy spread of the antiprotons exiting the RFQ. Since the  $\bar{p}$  energy spread is expected to be rather small ( $1\% \lesssim$ ), a 5% incremental increase in gate potential should suffice. The maximum potential on

the gates can be made rather high, however, in reasonable cost trap, this potential should not exceed 250 kV. Therefore, for an initial gate potential of 21 kV (to trap 20 keV antiprotons), 50 incremental increases of 5% each will result in a final gate voltage of 240.8 kV. Since the AGS cycle is 0.5 Hz, these 50  $\bar{p}$  pulses can be accumulated in 100 sec. The accumulation itself is done in a fashion similar to the trapping of the first  $\bar{p}$  pulse except that only incremental increases in gate voltages are made. After the first  $\bar{p}$  pulse is trapped (20 keV antiprotons in a 21 kV trap), a second  $\bar{p}$  pulse with an energy slightly exceeding 21 keV is injected into the trap while the voltage on the entry gate remains at 21 kV. The voltage on the other gate is raised by 5% before this pulse (to 22.05 kV) to repel these antiprotons. Next, the voltage on the entry gate is raised also to 22.05 kV just as the leading antiprotons from the second pulse reach it. This process is repeated for 50 pulses. Therefore, as many as  $5 \times 10^6$  antiprotons can be accumulated in this trap.

#### Cooling and Stacking

If one cools<sup>1</sup> antiprotons in the booster,  $10^8$   $\bar{p}$ /pulse can be injected into such a trap. Hence, in 50 pulses up to  $5 \times 10^9$  antiprotons can be accumulated in one trap. Since the accumulation time (100 sec) is much shorter than the storage time (2 hours), many traps can be filled up depending on the needed duty factor. The traps are to be stacked in series and loaded up sequentially starting with the trap furthest from the RFQ. Once the desired number of filled traps is reached, the potential on all the intermediate gates can be removed and the antiprotons can be "squeezed" into a single shorter trap.

For a 50% duty factor, i.e., one hour each for  $\bar{p}$  accumulation and for their availability for experiments, 1800  $\bar{p}$  pulses can be trapped (50 pulses in each of 36 traps). Thus, a total of  $1.8 \times 10^{11}$  antiprotons can be accumulated in one hour.

References

1. Y.Y. Lee, AGS/AD Technical Note No. 266 (1986).
2. Y.Y. Lee and D.I. Lowenstein, AGS/AD Technical Note No. 269 (1986).
3. A. Hershcovitch and P. Politzer, Phys. Rev. Lett. 36 (1976) 1365; A. Hershcovitch and P. Politzer, Phys. Fluids 22 (1979) 249; W. White, J. Malmberg and C. Driscoll, Phys. Rev. Lett. 49 (1982) 1822; C. Driscoll and J. Malmberg, Phys. Rev. Lett 50 (1983) 167.
4. W. Knauer, J. Appl. Phys. 37, 602 (1966).
5. J.S. Cohen, R.C. Martin, and W.R. Wadt, Phys. Rev. A, 27, 1821 (1983).

mvh  
ADY/TECH

## LOW ENERGY ANTIPROTON POSSIBILITIES AT BNL \*

Y.Y. Lee and D.I. Lowenstein  
Brookhaven National Laboratory  
Upton, NY 11973

Antinuclear physics in the energy range of 0-20 GeV has long been a mainstay of the high energy physics program at BNL. The emphasis of the experimental program in the last couple of years has however moved to other areas as new facilities in the world have come on line. The initiatives stimulated by the USAF has caused a renewed interest in the low energy capabilities at BNL, which are still very competitive and considerable for the production of low energy antiprotons. In the following, we present a synopsis of the present BNL accelerator plans and the near term possibilities for a high yield antiproton production experiment. In this paper we will not address the longer term facility possibilities of producing "large" amounts of antimatter. Parenthetically, even though several aspects of the program are of little interest for this audience, such as the Relativistic Heavy Ion Collider (RHIC) and the Stretcher, it is important to understand their parameters and impact upon various possible antinucleon initiatives at BNL.

### Accelerator Complex

The future BNL high-energy and heavy ion physics programs are centered about the 30 GeV Alternating Gradient Synchrotron (AGS) and the proposed 100-250 GeV/amu (gold-protons) Relativistic Heavy Ion Collider. The complex of accelerators is shown in Fig. 1. The high-energy physics complex consists of two 750 keV preinjectors (Cockcroft Walton for protons, RFQ linac for polarized protons, a second RFQ for protons is under construction) followed by a 200 MeV linac. Presently the 200 MeV protons are directly injected into the AGS and accelerated to 30 GeV. Under construction is a Booster Synchrotron that will boost the proton energy to 1.5 GeV prior to injection into the AGS. This will allow for an increase in delivered proton intensity by a factor of 4, to the  $5 \times 10^{13}$  protons/second level, and an increase in the delivered polarized proton intensity level by a factor of 20, to  $4 \times 10^{11}$  protons/pulse. The major machine parameters are listed in Table I. The heavy-ion physics complex consists of two 15 MV MP Tandems that inject several MeV/amu ions into the AGS. For the present, only fully stripped light ions ( $< {}^{32}\text{S}$ ) can be accelerated in the AGS. With the completion of the Booster Synchrotron, all ion species will be accelerated in the AGS to 10-15 GeV/amu (final energy is dependent on the ion species  $Z/A$ ). The AGS will then have the option to either slowly extract these ions for fixed target operations or inject them into RHIC. RHIC will be capable of accelerating all ion species with storage lifetimes of 10 hours at top energy and highest mass ion, e.g., 100 GeV/amu  ${}^{197}\text{Au}$ . Figure 2 describes as a function of collider energy, for various ion species, the design luminosity and central collision event rate for RHIC.

The AGS is now being required to provide, for experiments, a vast variety of particle species in several types of extraction modes that were never contemplated thirty years ago when it was being designed. From a

\*Work performed under the auspices of the U.S. Department of Energy and the U.S. Air Force Rocket Propulsion Laboratory.

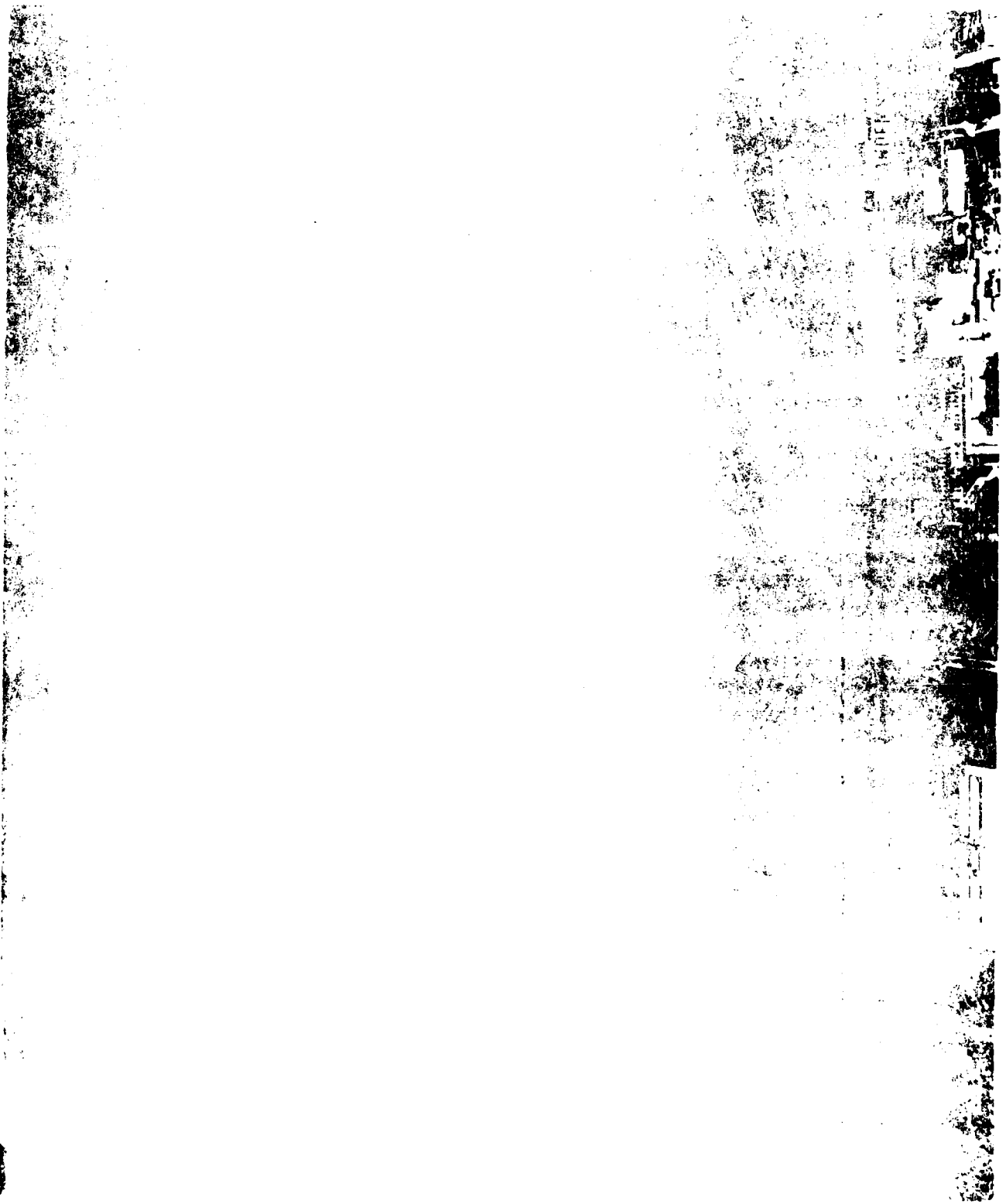


Figure 1. BNL accelerator site.

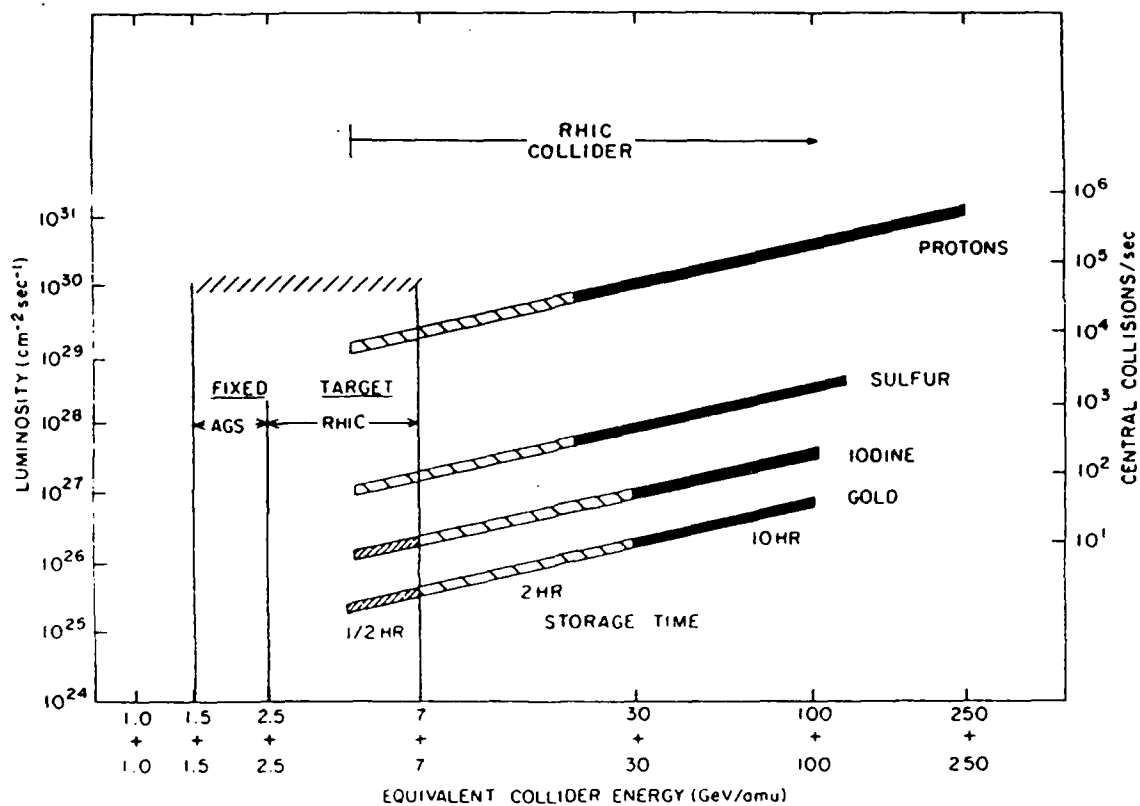


Figure 2 The design luminosity, for various ion masses, as a function of collision energy over the full range accessible with AGS and RHIC. On the left-hand scale, central collisions correspond to impact parameter less than 1 Fermi.



machine that was initially designed to accelerate  $10^{10}$  protons/pulse with internal target operation, the AGS now has accelerated  $1.9 \times 10^{13}$  protons/pulse,  $2.0 \times 10^{10}$  polarized protons/pulse (46% polarization @ 22 GeV/c and  $2 \times 10^8$   $^{28}\text{Si}$  ions to 15 GeV/amu). The internal targets have now been replaced with various slow and fast extraction modes of operation. With the completion of the Booster Synchrotron, the AGS operating modes will reach levels of  $5 \times 10^{13}$  protons/sec,  $4 \times 10^{11}$  polarized protons/pulse using the accumulator features of the Booster and the  $5 \times 10^{12}$  polarized protons/pulse level with significant improvements in ongoing ion source development, and the acceleration of  $10^9 - 10^{10}$  heavy ions (all species). In addition to the Booster construction, a Stretcher is under initial design to improve the slow extracted beam duty factor from 40% to  $\approx 100\%$  and

Table I. Booster Synchrotron Parameters

	Protons	Heavy Ions
Injection		
Energy	200 MeV	> 0.75 MeV/amu
Ejection		
Energy/ Momentum	1.5 GeV	$p=5.27 \frac{Q}{A}$ GeV/c/amu
Circumference (1/4 AGS)	201.78 m	
# Focusing Cells	24 FODO	
Cell Length	8.4 m	
Periodicity	6	
# Straight		
Section/Length	12/3.7 m	
Phase Advance/ Cell	72.3 °	
$\nu_x \sim \nu_y$	4.82	
$\beta_{\text{max}}/\beta_{\text{min}}$	14/3.7 m	
$\eta_{\text{max}}$	2.9 m	
Transition $\gamma$	4.86	
rf harmonics	3	3
# dipoles/length	36/2.4 m	
Field Injection	1.56 kG	> $0.105 \frac{A}{Q}$
Field Ejection	5.46 kG	12.78
# Quadrupole/ length	48/0.5 m	
Repetition Rate	7.5 Hz	1

increase the delivered slow extracted beam intensity by a factor of two to  $2.5$  to  $5.0 \times 10^{13}$  protons/sec. The fast extracted proton intensity of  $5 \times 10^{13}$  protons/sec would not be affected by the Stretcher. At this level of operation ( $8 \mu\text{A}$  current), the AGS could be classified as a mini-hadron factory. With additional alterations, such as, increasing the Booster energy to its maximum design energy of  $2.5 \text{ GeV}$  and several major AGS system modifications, e.g., main power supply, rf, shielding, etc., the AGS could provide  $2 \times 10^{14}$  protons/sec ( $32 \mu\text{A}$ ). Figure 3 summarizes the available proton intensity for each major enhancement for both fast extraction (FEB) and slow extraction (SEB). The AGS is presently the world's major hadron factory, and with the modest inclusion of a Stretcher, it could also serve as a very cost effective next step in the progression up the intensity frontier to the  $100 \mu\text{A}$  domain as proposed by at least four different laboratories around the world.

The mainstream future at BNL is directed, however, to the exploitation of a unique heavy ion collider, RHIC. RHIC consists of two independent rings of superconducting magnets in the former CBA tunnel, operating at a top field of  $3.5 \text{ Tesla}$  and  $4.5^\circ \text{ K}$ . Tables II and III list the general parameters for RHIC. Prototype magnets have been constructed at both BNL and in industry and meet the required specifications. In addition to the injector system (AGS), four of six experimental areas are complete, the liquid helium refrigeration system is complete and operational, the collider tunnel is complete, and the prototype control system is being implemented on the AGS. With this collider, one can accelerate all ion species from protons (polarized with the introduction of Siberian snakes) to gold and uranium. For proton-on-proton collisions, one could achieve a center-of-mass energy of  $500 \text{ GeV}$  with an average luminosity of  $8.4 \times 10^{30} \text{ cm}^{-2} \text{ sec}^{-1}$ . For gold-on-gold collisions, one could achieve a center-of-mass energy of  $40 \text{ TeV}$  ( $100 \text{ GeV/amu}$ ) with an average luminosity of  $4.4 \times 10^{26} \text{ cm}^{-2} \text{ sec}^{-1}$ . The maximum performance specifications for RHIC are defined by the beam physics of  $100 \text{ GeV/amu}$  gold ions. The major limiting condition is the intrabeam scattering process at the highest energy and the highest mass ion. At the lowest energies of RHIC, where beam lifetimes are less than one hour, one would operate RHIC in a fixed target mode by use of a gas jet target in one ring. RHIC will also allow for asymmetric operations, such as, protons in one ring and gold in the other. RHIC is expected to take four years to complete, with a requested start date of construction of October 1988.

#### Antiproton Production Experiment

The possibility of obtaining very low energy antiprotons of the order of  $20 \text{ keV}$  kinetic energy from the AGS was first described by Lee.<sup>1</sup> In this paper we would like to outline the requirements for such a facility (or experiment) to accomplish the very low energy antiproton source.

The basic magnetic cycle of the AGS and the Booster is given in Figure 4. After injecting  $1.5 \text{ GeV}$  protons into the AGS, the magnetic field of the Booster is ramped up to  $8.5 \text{ kG}$  in order to receive  $3.5 \text{ GeV/c}$  antiprotons produced by the AGS. The antiprotons are decelerated by the Booster and then extracted to the  $200 \text{ MeV}$  linac while the AGS delivers the rest of the

1. Y.Y. Lee, 59-61. Proc. 1986 Summer Workshop on Antiproton Beams in the 2-10 GeV/c Range, Brookhaven National Laboratory, August 18-22, 1986, Formal Report, BNL 52082 (1987).

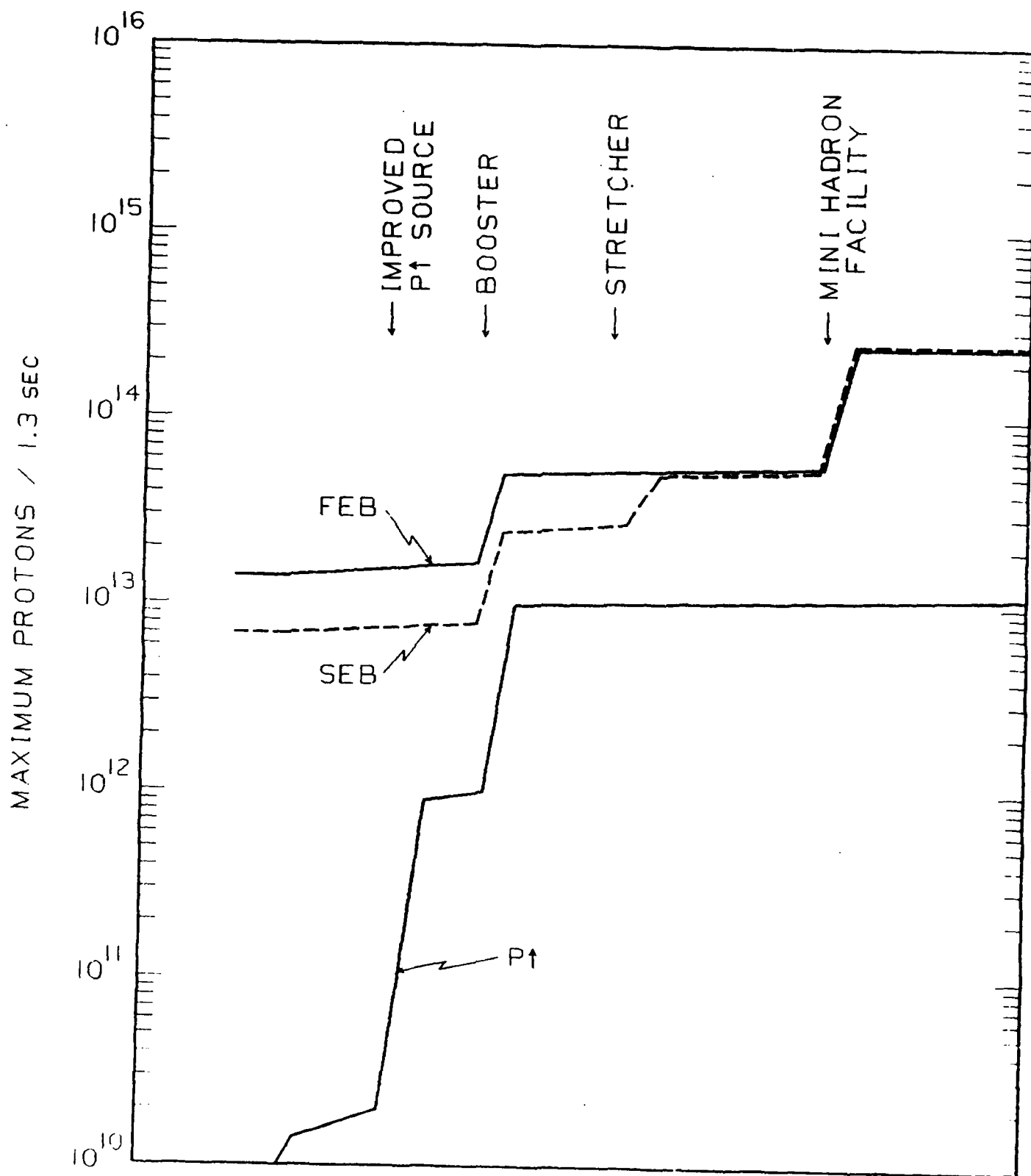


Figure 3

PROTON AND POLARIZED PROTON (P↑) INTENSITY

Table II RHIC General Parameters

Energy Range (each beam),	
Au	7-100 GeV/amu
protons	28.5-250 GeV
Luminosity, Au-Au @	
100 GeV/amu &	
10 H av.	$4.4 \times 10^{26} \text{ cm}^{-2} \text{ sec}^{-1}$
Operational lifetime	
Au @ $\gamma > 30$	> 10 h
Diamond length @	
100 GeV/amu	$\pm 27 \text{ cm rms}$
Circumference,	
4-3/4 C <sub>AGS</sub>	3833.87 m
Number of crossing	
points	6
Free space at	
crossing point	$\pm 9 \text{ m}$
Beta @ crossing,	
horizontal/vertical	6 m
low-beta/insertion	3 m
Betatron tune,	
horizontal/vertical	28.82
Transition energy, $\gamma_T$	25.0
Filling mode	Box-car
No. of bunches/ring	57
No. of Au-ions/bunch	$1.1 \times 10^9$
Filling time (ea. ring)	$\sim 1 \text{ min}$
Magnetic rigidity, $B\rho$	
@ injection	96.5 T·m
@ top energy	839.5 T·m
No. of dipoles	
(180/ring+12 common)	372
No. of quadrupoles	
(276/ring+216 insertion)	492
Dipole field @	
100 GeV/amu, Au	3.488 T
Dipole magnetic length	9.46 m
Coil i.d. arc magnets	8 cm
Beam separation in arcs	90 cm
rf frequency	26.7 MHz
rf voltage	1.2 MV
Acceleration time	1 min

Table III. RHIC Beam Parameters

Element	Proton	Deuterium	Carbon	Sulfur	Copper	Iodine	Gold
Atomic No. Z	1	1	6	16	29	53	79
Mass No. A	1	2	12	32	63	127	197
Rest energy (GeV/amu)	0.9383	0.9376	0.9310	0.9302	0.9299	0.9303	0.9308
<u>Injection:</u>							
Kinetic energy (GeV/amu)	28.5	13.6	13.6	13.6	12.4	11.2	10.7
$\bar{K}$	0.99947	0.99947	0.99793	0.99794	0.99757	0.99704	0.99680
Norm. emittance (mm.mrad)	20	10	10	10	10	10	10
Bunch area (eV.sec/amu)	0.3	0.3	0.3	0.3	0.3	0.3	0.3
Bunch length (nsec)	$\pm 8.6$	$\pm 8.6$	$\pm 8.6$	$\pm 8.6$	$\pm 8.6$	$\pm 8.6$	$\pm 8.6$
Energy spread ( $\times 10^{-4}$ )	$\pm 3.8$	$\pm 7.6$	$\pm 7.6$	$\pm 7.6$	$\pm 8.3$	$\pm 9.2$	$\pm 9.6$
No. ions/bunch ( $\times 10^9$ )	100	100	22	6.4	4.5	2.6	1.1
<u>Top Energy:</u>							
Kinetic energy (GeV/amu)	250.7	124.9	124.9	124.9	114.9	104.1	100.0
$\bar{E}_T$	268.2	134.2	135.2	135.3	124.6	112.9	108.4

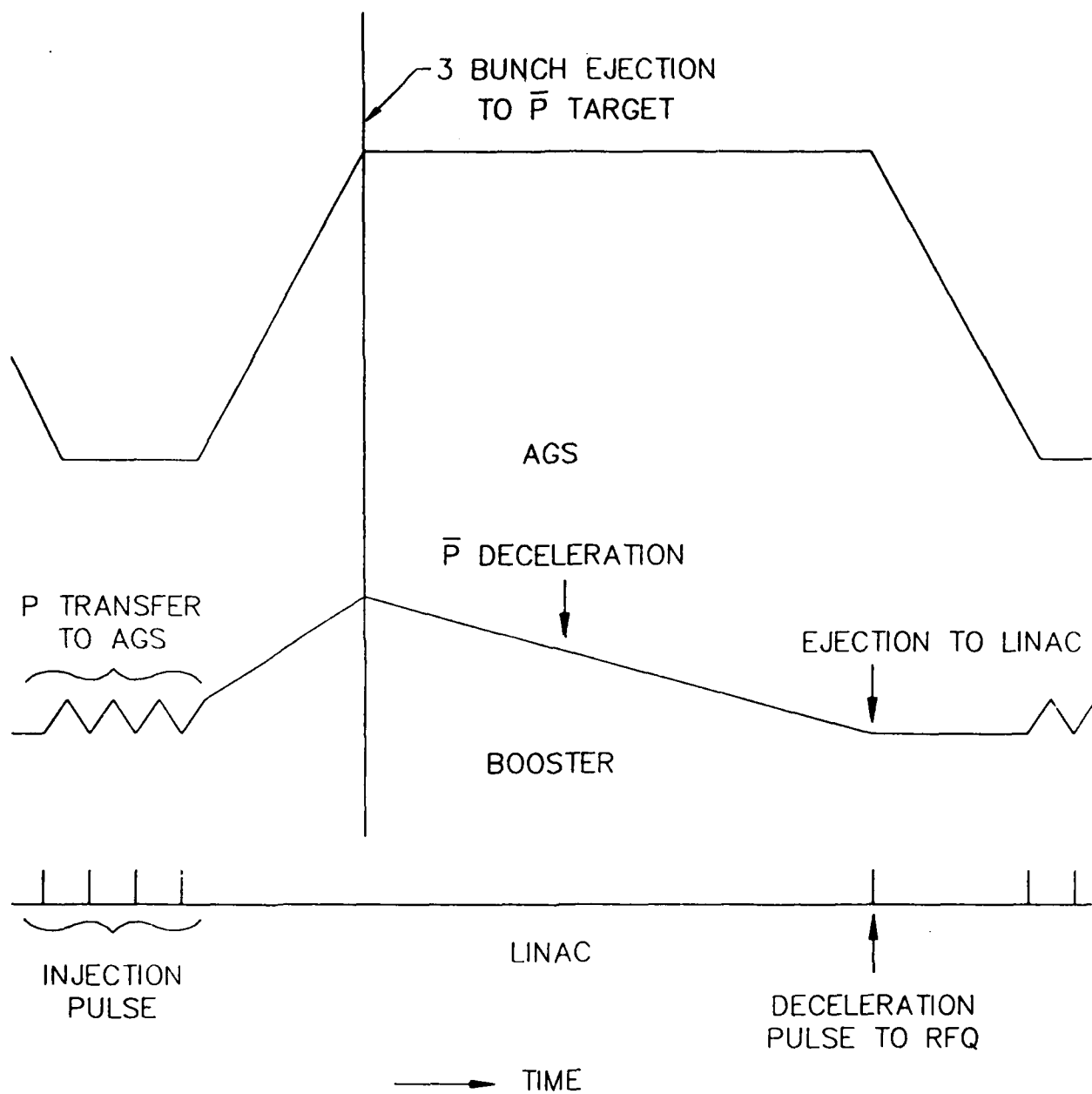


Figure 4  
Booster and AGS magnetic cycle

available protons for other experiments. The antiprotons are then decelerated in the linac to 750 keV and then to 20 keV in the RFQ linac. Figure 5 is a description of the accelerator complex.

At the end of the AGS acceleration cycle, the AGS rf voltage is raised to shorten the bunch length to a few nanoseconds before extracting three of the twelve bunches through the H10 extraction channel. This will increase the proton beam momentum spread and provide for a short antiproton bunch. The extraction channel and the beam transport should be able to accommodate the proton momentum spread. The additional equipment needed for the extraction is a ferrite kicker and power supply similar to the ones installed at H5 or E5, an extraction septum and power supply similar to the one at H10, and an AGS orbit bump and power supply.

The beam transport consists of six quadrupoles, a triplet in the AGS tunnel for beam shaping and another triplet upstream of the target for focusing the beam on to the target. A special target station similar to the ones at the CERN and Fermilab antiproton facilities must be constructed because of the high intensity beams involved. A focusing element such as a lithium lens is required in order to focus the produced antiprotons into the apertures of the transport quadrupoles. The antiprotons produced by the AGS are then transported to the Booster. The length of the line is approximately 150 meters and requires about 30 degrees of total bend. It requires the order of 10 quadrupoles and six 5 degree bending magnets. Injection into the booster is accomplished by duplicating the Booster extraction septum and kickers.

The antiprotons transported to the Booster will have a 50  $\pi$ -mm-mr emittance in both planes and a momentum bite of 2%. The length of the antiproton bunch is the same as the AGS proton bunch which was tailored to a few nanoseconds. By allowing the bunch to rotate in longitudinal phase space one can lengthen it to 50 nanoseconds and the antiproton momentum spread can then be reduced to about a tenth of a percent. No special equipment is needed to decelerate the beam to 200 MeV kinetic energy. One may have to install special instrumentation to detect the low intensity beam.

Decelerated antiprotons can be extracted at the Booster straight section C6. A fast ferrite kicker of strength 6 kG-meter can extract 200 MeV antiprotons from the Booster. A transport system identical to the injection line but of opposite polarity can transport the antiprotons to the HEBT line of the linac. A fast kicker can inject the beam into the upstream end of the linac.

At present we do not foresee any additional equipment required to decelerate the antiprotons through the linac and RFQ except increased sophistication in phase and amplitude controls. At the exit of the RFQ a kicker is required to deflect the decelerated antiprotons away from the regular proton channel and direct it to the detector region.

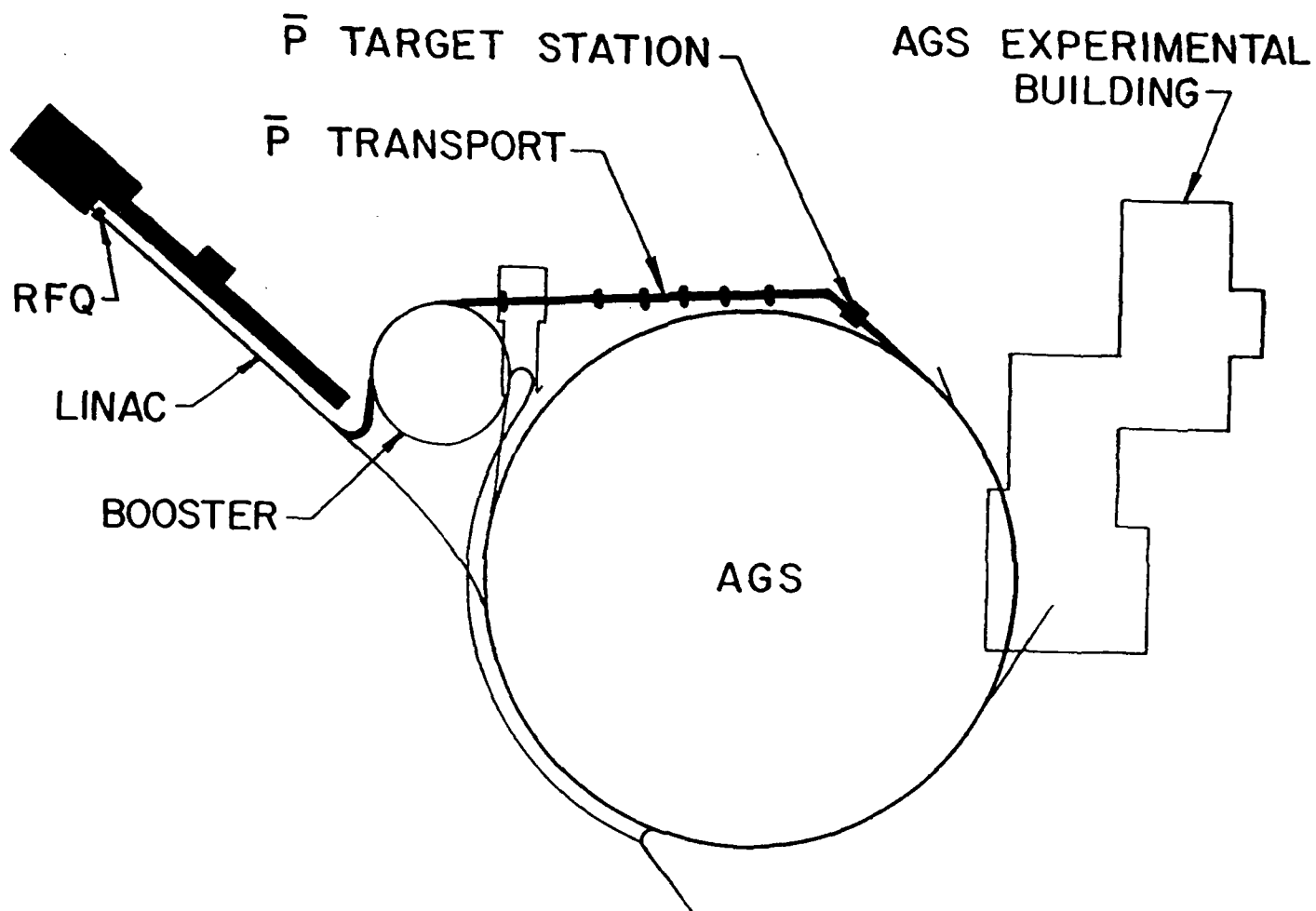


Figure 5  
AGS accelerator complex



Additional sophistication is needed in the control system of the AGS, Booster and linac. Pulse-to-pulse modulation of the system is required, not only for the magnetic cycle of the machines, but also to all other systems such as rf and extraction systems.

At present there are two modes of Booster operation, namely fast cycling proton operation and slower cycling heavy ion operation. The proton operation needs higher voltage and lower current while heavy ion operation needs lower voltage but higher current. Power supply modules are rearranged for each of the operations. For the proposed antiproton option, the range of antiproton deceleration current requirements forces one to use the arrangement of the heavy ion option which results in the Booster cycle period to be lengthened by a factor of two. If faster cycling of the Booster is important, one would add a set of modules to the present power supply to increase the repetition rate. It is inefficient to bunch and decelerate in the linac unless the antiproton beam is prebunched to the linac frequency. One would add a 200 MHz rf cavity to bunch the antiprotons in the Booster. This will bring the efficiency to about 80% compared to 50% for decelerating through the linac and RFQ.

It has been demonstrated that one can reduce the six dimensional emittance of the beam in a synchrotron either by stochastic or electron cooling. As a proof of principle experiment the option of cooling is not compelling. It has been calculated<sup>1</sup> that there is a factor of 900 decrease in the available antiproton flux at 20 keV without cooling versus with cooling because of the reduction in the 6-dimensional phase space. We have not estimated the additional costs of introducing stochastic cooling but refer the reader to the copious literature from both CERN and Fermilab.

We estimate the order of magnitude costs to carry out a test of the scheme. The estimate is scaled from either existing AGS equipment costs or scaled from the Booster proposal. We used a rule of thumb number of about \$150/kilowatt for the power supply estimates. We summarize them in Table IV.

### Conclusion

BNL's future high-energy and heavy ion physics plans consist of three major components. The first is to exploit the present and near-term upgraded AGS complex for 30 GeV physics, such as, the study of the TeV domain via flavor changing rare kaon decays, neutrino physics, glueball and exotics, spectroscopy, etc. The second is the primary BNL long-term goal of constructing RHIC to study the fundamental properties of matter in a state in which the primordial quarks and gluons are no longer confined as constituents of ordinary particles. The third component, which is now beginning to be considered are the possibilities of a mini-hadron factory with the AGS. Should the physics results of the next years justify the effort and cost, this would be a natural extension of the present and near-term AGS high-energy program.

TABLE IV  
(cost in thousands)

I. EXTRACTION FROM AGS-----	360.
FERRITE KICKER	50.
POWER SUPPLY	50.
EXTRACTION SEPTUM	100.
POWER SUPPLY	100.
ORBIT BUMP	10.
POWER SUPPLY	50.
II. TARGET STATION AND PROTON TRANSPORT-----	1070.
QUADRUPOLES (6)	240.
POWER SUPPLIES	180.
TARGET STATION AND LI LENS	650.
III. P-BAR TRANSPORT AND BOOSTER INJECTION-----	1750.
TRANSPORT TUNNEL(450 FT)	450.
QUADRUPOLES (10)	400.
POWER SUPPLIES	300.
DIPOLES ( 5)	200.
POWER SUPPLIES	100.
INJECTION SEPTUM	100.
POWER SUPPLY	100.
FAST KICKER	50.
POWER SUPPLY	50.
IV. BOOSTER EXTRACTION AND TRANSPORT TO LINAC-----	1010.
EXTRACTION KICKER	100.
POWER SUPPLY	100.
QUADRUPOLES (15)	150.
POWER SUPPLIES	250.
DIPOLES ( 8)	160.
POWER SUPPLY	150.
KICKER	50.
POWER SUPPLY	50.
V. INSTRUMENTATION AND CONTROLS-----	500.
VI. CHANGES IN BOOSTER TUNNEL AND BUILDING 914-----	100.
VII. BOOSTER POWER SUPPLY ADDITION-----	1000.
VIII. 200 MHz CAVITY SYSTEM-----	450.
SUBTOTAL-----	6240.
EDIA(@15%)	940.
CONTINGENCY(@20%)	1440.
TOTAL	<u>8620.</u>



Accelerator Division  
Alternating Gradient Synchrotron Department  
BROOKHAVEN NATIONAL LABORATORY  
Associated Universities, Inc.  
Upton, New York 11973

Accelerator Division  
Technical Note

AGS/AD/Tech. Note No. 299

A HIGH INTENSITY HADRON FACILITY, AGS II

Y. Y. LEE and D. I. LOWENSTEIN

April 25, 1988

There is a large and growing community of particle and nuclear physicists around the world who are actively lobbying for the construction of an accelerator that could provide 1-2 orders of magnitude increase in proton intensity above that of the present AGS. There have been a series of proposals from Canada, Europe, Japan, and the U.S.A. They can all be characterized as machines varying in energy from 12-60 GeV and intensities of 30-100  $\mu$ A. The community of physicists using the AGS are in a unique position however. The AGS is the only machine available that can provide the beams to execute the physics program that this large international community is interested in. The BNL approach to the communities interests involves a stepwise intensity upgrade program. At present the AGS slow extracted beam current is 1  $\mu$ A. With the completion of the Booster in 1990 and the associated AGS modifications, the current will rise to 4  $\mu$ A. With the subsequent addition of the Stretcher the current will rise to 8  $\mu$ A and approximately 100% duty factor. In this note we examine the possibility of a further enhancement to a current level of 40  $\mu$ A CW.

Let us first examine the capabilities of each of the present AGS accelerators. The Linac is capable of running ten pulses a second of 30 mA  $H^-$  ions with a 500  $\mu$ sec pulse length. The Linac output current exceeds the input capabilities of the Booster. The Booster is capable of pulsing ten cycles a second. Because of the large power swing both in real and reactive power, the Booster is limited presently to operate at 7.5 Hz and an energy to 1.5 GeV. If the Booster were operated beyond these limits, the electrical line voltage fluctuation due to its pulsing would severely affect other parts of the Laboratory. In certain resonant situations, the entire LILCO power grid and some generating stations would be adversely effected. One way to overcome this limitation would be to pulse, out-of-phase, an equivalent electrical device as an analog to a flywheel so as to smooth the power swing. Once the power swing problem is corrected one could cycle the Booster faster and to a higher energy.

At present the AGS is capable of cycling every 1.2 seconds. The pulse rate is limited mainly by two factors. One is the limitations of the main magnet power supply and the second is the peak voltage of the present radio frequency acceleration system. Both of these can be improved. An important consideration that minimizes the scope of the improvements is that with the Stretcher used for slow extraction one no longer needs to operate the AGS with a magnetic flattop. The highest current that can be achieved is when one matches all the accelerators to the repetition rate of the Linac. Our scheme assumes that one does not replace either the Linac or the AGS. We previously mentioned the problems with the Booster power swing, AGS main magnet power supply and radio frequency systems. There are other problem areas, such as, crossing AGS transition energy with no beam losses, space charge effects, etc.

AD-A207 482

POTENTIAL FOR A NEAR TERM VERY LOW ENERGY ANTIPROTON  
SOURCE AT BROOKHAVEN NATIONAL LABORATORY(U) AIR FORCE  
ASTRONAUTICS LAB EDWARDS AFB CA G D NORDLEY APR 89  
AFAL-SR-89-001

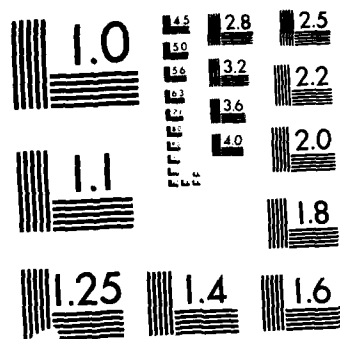
3/3

UNCLASSIFIED

F/G 20/7

NL





RESOLUTION TEST CHART  
NBS 1010-A

We first propose to increase the Booster energy to 2.8 GeV and the repetition rate to 10 Hz. This is below the Booster transition energy and well within the capabilities of this machine. The Booster is already designed to operate at the increased dB/dt rate. The increased Booster energy is motivated by the energy swing solution described below.

We next propose to introduce a Post Booster accelerator (see Table I) after the Booster. This machine would operate at 10 Hz and accelerate protons to an energy above the AGS transition energy. This machine would be capable of accelerating the full Booster beam pulse to an energy above 9 GeV. The Post Booster power swing could be made to complement that of the Booster and thus overcome the Booster repetition rate limitations. The AGS main ring power supply cycling limitations would also be eased due to the reduced AGS beam energy swing. By adjusting the Post Booster magnet aperture, magnetic field range and radius, the Post Booster would be designed to have the same magnetic energy difference swing as the Booster. These two machines would operate at the same repetition rate but 180° out of phase with each other. To reduce the construction costs by minimizing the number of tunnels, it would be desirable to install the Post Booster in the same tunnel as the Collector ring. The Collector ring that is introduced below requires a minimum circumference of three times that of the Booster ring. The Post Booster would thus have a circumference three times that of the Booster, 75% of the AGS. The spacing of the Booster pulses would be preserved in the Post Booster. Table II shows the proposed parameters for the Booster, the Post Booster, Collector, and the AGS. We note that the space charge intensity limit for a given normalized emittance is proportional to  $\beta\gamma^2$  of the proton. Thus once one is below the space charge tune shift limit in the Booster, the space charge problem is minimal for all subsequent accelerators in the chain.

Table I  
Post Booster Parameters

Injection energy	2.815 GeV (3.634 GeV/c)
Ejection energy	9.26 GeV ( 10.2 GeV/c)
Circumference	605.25 m
Superperiods	6
# cells	48
Cell length	12.61 m
$v_x/v_y$	12.75/11.75
Phase advance/cell	95.6/88.1 °
$\beta_{max}/\beta_{min}$	22/3.3
$\eta_{max}$	0.62
# long straight section/length	12/5.3 m
Dipoles	
No.	80
Length	3.8 m
Field injection/ejection	2.5 kG/7 kG
Aperture	17.96/5.84 cm
Quadrupoles	
No.	96
Length	1 m
Aperture	13 cm
Max. poletip field	5.2 kG

Table II

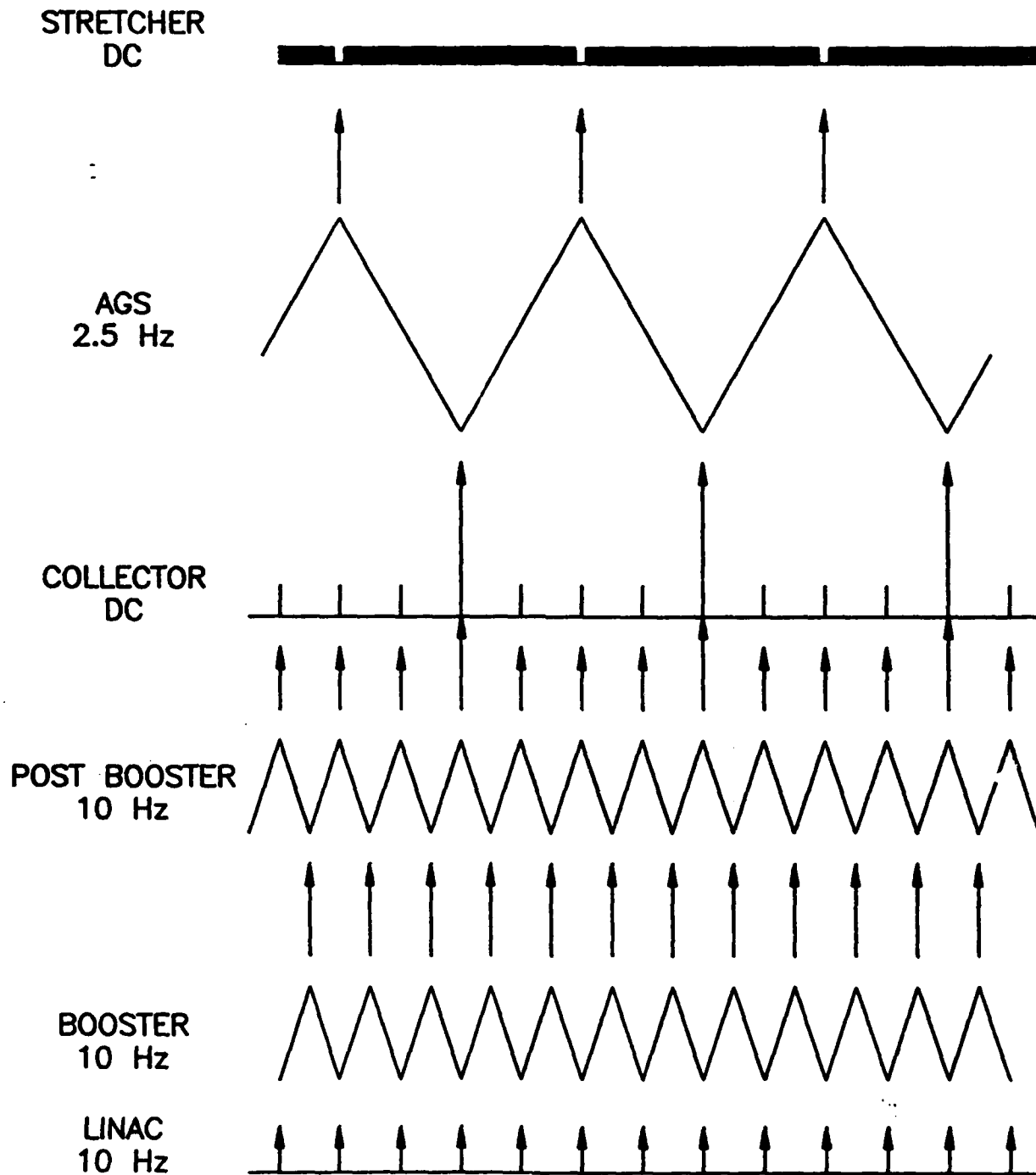
	Input Energy	Input $\beta\gamma^2$	Output Energy	# Bunches	# rf Buckets
Booster	200 MeV	0.833	2.8 GeV	3	3
Post Booster	2.8 GeV	14.87	9.3 GeV	3	9
Collector	9.3 GeV	117.6	9.3 GeV	12	12
AGS	9.3 GeV	117.6	30 GeV	12	12

The next accelerator in the chain is the Collector ring (see Table III). The AGS cycling limitations require the introduction of an intermediate storage ring so as not to lose the advantages of the 10 Hz capabilities of the preinjectors. The Collector would be a short term (0.4 sec) intermediate storage ring. This machine would reside in the Post Booster tunnel. The function of this ring is to temporarily store three Post Booster pulses prior to injection into the AGS (the Post Booster accelerates with only one-third of its rf buckets filled). The AGS would accept the three Post Booster pulses (9 bunches) stored in the Collector and one additional pulse (3 bunches) directly from the Post Booster for a total of 12 bunches. The Post Booster and the Collector would inject into the AGS every 400 milliseconds. A proposed cycle for the Booster, Post Booster, Collector, AGS, and Stretcher is shown in Figure 1. Potential locations for the proposed Accelerators are shown in Figure 2. We show in Table IV the estimated proton currents at various implementation stages of the above-mentioned proposal. The delivered currents are for slow extracted beam operation.

Table III  
Collector Ring Parameters

Energy	9.26 GeV (10.2 GeV/c)
Circumference	605.25 m
Superperiods	6
# cells	30
Cell length	20.175
$v_x/v_y$	7.25
Phase advance	87 °
$\beta_{max}/\beta_{min}$	34.1/6.3 m
$\eta_{max}$	3.3 m
straight section	12/9 m
Dipoles	
No.	96
Length	3.55
B	6.26 kG
Aperture	14/5 cm
Quadrupoles	
No.	60
Length	0.5 m
Aperture	11 cm
Polatip	5.1 kG





## AGS II OPERATING CYCLE

Figure 1. Accelerator Cycles

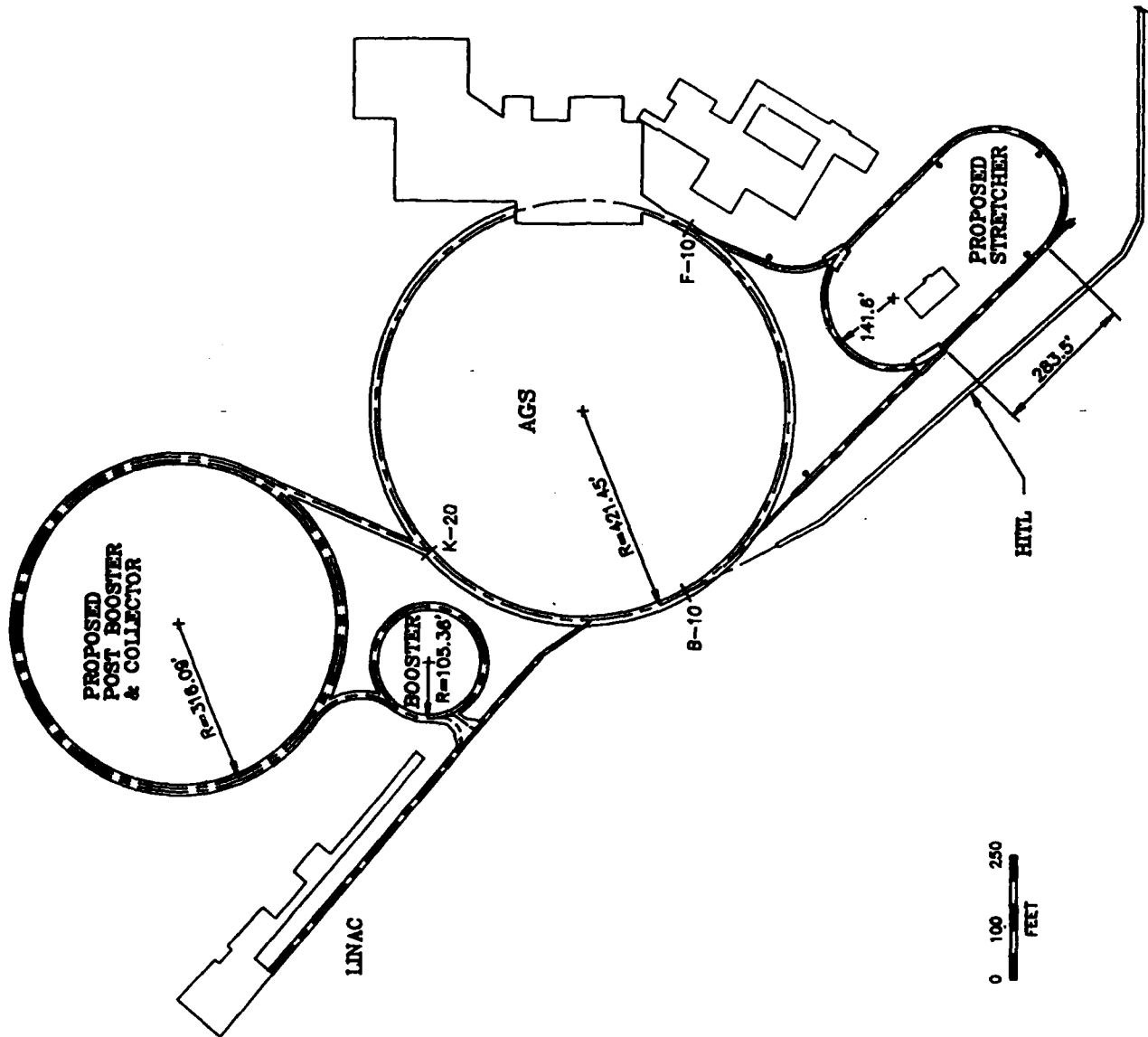


Figure 2. Accelerator Complex Layout

Table IV

Option	AGS Protons per pulse	AGS Cycle Time (sec)	Duty Factor (%)	Delivered Current ( $\mu$ A)
AGS	$1.5 \times 10^{13}$	2.5	35	1.0
+ Booster	$6 \times 10^{13}$	2.5	35	4.0
+ Stretcher	$6 \times 10^{13}$	1.2	100	8.0
+ Post Booster and Collector	$2.5 \times 10^{14}$	0.4	100	40.0

The proposed scheme utilizes every Linac pulse and thus there is no advantage to accumulate polarized protons in the Booster. The higher ejection energy however requires the crossing of one intrinsic depolarizing resonance at 1.57 GeV in the Booster. We have not calculated the depolarizing effect of this resonance nor yet considered a resonance crossing scheme. The Post Booster and the Collector, would be designed to avoid serious depolarizing resonances. For heavy ion operations we would consider moving the final electron stripping foil from the Booster to the Post Booster extraction line. For the heaviest ions the beam intensity would increase due to the larger stripping efficiencies at higher energy.

We have presented one of several possibilities for the evolution of the AGS complex into a high intensity hadron facility. One could consider other alternatives, such as using the AGS as the Collector and constructing a new 9-30 GeV machine. We believe the most responsible scenario must minimize the cost and downtime to the ongoing physics program. With a stepwise approach, starting with the Booster, the physics program can evolve without a single major commitment in funds. At each step an evaluation of the funds versus physics merit can be made. As a final aside, each upgrade at the AGS and Booster is presently being implemented to support an interleaved operation of both protons and ions.

END

FILMED

6-89

DTIC